



**Medical University of Gdansk**

**Doctoral Thesis**

**“The role of PDIA3 in vitamin D signaling”**

**mgr Joanna I. Nowak**

Supervisor: prof. dr hab. Michał Żmijewski

Faculty of Medicine,  
Department of Histology

**Gdansk 2023**

**To my supervisor prof. dr hab. Michał Żmijewski**  
**Thank you for believing in me, all guidance, and encouragement during this project.**  
**This journey wouldn't be possible without your support.**

**To all my laboratory colleagues,**  
**Thank you for helping me overcome all the obstacles during my Ph.D.**

**To my beloved family,**  
**Thank you for your tremendous understanding and encouragement**  
**in the past few years.**

## **Grants**

The study was supported by a National Science Center OPUS Program under contracts  
2017/25/B/NZ3/00431

## **TABLE OF CONTENTS**

<b>I. LIST OF PUBLICATIONS</b> .....	4
<b>II. ABBREVIATIONS</b> .....	5
<b>III. ABSTRACT</b> .....	7
<b>IV. ABSTRACT IN POLISH</b> .....	9
<b>V. INTRODUCTION</b> .....	11
<b>VI. AIMS</b> .....	14
<b>VII. DISCUSSION OF PUBLICATIONS INCLUDED IN THE DOCTORAL DISSERTATION</b> .....	15
<b>VIII. CONCLUSIONS</b> .....	23
<b>IX. LIST OF REFERENCES</b> .....	25
<b>X. PUBLICATIONS</b> .....	29
<b>XI. STATEMENTS OF CO-AUTHORS</b> .....	71

## I. LIST OF PUBLICATIONS

### 1. Publication 1 (Original)

Authors: Joanna I. Nowak, Anna M. Olszewska, Anna Piotrowska, Kamil Myszczyński, Paweł Domżański, Michał A. Żmijewski

title: PDIA3 modulates genomic response to 1,25-dihydroxy vitamin D3 in squamous cell carcinoma of the skin

Steroids, 2023, <https://doi.org/10.1016/j.steroids.2023.109288>

IF = 2,76 | MNI<sub>SW</sub> = 70 | Q4

### 2. Publication 2 (Original)

Authors: Joanna I. Nowak, Anna M. Olszewska, Oliwia Król, Michał A. Żmijewski

title: Protein Disulfide Isomerase Family A Member 3 Knockout Abrogate Effects of Vitamin D on Cellular Respiration and Glycolysis in Squamous Cell Carcinoma

Nutrients, 2023, <https://doi.org/10.3390/nu15214529>

IF = 5,9 | MNI<sub>SW</sub> = 140 | Q1

### 3. Publication 3 (Original)

Authors: Joanna I. Nowak, Anna M. Olszewska, Magdalena Gebert, Rafał Bartoszewski, Michał A. Żmijewski

title: VDR and PDIA3 are essential for activation of calcium signaling and membrane response to 1,25(OH)<sub>2</sub>D<sub>3</sub> in squamous cell carcinoma cells

Cells, 2023, <https://doi.org/10.3390/cells13010011>

IF = 6,0 | MNI<sub>SW</sub> = 140 | Q2

Bibliometrics:

Impact Factor: 14,66

MNI<sub>SW</sub>: 350



## II. ABBREVIATIONS

1,25-MARRS - *Membrane-associated, rapid response steroid-binding*

A431- *Squamous Cell Carcinoma cell line*

BNIP3 - *BCL2 Interacting Protein 3*

CAMKIIA - *Calcium/Calmodulin Dependent Protein Kinase II Alpha*

CAMP - *Cathelicidin Antimicrobial Peptide*

CDKN1A - *Cyclin-Dependent Kinase Inhibitor 1A*

CDKN2A - *Cyclin-Dependent Kinase Inhibitor 2A*

Cyp24A1 - *Cytochrome P450 Family 24 Subfamily A Member 1*

DEG - *Differentially expressed genes*

ECAR - *Extracellular Acidification Rate*

Erk1/2 - *Extracellular Signal-Regulated Kinase 1/2*

ERp57- *Endoplasmic Reticulum Resident Protein 57*

GO - *Gene ontology*

GRP58 - *Glucose Regulated Protein, 58kDa*

HaCaT - *Immortalized human keratinocyte cell line*

HNSCC- *Head and neck squamous cell carcinoma*

MAPK - *Mitogen-activated protein Kinase*

MKI67 - *Marker Of Proliferation Ki-67*

mtDEGs - *mitochondria-associated differently expressed genes*

NFAT - *Nuclear Factor of Activated T-cells*

OCR - *Oxygen Consumption Rate*

PDIA3 - *Protein Disulfide Isomerase Family A Member 3*

PERK - *Protein Kinase RNA-Like ER Kinase*

PKC - *Protein Kinase C*

PKC $\alpha$  - *Protein Kinase C-alpha*

PLA2 - *Phospholipase A2*

PLAA - *Phospholipase A2 Activating Protein*

PLC $\gamma$  - *Phospholipase C Gamma 1*

PTGS2 - *Prostaglandin-Endoperoxide Synthase 2*

RXR - *Retinoid X Receptor*

SCC - *Squamous Cell Carcinoma*

STAT3 - *Signal Transducer And Activator Of Transcription 3*

TEM - *Transmission electron microscopy*

TRPV6 - *Transient Receptor Potential Cation Channel Subfamily V Member 6*

VDR - *Vitamin D Receptor*

VDRE - *Vitamin D Response Elements*

### III. ABSTRACT

PDIA3 is a membrane-associated disulfide isomerase involved in processes such as disulfide bond formation, protein folding, transport, and remodeling. The main localization of the PDIA3 protein is the endoplasmic reticulum, where it functions as a chaperon protein. However, PDIA3 was also localized in the nucleus, at the cell membrane, or within mitochondria, where it affects various physiological processes, such as participation in signal transduction through STAT3 protein, proapoptotic activities, and membrane response to 1,25(OH)<sub>2</sub>D<sub>3</sub>.

An active form of vitamin D (1,25(OH)<sub>2</sub>D<sub>3</sub>) acts through vitamin D receptor (VDR) initiating genomic response and modulating the expression of more than 3000 genes in the human genome. However, not all of the effects can be attributed to genomic actions of VDR, thus nongenomic actions of vitamin D were described. In recent years, PDIA3 was connected to those rapid, non-genomic activities of 1,25(OH)<sub>2</sub>D<sub>3</sub> as its membrane receptor.

Here, the role of PDIA3 in alternative pathways of vitamin D in squamous cell carcinoma was investigated. Using a transcriptomic-based approach changes in expression of 2000 genes were identified after *PDIA3* deletion in A431 cells. Further, PDIA3-deficient cells have shown changes in proliferation, migration, and cell cycle, suggesting an important physiological role of PDIA3. A431Δ*PDIA3* cells showed increased sensitivity to 1,25(OH)<sub>2</sub>D<sub>3</sub>. Interestingly, it was observed that expression of some of the classical VDR targets, including *CAMP* (Cathelicidin Antimicrobial Peptide), *TRPV6* (Transient Receptor Potential Cation Channel Subfamily V Member 6), were regulated differently by 1,25(OH)<sub>2</sub>D<sub>3</sub>, in A431Δ*PDIA3*. The group of PDIA3-dependent genes (PTGS2, MMP12, FOCAD) was identified, using Venn analysis as a graphical illustration of the logical relationship between DEGs expressed in A431WT, A431Δ*PDIA3* 1,25(OH)<sub>2</sub>D<sub>3</sub>-treated and A431Δ*PDIA3* nontreated cells. Additionally, response to 1,25(OH)<sub>2</sub>D<sub>3</sub> in cancerous A431 cells differed from immortalized HaCaT keratinocytes, used as non-cancerous control. Furthermore, *PDIA3* deletion resulted in changes in mitochondria morphology and bioenergetics. Morphology parameters such as perimeter, section area, and maximal diameter were decreased in A431Δ*PDIA3* cells, while 1,25(OH)<sub>2</sub>D<sub>3</sub> treatment partially reversed the effect of *PDIA3* deletion. Moreover, *PDIA3* knockout affected mitochondrial bioenergetics (oxidative phosphorylation and glycolysis) and modulated STAT3 signaling. Oxygen consumption rate (OCR) and Extracellular Acidification Rate (ECAR) were

significantly higher in A431 $\Delta$ *PDIA3* than in A431WT cell, with no significant effect 1,25(OH) $_2$ D $_3$  treatment. Interestingly, it seems that the *PDIA3* effect on mitochondria might be not direct but involves modulation of transcription of several mitochondria-related genes. Next, membrane response to 1,25(OH) $_2$ D $_3$  and calcium signaling were investigated. in squamous cell carcinoma A431 cell line with or without deletion of *VDR* and *PDIA3* genes. Deletion of either *PDIA3* or *VDR* resulted in decreased baseline calcium levels and its responsiveness to 1,25(OH) $_2$ D $_3$ , however, the effect was more pronounced in A431 $\Delta$ *PDIA3*. The knockout of either of these genes disrupted 1,25(OH) $_2$ D $_3$ -elicited membrane signaling in A431 cells. The results indicate that *VDR* is essential for the activation of Calcium/calmodulin-dependent protein Kinase II Alpha (*CAMK2A*), while *PDIA3* is required for 1,25(OH) $_2$ D $_3$ -induced calcium mobilization in A431 cells.

Taken together, it was established that *PDIA3* is involved in 1,25(OH) $_2$ D $_3$  action on gene expression profile and a range of phenotypic effects, such as proliferation and migration of A431 squamous cell carcinoma. *PDIA3* affects mitochondrial morphology and bioenergetics, possibly by regulating *STAT3* signaling. Further, a major role of *PDIA3* in membrane response to 1,25(OH) $_2$ D $_3$  was shown. However, it seems that *VDR* is also required for the activation of nongenomic response to 1,25(OH) $_2$ D $_3$ . Thus, the results presented here emphasize the important role of *PDIA3* in regulating the response to 1,25(OH) $_2$ D $_3$  and maintaining normal cellular physiology. Furthermore, *PDIA3* could be considered a predictive marker as well as a target for anticancer therapy.

**Keywords:** Vitamin D, *VDR*, *PDIA3*, transcriptome analysis, Ca $^{2+}$  signaling, cellular bioenergetics, squamous cell carcinoma

#### IV. ABSTRACT IN POLISH

PDIA3 to białkiem o aktywności izomerazy dwusiarczkowej, zaangażowane w procesy takie jak tworzenie wiązań dwusiarczkowych, zwijanie, transport i remodelowanie białek. Główną lokalizacją białka PDIA3 jest siateczka śródplazmatyczna, gdzie funkcjonuje jako białko chaperonowe. PDIA3 zostało także zlokalizowane w obrębie jądra komórkowego, błony komórkowej czy mitochondriach, gdzie zaangażowane jest w regulację wielu procesów fizjologicznych, takich jak: transdukcji sygnału przez regulację aktywności białka STAT3, aktywność proapoptotyczną i odpowiedź błonową na  $1,25(\text{OH})_2\text{D}_3$ .

Aktywna forma witaminy D ( $1,25(\text{OH})_2\text{D}_3$ ) działa poprzez swój klasyczny receptor witaminy D (VDR) inicjując odpowiedź genomową, podczas której moduluje ekspresję ponad 3000 genów w ludzkim genomie. Jednakże, nie wszystkie efekty działania  $1,25(\text{OH})_2\text{D}_3$  można przypisać klasycznej ścieżce odpowiedzi na witaminę D, dlatego zasugerowano istnienie alternatywnych, poza genomowych szlaków witaminy D. W ostatnich latach białko PDIA3 zostało powiązane z szybkimi, niegenomowymi działaniami  $1,25(\text{OH})_2\text{D}_3$  jako jej receptor błonowy.

W poniższym cyklu publikacji zbadano rolę białka PDIA3 w alternatywnych szlakach aktywowanych przez witaminę D w modelu raka płaskonabłonkowego skóry. Stosując podejście oparte na zsekwencjonowaniu całego transkryptomu komórek A431 zidentyfikowano zmiany w ekspresji około 2000 genów po delecji genu *PDIA3*. Ponadto, komórki pozbawione *PDIA3* wykazały zmiany w proliferacji, migracji i cyklu komórkowym, co podkreśla ważną rolę regulacyjną białka PDIA3. Komórki *A431ΔPDIA3* wykazywały zwiększoną wrażliwość na działanie  $1,25(\text{OH})_2\text{D}_3$ . Co ciekawe, zaobserwowano, że ekspresja niektórych klasycznych genów zależnych od VDR, w tym *CAMP* (*Cathelicidin Antimicrobial Peptide*), *TRPV6* (*Transient Receptor Potential Cation Channel Subfamily V Member 6*), była regulowana w inny sposób przez  $1,25(\text{OH})_2\text{D}_3$  w komórkach *A431ΔPDIA3*. Grupa genów których ekspresja była zależnych od PDIA3 (*PTGS2*, *MMP12*, *FOCAD*) została zidentyfikowana na podstawie graficznej analizy Venna, ilustrującą logiczny związek pomiędzy genami ulegającymi ekspresji w komórkach *A431WT*, *A431ΔPDIA3* traktowanym  $1,25(\text{OH})_2\text{D}_3$  oraz nietraktowanymi komórkami *A431ΔPDIA3*. Dodatkowo, odpowiedź komórek nowotworowych A431 na traktowanie  $1,25(\text{OH})_2\text{D}_3$  różniła się od odpowiedzi unieśmiertelnionej linii keratynocytów HaCaT,

stosowanych jako kontrola nienowotworowa. Ponadto, delecja *PDIA3* wywoływała zmiany w morfologii i bioenergetyce mitochondriów. Parametry morfologiczne, takie jak obwód, pole przekroju mitochondriów i ich maksymalna średnica były znacząco zmniejszone w komórkach A431 $\Delta$ *PDIA3*, podczas gdy traktowanie 1,25(OH)<sub>2</sub>D<sub>3</sub> częściowo odwracało efekt delecji *PDIA3*. Co więcej, delecja *PDIA3* zmieniała bioenergetykę mitochondriów (fosforylację oksydacyjną i glikolizę) i modulowała sygnalizację STAT3. Szybkość zużycia tlenu (OCR) i szybkość zakwaszania zewnątrzkomórkowego (ECAR) były podwyższone w komórkach A431 $\Delta$ *PDIA3*, w porównaniu do komórek A431WT, bez znaczącego wpływu 1,25(OH)<sub>2</sub>D<sub>3</sub>. Następnie zbadana została odpowiedź błonową na 1,25(OH)<sub>2</sub>D<sub>3</sub> wraz z sygnalizacją wapniową w liniach komórkowych raka płaskonabłonkowego skóry z delecją lub bez delecji genów *VDR*, bądź *PDIA3*. Zarówno delecja *PDIA3* lub *VDR* powodowała obniżenie wyjściowego poziomu wapnia i odpowiedzi komórek na 1,25(OH)<sub>2</sub>D<sub>3</sub>, jednakże efekt był bardziej wyraźny w linii A431 $\Delta$ *PDIA3*. Knockout któregośkolwiek z tych genów zakłócał sygnalizację odbłonową indukowaną przez 1,25(OH)<sub>2</sub>D<sub>3</sub> w komórkach A431. Wyniki wskazują, że *VDR* jest niezbędny do aktywacji zależnej od wapnia/kalmoduliny kinazy białkowej II Alpha (*CAMK2A*), podczas gdy białko *PDIA3* jest wymagane do mobilizacji wapnia w komórkach A431 indukowanej 1,25(OH)<sub>2</sub>D<sub>3</sub>.

Podsumowując, białko *PDIA3* jest zaangażowany w odpowiedź genomową na 1,25(OH)<sub>2</sub>D<sub>3</sub>, poprzez modulowanie profilu ekspresji genów oraz szerokiego zakresu efektów fenotypowych, takich jak proliferacja i migracja komórek A431. *PDIA3* wpływa na morfologię i bioenergetykę mitochondriów, prawdopodobnie poprzez regulację sygnalizacji STAT3. Ponadto, wykazano istotną rolę białka *PDIA3* w odpowiedzi błonowej na 1,25(OH)<sub>2</sub>D<sub>3</sub>. Wydaje się jednak, że *VDR* jest również niezbędny do aktywacji nie genomowej odpowiedzi na 1,25(OH)<sub>2</sub>D<sub>3</sub>. Przedstawione w poniższej rozprawie wyniki podkreślają istotną rolę *PDIA3* w regulacji odpowiedzi na 1,25(OH)<sub>2</sub>D<sub>3</sub> i utrzymaniu prawidłowej fizjologii komórkowej. Ponadto *PDIA3* można uznać za marker predykcyjny, a także potencjalny cel terapii przeciwnowotworowej.

**Słowa kluczowe:** Witamina D, *VDR*, *PDIA3*, analiza transkryptomyczna, sygnalizacja Ca<sup>2+</sup>, bioenergetyka komórki, rak płaskonabłonkowy skóry

## V. INTRODUCTION

Protein Disulfide Isomerase Family Member A3 (PDIA3 also known as GRP58, 1,25-MARRS) belongs to the PDI family of oxidoreductase proteins which control protein disulfide bridges isomerization [1, 2]. PDIA3 is a resident chaperone protein within the endoplasmic reticulum, where it regulates the folding of other proteins and refolding of misfolded proteins [3]. Besides classical ER localization, PDIA3 may also be present in the nucleus, at the cell membrane, or in the mitochondria-associated membranes (MAM) region of ER [4-6]. Due to its varied location, PDIA3 affects a wide range of physiological processes including signal transduction through STAT3 protein in the nucleus [7], proapoptotic activities within mitochondria [4], and functioning as a membrane receptor for 1,25(OH)<sub>2</sub>D<sub>3</sub> at the cell membrane [8, 9]. PDIA3 can function as a chaperone protein for STAT3 and modulate its transcriptional activity by regulating its phosphorylation at Y705 [7, 10, 11]. It was suggested that the second phosphorylation site of STAT3 at S727 residue, targets mitochondrial import of this transcription factor and it could be suppressed by PDIA3 [12, 13]. In recent years, PDIA3 has been linked to various pathological processes such as cancer or neurodegenerative diseases. Dysregulation of PDIA3 expression in cancer patients correlates with poor prognosis [14, 15] and can serve as a prognostic marker and pharmacological target [11, 16, 17]. The importance of PDIA3 for maintaining normal physiology is further emphasized by the fact that its deletion in mice is lethal [18, 19], and even a single mutation within its sequence can lead to dysregulation of cell adhesion and cytoskeleton dynamics causing developmental defects [20].

Vitamin D is a powerful secosteroid hormone responsible for the regulation of calcium-phosphorus homeostasis [21]. Naturally, vitamin D is produced upon ultraviolet type B (UVB) radiation in basal layers of skin epidermis [22, 23]. For its activation into a fully functional hormone (1,25(OH)<sub>2</sub>D<sub>3</sub>), two subsequent hydroxylations are required [24, 25]. 1,25(OH)<sub>2</sub>D<sub>3</sub> was shown to have a broad range of effects on cellular processes. Classical genomic actions of 1,25(OH)<sub>2</sub>D<sub>3</sub> are mediated by vitamin D receptor (VDR), which binds its co-receptor Retinoid X Receptor (RXR), forming a powerful transcription factor. After binding to the ligand, the complex is translocated into the nucleus, where it modulates the expression of more than 3000 genes including genes involved in cell differentiation, proliferation, and migration [23, 26, 27]. Vitamin D has been proven to be essential for proper functioning of musculoskeletal, immune, and nervous systems [28-30]. Moreover,

1,25(OH)<sub>2</sub>D<sub>3</sub> is beneficial in the prevention and treatment of various diseases, including cancer [31-35], psoriasis [36], and preeclampsia [37].

Despite the well-established role of vitamin D in cellular physiology not all effects can be attributed to genomic activity of VDR. Thus, the existence of membrane-associated, rapid-response steroid-binding protein (1,25-MARRS) was suggested. The presence of such a pathway explained, for example, a rapid influx of calcium ions induced by 1,25(OH)<sub>2</sub>D<sub>3</sub> [38, 39]. In numerous studies, PDIA3 has been connected to those rapid, non-genomic activities of 1,25(OH)<sub>2</sub>D<sub>3</sub> as its membrane receptor [40-42]. After stimulation with 1,25(OH)<sub>2</sub>D<sub>3</sub>, PDIA3 was shown to interact with phospholipase A2 activating protein (PLAA), subsequently leading to the activation of phospholipase A2. As a result of this action, calcium is released to the cytoplasm, where it can activate protein kinase C (PKC) or calcium/calmodulin-dependent protein kinase II (CaMKII). Sequentially, downstream signaling pathways, such as mitogen-activated protein kinases (MAPK) and other transcription factors (STAT1-3, NF-κB) are activated. Importantly, PDIA3 was proven to be involved in a 1,25(OH)<sub>2</sub>D<sub>3</sub>-induced rapid calcium uptake within the intestine cells [19, 43]. Thus, PDIA3 is closely related to calcium homeostasis. All signaling pathways activated by vitamin D are shown in **Figure 1**.



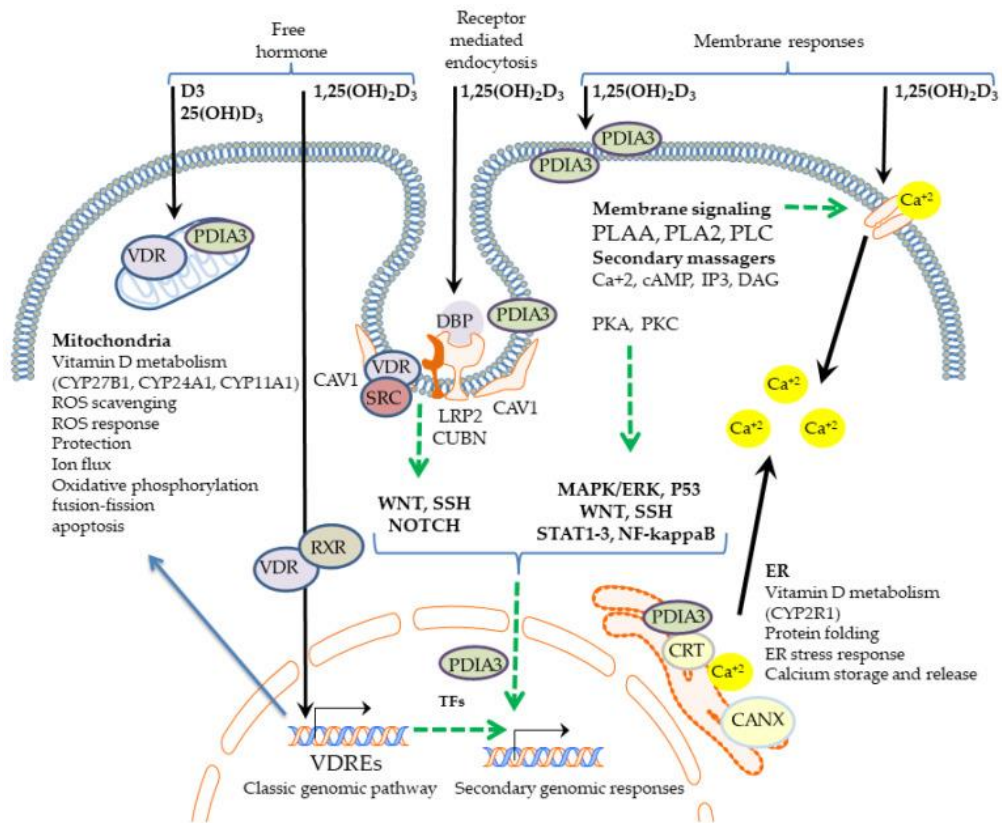


**Figure 1.** Signaling pathways activated by  $1,25(\text{OH})_2\text{D}_3$ .  $1,25(\text{OH})_2\text{D}_3$  can enter the cell through the cell membrane according to the free hormone hypothesis or might be imported by the megalin/cubulin complex through receptor-mediated endocytosis.  $1,25(\text{OH})_2\text{D}_3$  is bound by the complex of VDR/RXR heterodimer, which is translocated into the nucleus where it modulates the expression of VDR-target genes. PDIA3 mediates activation of  $1,25(\text{OH})_2\text{D}_3$ -dependent membrane signaling cascades including activation of PLAA, PLA2, PKC, and opening of calcium channels, followed by activation of downstream targets such as PKA, PKC, or CAMK2G. Those membrane activities of  $1,25(\text{OH})_2\text{D}_3$  were linked to the modulation of transcription factors NF- $\kappa$ B, STAT3, and p53, through both VDR and PDIA3[42].

## VI. AIMS

The involvement of PDIA3 in vitamin D signaling, although proven, still remains not fully understood. **The primary objective of this research project was to investigate the role of PDIA3 in vitamin D genomic and non-genomic activities using squamous cell carcinoma as a model.**

The project was part of NCN OPUS 13 grant “Alternative pathways of vitamin D” under contracts 2017/25/B/NZ3/00431, where I was employed as a Ph.D. student.

The goal of the first publication (Nowak JI, Olszewska AM, Piotrowska A, Myszczyński K, Domzalski P, Zmijewski MA. *PDIA3 modulates genomic response to 1,25-dihydroxyvitamin D<sub>3</sub> in squamous cell carcinoma of the skin*. *Steroids*. 2023;109288) was to investigate the effects of 1,25(OH)<sub>2</sub>D<sub>3</sub> on gene expression profile in squamous cell carcinoma A431 cell line, in the presence or absence of PDIA3. In addition, the impact of VDR and PDIA3 deletion on biological features, such as proliferation, migration, and cell cycle, after 1,25(OH)<sub>2</sub>D<sub>3</sub> treatment was assessed.

The second publication (Nowak JI, Olszewska AM, Król O, Żmijewski MA. *Protein Disulfide Isomerase Family A Member 3 Knockout Abrogate Effects of Vitamin D on Cellular Respiration and Glycolysis in Squamous Cell Carcinoma*. *Nutrients*. 2023;15(21):4529) was focused on the impact of PDIA3 on mitochondrial bioenergetics and morphology in squamous cell carcinoma and its potential involvement in vitamin D action within mitochondria.

The last publication (Nowak JI, Olszewska AM, Wierzbicka JM, Gebert M, Bartoszewski R, Zmijewski MA. *VDR and PDIA3 are essential for the activation of calcium signaling and membrane response to 1,25(OH)<sub>2</sub>D<sub>3</sub> in squamous cell carcinoma cells*. *Cells*. 2024; 13(1):11) investigated the topic of PDIA3 involvement in 1,25(OH)<sub>2</sub>D<sub>3</sub>-induced calcium signaling and membrane response to 1,25(OH)<sub>2</sub>D<sub>3</sub> in squamous cell carcinoma.

## VII. DISCUSSION OF PUBLICATIONS INCLUDED IN THE DOCTORAL DISSERTATION

To explore the topic of the role of PDIA3 in vitamin D activities in squamous cell carcinoma, the knockout of *PDIA3* was introduced to the A431 cell line using CRISPR/Cas9 technology. An analogous procedure was used to establish a stable cell line with impaired vitamin D receptor (VDR) expression, which was used as an additional control. The *PDIA3* or *VDR* knockout cells were obtained from Synthego corporation (Melano Park, CA, USA) as a mixture of several clones (pooled cells, separately for each knockout), thus clonal selection was performed, and the identity of selected clones verified by qPCR, western blot followed by Sanger sequencing. For further experiments, A431WT (wild type), A431 $\Delta$ VDR, and A431 $\Delta$ PDIA3 were used.

In the first publication of my PhD cycle, the effects of 1,25(OH)<sub>2</sub>D<sub>3</sub> on biological features and gene expression in squamous cell carcinoma (SCC) cells line A431, in the presence or absence of PDIA3 protein was investigated. To assess how *PDIA3* deletion affects the physiological activities of 1,25(OH)<sub>2</sub>D<sub>3</sub>, an analysis of proliferation, migration, and cell cycle was performed. An SRB assay showed that 1,25(OH)<sub>2</sub>D<sub>3</sub> inhibited the proliferation of about 18% of A431WT cells with half-maximum effective concentration (EC<sub>50</sub>) for 1,25(OH)<sub>2</sub>D<sub>3</sub> equaled 39,355nM. Knockout of either *VDR* or *PDIA3* in the A431 cell line impaired inhibition effectiveness of 1,25(OH)<sub>2</sub>D<sub>3</sub> to 10%. Interestingly, both deletions sensitized cells to 1,25(OH)<sub>2</sub>D<sub>3</sub> (EC<sub>50</sub>=1,346 nM and 0,019 nM respectively). In previous studies of our team, it was shown that in HaCaT cells 1,25(OH)<sub>2</sub>D<sub>3</sub>-treatment reduced the proliferation rate by around 20% with EC<sub>50</sub> = 0,089 nM [44]. It suggests that A431 cells are more resistant to 1,25(OH)<sub>2</sub>D<sub>3</sub> treatment than HaCaT cells. Moreover, to see how 1,25(OH)<sub>2</sub>D<sub>3</sub> affected the distribution of A431 cells through cell cycle phases was analyzed by flow cytometry. Prolongated treatment of cells for 72h, decreased the number of cells in the SubG1 and G1 phases of the cell cycle in all A431 sublines. Further, 1,25(OH)<sub>2</sub>D<sub>3</sub> triggered cell cycle arrest in the S phase with the most prominent effect in A431  $\Delta$ VDR cells. In general, prolonged incubation with 1,25(OH)<sub>2</sub>D<sub>3</sub> resulted in limited accumulation of cells in subG1 representing dying cells and the effect was more pronounced in  $\Delta$ PDIA3 cells. Additionally, the expression of genes associated with proliferation and cell cycle was assessed by qPCR. The expression of both cycle inhibitors, Cyclin-Dependent Kinase Inhibitor 2A (*CDKN2A*) and *Cyclin-Dependent Kinase Inhibitor 1A* (*CDKN1A*) was increased significantly upon treatment with 1,25(OH)<sub>2</sub>D<sub>3</sub> in A431 cells, while deletion of

either *VDR* or *PDIA3* abrogated effects of  $1,25(\text{OH})_2\text{D}_3$ . To compare motility and migration of A431 sublines wound closure assay was recorded live with Olympus CellVivo IX83 for 72h. In agreement with other studies [34],  $1,25(\text{OH})_2\text{D}_3$  treatment inhibited cell motility of A431WT cells, while *VDR* deletion abolished that effect, enhancing cell migration. That is supported by other studies, where *VDR* silencing reduced the responsiveness of melanoma cells to  $1,25(\text{OH})_2\text{D}_3$  treatment [45], and its deletion induced hyperproliferation of melanoma cells [46]. Surprisingly, *PDIA3* deletion alone greatly reduced the mobility of A431, which was further decreased after  $1,25(\text{OH})_2\text{D}_3$  treatment.

Previously, we have shown that *VDR* deletion completely abolished  $1,25(\text{OH})_2\text{D}_3$ -induced gene expression in A431 after 24h treatment [47]. To verify the effect of *PDIA3* on the gene expression profile of A431 cells, the whole transcriptome of non-treated A431-derived cell lines was sequenced. Unexpectedly, *PDIA3* deletion in A431 cells resulted in the appearance of 2184 differently expressed genes (DEGs). Gene ontology (GO) analysis revealed significant enrichment of DEGs associated with calcium-phosphorus signaling, phospholipase C activity, MHC class II receptor activity, and calcium-dependent phospholipid binding. That is in agreement with the results of Wang and coworkers, as they showed that *PDIA3* deletion impaired the process associated with calcium homeostasis [48]. Moreover, among DEGs affected by deletion of *PDIA3*, several classic targets of  $1,25(\text{OH})_2\text{D}_3$  transcriptional activity driven by *VDR*, including *Cytochrome P450 Family 24 Subfamily A Member 1 (CYP24A1)*, *Cathelicidin Antimicrobial Peptide (CAMP)* and *Transient Receptor Potential Cation Channel Subfamily V Member (TRPV6)* were observed. Interestingly, *PDIA3* deletion resulted in almost complete attenuation of *TRPV6* channel expression, which is strongly involved in maintaining calcium ion homeostasis [49]. Next, the effects of incubation of A431 cells lacking *PDIA3* with  $1,25(\text{OH})_2\text{D}_3$  for 24h were studied. The analysis revealed regulation of 704 DEGs, which were connected to the phosphorus metabolic process, MAPK cascade, positive regulation of apoptotic process, and calcium ion binding. To graphically presentation the logical relationship between DEGs expressed in A431WT, A431 $\Delta$ *PDIA3*  $1,25(\text{OH})_2\text{D}_3$  treated and A431 $\Delta$ *PDIA3* nontreated cells, and to identify *PDIA3*-dependent DEGs regulated by  $1,25(\text{OH})_2\text{D}_3$  Venn analysis was used (**Fig. 2**). Among  $1,25(\text{OH})_2\text{D}_3$ -dependent DEGs detected in both A431WT and A431 $\Delta$ *PDIA3*, 59 were solely found in A431 WT cells, which suggested that the regulation of those DEGs by  $1,25(\text{OH})_2\text{D}_3$  depends on *PDIA3* expression. On the other hand, 191 DEGs were unique for A431 $\Delta$ *PDIA3* cells, while 168 genes were commonly regulated by

1,25(OH)<sub>2</sub>D<sub>3</sub> in A431WT and A431Δ*PDIA3*, thus their expression was not affected by *PDIA3* presence. In A431Δ*PDIA3* nontreated, a group of 102 DEGs was identified as 1,25(OH)<sub>2</sub>D<sub>3</sub>-dependent and *PDIA3*-regulated, while 109 DEGs were affected by either *PDIA3* deletion and 1,25(OH)<sub>2</sub>D<sub>3</sub> in both cell lines. Finally, 58 DEGs, which were found in nontreated A431Δ*PDIA3* cells were modulated by 1,25(OH)<sub>2</sub>D<sub>3</sub>, but only in A431WT cells, suggesting that *PDIA3* presence is required for their regulation upon 1,25(OH)<sub>2</sub>D<sub>3</sub> treatment. Venn analysis of all 1,25(OH)<sub>2</sub>D<sub>3</sub> regulated DEGs allowed us to distinguish *PDIA3*-dependent (*PTGS2*, *MMP12*, *FOCAD*), and -independent (*NKAIN2*, *SERPINB7*, *ZNF185*) genes in A431 cells. Additionally, expression of those genes, together with classical vitamin D targets (*CYP24A1*, *CAMP*, and *TRPV6*), was evaluated by qPCR in HaCaT cell line, which served as noncancerous control, and A431 sublines. It was observed that squamous cell carcinoma cells were less responsive to 1,25(OH)<sub>2</sub>D<sub>3</sub> treatment than immortalized keratinocytes (HaCaT).

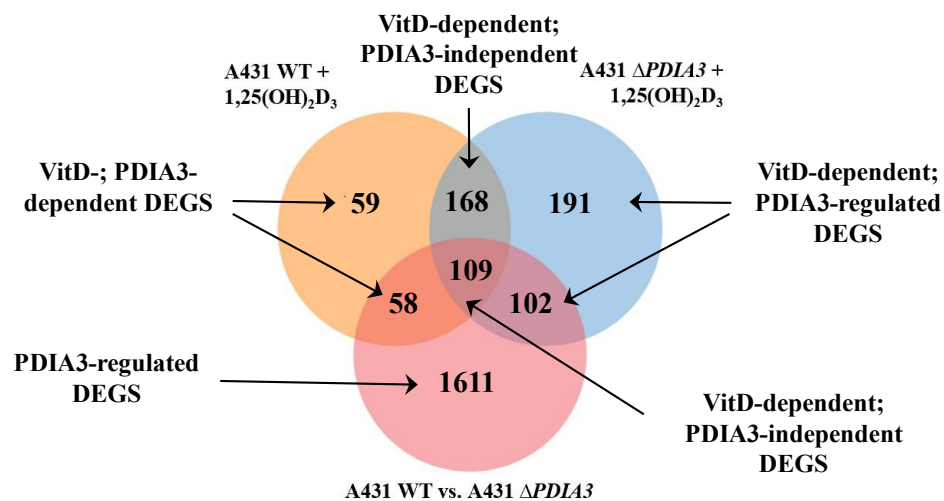


**Figure 2.** Venn diagram showing the distribution of DEGs between A431WT and A431Δ*PDIA3* cells treated with 1,25(OH)<sub>2</sub>D<sub>3</sub> and non-treated A431Δ*PDIA3*.

In summary, data presented in this publication demonstrated an impaired genomic response to 1,25(OH)<sub>2</sub>D<sub>3</sub> of cancer cells in comparison to HaCaT keratinocytes. Moreover, the deletion of *PDIA3* radically changed the response of A431 cells to 1,25(OH)<sub>2</sub>D<sub>3</sub> treatment, not only on the genomic response but sensitized cells to 1,25(OH)<sub>2</sub>D<sub>3</sub>, as shown within proliferation and migration assays. It could be postulated that *PDIA3* affects directly or indirectly several intracellular pathways essential for genomic and/or nongenomic activity of vitamin D, modulating cellular response to this powerful secosteroid. Furthermore,

PDIA3 could also be considered a target for anticancer therapy as well as a modulator of response to 1,25(OH)<sub>2</sub>D<sub>3</sub>.

As the involvement of PDIA3 in the modulation of cellular responses to 1,25(OH)<sub>2</sub>D<sub>3</sub> including gene expression and a range of phenotypic effects was established, in the second publication the impact of PDIA3 on mitochondrial morphology and bioenergetics in A431 SCC cells treated with 1,25(OH)<sub>2</sub>D<sub>3</sub> was investigated.

The microphotographs of mitochondria in A431WT and A431Δ*PDIA3* in 1,25(OH)<sub>2</sub>D<sub>3</sub> treated, or nontreated cells were taken using transmission electron microscopy (TEM), and parameters of mitochondrial morphology (section, diameter, and perimeter) were calculated with cellSens Olympus Software v.4.1. Live imaging of fluorescence probes, MitoGreen and JC-1, was used to observe changes in mitochondrial surface and membrane potential, respectively. Next, the effect of 1,25(OH)<sub>2</sub>D<sub>3</sub> treatment on mitochondrial bioenergetics in A431WT and A431Δ*PDIA3* was determined using the Seahorse XF24. An oxygen consumption rate (OCR) was monitored in real-time with the following addition of oligomycin, FCCP, rotenone, and antimycin, while the extracellular acidification rate (ECAR) was measured in real time by adding glucose to the culture medium. Further, to assess the impact of *PDIA3* deletion on the mitochondria-associated genes (mtDEGs), data from our transcriptomic study (Publication 1) were compared to publicly available data (MitoCarta 3.0) by using Venn analysis. Finally, as the interaction of PDIA3 with transcription factor STAT3 was described in the context of cellular respiration, it was checked whether 1,25(OH)<sub>2</sub>D<sub>3</sub> affects this signaling. To investigate the issue western blot and immunofluorescence staining were performed in A431 sublines.

*PDIA3* knockout decreased the volume, perimeter, and diameter of mitochondria. The 1,25(OH)<sub>2</sub>D<sub>3</sub> treatment of A431Δ*PDIA3* cells partially reversed the effect of *PDIA3* deletion by increasing the aforementioned parameters. Interestingly, a more potent effect of 1,25(OH)<sub>2</sub>D<sub>3</sub> treatment on mitochondria was observed in A431Δ*PDIA3* cells in comparison to A431WT. Surprisingly, no statistically significant changes in mitochondrial surface area, or mitochondrial membrane potential were observed after 1,25(OH)<sub>2</sub>D<sub>3</sub> treatment in A431 Δ*PDIA3*, even though in A431WT cells mitochondrial potential was significantly reduced [50], suggesting that the effect of 1,25(OH)<sub>2</sub>D<sub>3</sub> on membrane potential might be PDIA3-dependent. Deletion of *PDIA3* significantly increased both OCR and ECAR in the A431 squamous cell carcinoma line. All parameters of oxidative phosphorylation were increased

in A431 cells lacking *PDIA3*. Furthermore, *PDIA3* knockout abrogated the effect of 1,25(OH)<sub>2</sub>D<sub>3</sub> on those parameters. The presented data are in line with results published by Keasey et al., who showed that *PDIA3* inhibits respiratory function in endothelial cells and *C. elegans* [13]. In terms of glycolysis and other glycolytic parameters (reserve, capacity, and non-glycolytic acidification) 1,25(OH)<sub>2</sub>D<sub>3</sub> treatment resulted in a marginally statistically significant decrease. This is in agreement with other studies showing reduced glycolysis after vitamin D treatment in breast cancer cells [51, 52] and colorectal cancer [51, 52]. Although *PDIA3* deletion enhanced glycolysis, the effect of 1,25(OH)<sub>2</sub>D<sub>3</sub> treatment was not as pronounced as in A431WT cells. Next, Venn analysis revealed that among genes annotated in MitoCarta 3.0, 302 mtDEGs, identified in A431Δ*PDIA3*, were affected solely by *PDIA3* deletion, while 149 mtDEGs were changed by 1,25(OH)<sub>2</sub>D<sub>3</sub> treatment. Interestingly, 111 mtDEGs were commonly regulated after *PDIA3* deletion and 1,25(OH)<sub>2</sub>D<sub>3</sub> treatment. GO analysis in terms of molecular processes revealed that knockout of *PDIA3* in A431 cells mainly affected cellular respiration, aerobic electron transport chain, and mitochondrial ATP synthesis. Curiously, the 1,25(OH)<sub>2</sub>D<sub>3</sub> treatment of knockout cells entirely changed the expression of the genes linked to mitochondrial transcription/translation, such as mitochondrial translation, mitochondrial gene expression, and mitochondrial transport. However, we did not identify any *PDIA3*-dependent mtDEGs, which were also regulated by 1,25(OH)<sub>2</sub>D<sub>3</sub>. In other studies, *PDIA3* was localized within mitochondria [53] and co-localized with STAT3 [54], suggesting its role in STAT3 signaling. The most pronounced translocation of STAT3 into the nucleus was observed in A431WT cells after 8h 1,25(OH)<sub>2</sub>D<sub>3</sub> treatment. Deletion of the *VDR* decreased the basal signal, both nuclear and cytoplasm, resulting in a higher nucleus/cytoplasm ratio for STAT3, but the effect of 1,25(OH)<sub>2</sub>D<sub>3</sub> treatment was not observed. Interestingly, deletion of *PDIA3* did not change basal intensity for STAT3, and similarly to A431Δ*VDR* cells, there was no visible effect of 1,25(OH)<sub>2</sub>D<sub>3</sub> treatment. Next, the level of STAT3 as well as its phosphorylation at Tyr705 and Ser727 were analyzed. The total amount of STAT3 increased in time after 1,25(OH)<sub>2</sub>D<sub>3</sub> treatment, however either deletion (*VDR* or *PDIA3*) increased the initial level of STAT3. Interestingly, the STAT3 phosphorylation at the S727 site, which is linked to mitochondria, was strongly increased by both knockouts in A431 cells (A431Δ*VDR* and A431Δ*PDIA3*) and further amplified by treatment with 1,25(OH)<sub>2</sub>D<sub>3</sub> for 4 h. This observation is consistent with previous studies showing that *PDIA3* can inhibit STAT3 phosphorylation and thereby influence mitochondrial bioenergetics [13, 55].

Taken together, data presented in the second article indicate that PDIA3 is strongly engaged in the regulation of cellular respiration and glycolysis. The possible mechanism of its action is through the regulation of STAT3. Here, for the first time, it was shown that phosphorylation of STAT3 at Tyr705 and Ser727 can be induced by 1,25(OH)<sub>2</sub>D<sub>3</sub> and depends on the presence of both VDR and PDIA3. However, none PDIA3-dependent mtDEGs were identified, suggesting that the main effect of 1,25(OH)<sub>2</sub>D<sub>3</sub> on mitochondrial gene expression is mediated by VDR and partially RXR genomic actions [50]. Data presented in this publication strongly supports the importance of PDIA3 in cellular bioenergetics and cell physiology.

In the last publication, the topic of VDR and PDIA3 involvement in the activation of calcium signaling and membrane response to 1,25(OH)<sub>2</sub>D<sub>3</sub> was investigated.

Since transcriptome analysis revealed multiple changes in A431  $\Delta$ PDIA3 cells, obtained data were once more analyzed in the context of calcium-associated genes. Next, changes in intracellular calcium concentration were measured by two fluorescence probes (Fluo-4AM or Fura-2AM) by fluorescent measurement using live microscopy on Olympus Cell-Vivo IX 83 or plate reader, respectively. Moreover, the effects of VDR or PDIA3 deletion on the activity of calcium-associated nuclear factor of activated T-cells (NFAT) and vitamin D response elements (VDRE) were investigated by using dual-luciferase promoter assay. Next, to investigate the role of VDR and PDIA3 in calcium signaling as a part of membrane response to 1,25(OH)<sub>2</sub>D<sub>3</sub> western blot analysis of calcium signaling-related proteins, including PLAA, PLC $\gamma$ , PKC $\alpha$ , CAMK2 $\alpha$ , pCAMK2 $\alpha$  (T204), ERK1/2, and pERK1/2 (Thr202/tyr204) in A431 cell lines was performed.

Calcium acts as a second messenger molecule and is critical for proper cell physiology and signal transduction [56, 57]. Here, after deletion of either VDR or PDIA3, a decreased baseline level of calcium, with a less pronounced effect for A431 $\Delta$ VDR, was observed. That's in line with another study where PDIA3 deletion inhibited mitochondrial calcium uptake in HeLa cells, possibly through regulation of mitochondrial calcium uniporter (MCU) expression [58]. The addition of 100nM 1,25(OH)<sub>2</sub>D<sub>3</sub> elicited an influx of calcium ions in A431 cells, however, the increase in both knockout cell lines was significantly smaller. Lower and higher concentrations (10nM and 1 $\mu$ M) were tested with similar effects, suggesting that even low concentrations of 1,25(OH)<sub>2</sub>D<sub>3</sub> are sufficient for the activation of calcium influx within A431 cells. Interestingly, a calimycin-induced calcium



influx was also impaired by *VDR* or *PDIA3* deletion. In the transcriptomic study, it was observed that deletion of *PDIA3* can impact not only the calcium-associated genes but also a classic *VDR*-target gene like *TRPV6*- a well-known calcium channel, which is well known to be essential for vitamin D-induced active calcium transport in the intestine [59]. It was observed that  $1,25(\text{OH})_2\text{D}_3$  treatment increased levels of *TRPV6* in A431WT cells, but the effect was slightly reduced in A431 $\Delta$ *VDR* cells. Interestingly, *PDIA3* deletion abolished  $1,25(\text{OH})_2\text{D}_3$ -induced increase of *TRPV6* protein. Bianco *et al.*, have shown that deletion of *TRPV6* calcium channel resulted in no response to PTH or  $1,25(\text{OH})_2\text{D}_3$  treatment on mice model [60], thus decreased levels of *TRPV6* in A431 $\Delta$ *PDIA3* may explain the partial impairment of calcium influx observed with Fura-2AM probe. Next, changes in the activity of calcium-associated nuclear factor of activated T-cells (NFAT) and vitamin D responding element (VDRE) in the A431 sublines were investigated. The NFAT activity was increased by  $1,25(\text{OH})_2\text{D}_3$  treatment in A431WT cells 3 folds after 8h. Deletion of *VDR* didn't affect NFAT activity, while in A431 $\Delta$ *PDIA3* rapid increase of activity was observed after 4h with further decrease in time. VDRE served as additional control. The VDRE activity was highest in A431WT cells after 24h  $1,25(\text{OH})_2\text{D}_3$  treatment. In A431 $\Delta$ *VDR* no activation of VDRE was observed. On opposite *PDIA3* deletion slightly enhanced VDRE activation after 4 or 8h  $1,25(\text{OH})_2\text{D}_3$  treatment. Calcium is a known secondary messenger, which activates several downstream targets such as PKC or CAMKII. Thus, downstream targets of calcium signaling as a part of membrane response to  $1,25(\text{OH})_2\text{D}_3$  were investigated. Although we observed that the baseline total levels of PLAA, PLC $\gamma$ , and PKC $\alpha$  were increased by *PDIA3* deletion, the change in PLA2 and PKC $\alpha$  activity measured by ELISA assays after  $1,25(\text{OH})_2\text{D}_3$  stimulation was not observed in our cellular model, as suggested previously [61]. Further, the knockout of the *PDIA3* gene disrupted the response of Erk1/2 and its phosphorylation after  $1,25(\text{OH})_2\text{D}_3$  treatment. While *VDR* deletion decreased the expression of PKC $\alpha$  induced by  $1,25(\text{OH})_2\text{D}_3$ . *VDR* knockout also abolished the response of CAMKII $\alpha$  and its phosphorylation. Interestingly,  $1,25(\text{OH})_2\text{D}_3$  treatment induced a slight increase in *PDIA3* level after 24h incubation and *VDR* deletion enhanced this effect.

To sum up the last publication, this study showed a major role of *PDIA3* in membrane response to  $1,25(\text{OH})_2\text{D}_3$ . The results indicate that *PDIA3* is not solely responsible for the activation of nongenomic pathways of  $1,25(\text{OH})_2\text{D}_3$  in A431 squamous cell carcinoma, but *VDR* is also required, and possibly acts through CAMKII $\alpha$  activation, while *PDIA3* seems to play a major role in the regulation of calcium homeostasis with possibly through

involvement of epithelial channel TRPV6 and regulation of its stability. Moreover, it seems that both VDR and PDIA3 are required for the regulation of calcium influx induced by  $1,25(\text{OH})_2\text{D}_3$  in squamous cell carcinoma.

## VIII. CONCLUSIONS

PDIA3 is a protein involved in multiple physiological processes, such as mediation of protein folding, modulation of store-operated  $\text{Ca}^{2+}$  channels, cellular bioenergetics, and rapid response for  $1,25(\text{OH})_2\text{D}_3$ . In my PhD project, it was shown that PDIA3 can directly or indirectly modulate  $1,25(\text{OH})_2\text{D}_3$ -regulated gene expression in A431 squamous cell carcinoma. Moreover,  $1,25(\text{OH})_2\text{D}_3$  treatment partially reversed the expression of cancer-related genes. Thus, it seems that PDIA3 could be also considered as a target for anticancer therapy as well as a modulator of response to  $1,25(\text{OH})_2\text{D}_3$ . Further, PDIA3 possibly through STAT3 regulation affected mitochondria morphology and bioenergetics in A431 cells as well as mitochondrial response to  $1,25(\text{OH})_2\text{D}_3$ . PDIA3 together with VDR is required for regulation of calcium signaling induced by  $1,25(\text{OH})_2\text{D}_3$ . However, it seems that membrane response to  $1,25(\text{OH})_2\text{D}_3$  is regulated differently by PDIA3 and VDR, through CAMKII $\alpha$  and impairment of  $1,25(\text{OH})_2\text{D}_3$ -induced calcium mobilization respectively. Taken together, those results demonstrate the importance of PDIA3 in cellular physiology, and activities of  $1,25(\text{OH})_2\text{D}_3$ , as it directly or indirectly affects several intracellular pathways. The proposed role of PDIA3 and VDR in the regulation of intracellular response to  $1,25(\text{OH})_2\text{D}_3$  were summarized in **Figure 3**.

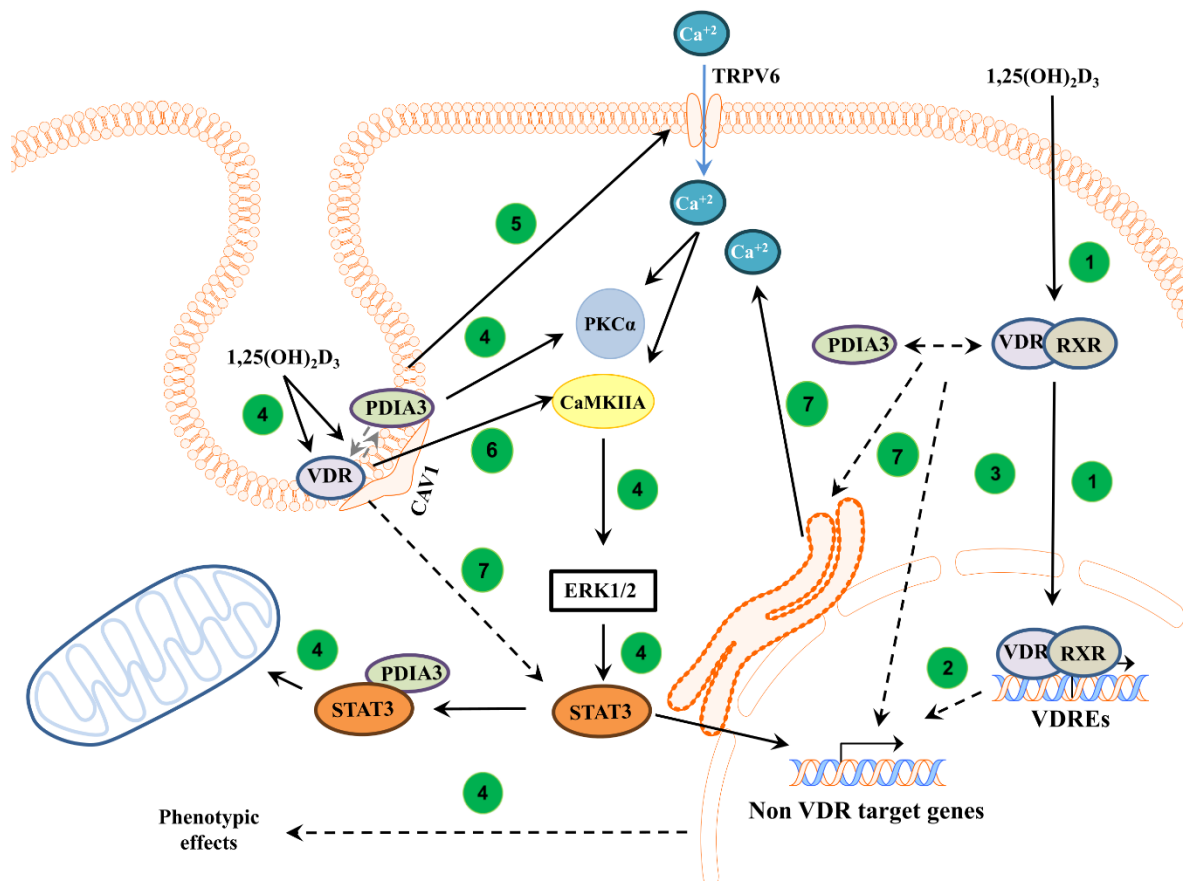


**Figure 3.** Proposed mechanism of action of VDR and PDIA3 to 1,25(OH)<sub>2</sub>D<sub>3</sub> membrane response in squamous cell carcinoma. In classical pathway 1,25(OH)<sub>2</sub>D<sub>3</sub> is bound by a heterodimer of VDR/RXR proteins and subsequently, complex is translocated into the nucleus where it regulates transcription of vitamin D target genes (1) [26]. Further, primary VDR target transcription factors can regulate secondary non-vitamin D target genes (2) [62]. It was also postulated that PDIA3 can modulate genomic response to 1,25(OH)<sub>2</sub>D<sub>3</sub> (3)[63]. In non-genomic pathways, VDR and PDIA3 were shown to interact with caveolin-1 [64]. PDIA3 was shown to be essential to activate PKC after 1,25(OH)<sub>2</sub>D<sub>3</sub> treatment [48] (4). Moreover, PDIA3 affects TRPV6 levels within SCC cells, possibly disrupting calcium response (5). Either PDIA3 or VDR is needed to activate STAT3, possibly regulating mitochondrial bioenergetics and non-VDR target genes (4) [63, 65]. Interestingly, it seems that VDR is required to activate CAMK2IIA kinase (6), while either protein is essential for valid calcium signaling (7).

## IX. LIST OF REFERENCES

1. Powell, L.E. and P.A. Foster, *Protein disulphide isomerase inhibition as a potential cancer therapeutic strategy*. *Cancer Med*, 2021. **10**(8): p. 2812-2825.
2. Appenzeller-Herzog, C. and L. Ellgaard, *The human PDI family: versatility packed into a single fold*. *Biochim Biophys Acta*, 2008. **1783**(4): p. 535-48.
3. Hettinghouse, A., R. Liu, and C.J. Liu, *Multifunctional molecule ERp57: From cancer to neurodegenerative diseases*. *Pharmacol Ther*, 2018. **181**: p. 34-48.
4. Zhao, G., H. Lu, and C. Li, *Proapoptotic activities of protein disulfide isomerase (PDI) and PDIA3 protein, a role of the Bcl-2 protein Bak*. *J Biol Chem*, 2015. **290**(14): p. 8949-63.
5. Grindel, B.J., et al., *Tumor necrosis factor- $\alpha$  treatment of HepG2 cells mobilizes a cytoplasmic pool of ERp57/1,25D<sub>3</sub>-MARRS to the nucleus*. *J Cell Biochem*, 2011. **112**(9): p. 2606-15.
6. Wu, W., et al., *Nuclear translocation of the 1,25D<sub>3</sub>-MARRS (membrane associated rapid response to steroids) receptor protein and NFkappaB in differentiating NB4 leukemia cells*. *Exp Cell Res*, 2010. **316**(7): p. 1101-8.
7. Chichiarelli, S., et al., *Role of ERp57 in the signaling and transcriptional activity of STAT3 in a melanoma cell line*. *Arch Biochem Biophys*, 2010. **494**(2): p. 178-83.
8. Gaucci, E., et al., *Analysis of the interaction of calcitriol with the disulfide isomerase ERp57*. *Sci Rep*, 2016. **6**: p. 37957.
9. Khanal, R. and I. Nemere, *Membrane receptors for vitamin D metabolites*. *Crit Rev Eukaryot Gene Expr*, 2007. **17**(1): p. 31-47.
10. Eufemi, M., et al., *ERp57 is present in STAT3-DNA complexes*. *Biochem Biophys Res Commun*, 2004. **323**(4): p. 1306-12.
11. Choe, M.H., et al., *ERp57 modulates STAT3 activity in radioresistant laryngeal cancer cells and serves as a prognostic marker for laryngeal cancer*. *Oncotarget*, 2015. **6**(5): p. 2654-66.
12. Tammineni, P., et al., *The import of the transcription factor STAT3 into mitochondria depends on GRIM-19, a component of the electron transport chain*. *J Biol Chem*, 2013. **288**(7): p. 4723-32.
13. Keasey, M.P., et al., *PDIA3 inhibits mitochondrial respiratory function in brain endothelial cells and C. elegans through STAT3 signaling and decreases survival after OGD*. *Cell Commun Signal*, 2021. **19**(1): p. 119.
14. Ramos, F.S., et al., *PDIA3 and PDIA6 gene expression as an aggressiveness marker in primary ductal breast cancer*. *Genet Mol Res*, 2015. **14**(2): p. 6960-7.
15. Takata, H., et al., *Increased expression of PDIA3 and its association with cancer cell proliferation and poor prognosis in hepatocellular carcinoma*. *Oncol Lett*, 2016. **12**(6): p. 4896-4904.
16. Wang, K., et al., *Combination of CALR and PDIA3 is a potential prognostic biomarker for non-small cell lung cancer*. *Oncotarget*, 2017. **8**(57): p. 96945-96957.
17. Pressinotti, N.C., et al., *Differential expression of apoptotic genes PDIA3 and MAP3K5 distinguishes between low- and high-risk prostate cancer*. *Mol Cancer*, 2009. **8**: p. 130.
18. Garbi, N., et al., *Impaired assembly of the major histocompatibility complex class I peptide-loading complex in mice deficient in the oxidoreductase ERp57*. *Nat Immunol*, 2006. **7**(1): p. 93-102.
19. Nemere, I., et al., *Intestinal cell calcium uptake and the targeted knockout of the 1,25D<sub>3</sub>-MARRS (membrane-associated, rapid response steroid-binding) receptor/PDIA3/Erp57*. *J Biol Chem*, 2010. **285**(41): p. 31859-66.
20. Bilches Medinas, D., et al., *Mutation in protein disulfide isomerase A3 causes neurodevelopmental defects by disturbing endoplasmic reticulum proteostasis*. *Embo j*, 2022. **41**(2): p. e105531.

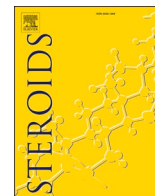
21. Khammissa, R.A.G., et al., *The Biological Activities of Vitamin D and Its Receptor in Relation to Calcium and Bone Homeostasis, Cancer, Immune and Cardiovascular Systems, Skin Biology, and Oral Health*. Biomed Res Int, 2018. **2018**: p. 9276380.
22. Wacker, M. and M.F. Holick, *Sunlight and Vitamin D: A global perspective for health*. Dermatoendocrinol, 2013. **5**(1): p. 51-108.
23. Piotrowska, A., J. Wierzbicka, and M.A. Żmijewski, *Vitamin D in the skin physiology and pathology*. Acta Biochim Pol, 2016. **63**(1): p. 17-29.
24. Kato, S., *The function of vitamin D receptor in vitamin D action*. J Biochem, 2000. **127**(5): p. 717-22.
25. Żmijewski, M.A. and C. Carlberg, *Vitamin D receptor(s): In the nucleus but also at membranes?* Exp Dermatol, 2020. **29**(9): p. 876-884.
26. Haussler, M.R., et al., *Vitamin D receptor (VDR)-mediated actions of 1  $\alpha$ ,25(OH)<sub>2</sub>vitamin D<sub>3</sub>: genomic and non-genomic mechanisms*. Best Pract Res Clin Endocrinol Metab, 2011. **25**(4): p. 543-59.
27. Slominski, A.T., et al., *Differential and Overlapping Effects of 20,23(OH)<sub>2</sub>D<sub>3</sub> and 1,25(OH)<sub>2</sub>D<sub>3</sub> on Gene Expression in Human Epidermal Keratinocytes: Identification of AhR as an Alternative Receptor for 20,23(OH)<sub>2</sub>D<sub>3</sub>*. Int J Mol Sci, 2018. **19**(10).
28. Xue, Y. and J.C. Fleet, *Intestinal vitamin D receptor is required for normal calcium and bone metabolism in mice*. Gastroenterology, 2009. **136**(4): p. 1317-27, e1-2.
29. Motiwala, S.R. and T.J. Wang, *Vitamin D and cardiovascular risk*. Curr Hypertens Rep, 2012. **14**(3): p. 209-18.
30. Trochoutsou, A.I., et al., *Vitamin-D in the Immune System: Genomic and Non-Genomic Actions*. Mini Rev Med Chem, 2015. **15**(11): p. 953-63.
31. Sutedja, E.K., et al., *Calcitriol Inhibits Proliferation and Potentially Induces Apoptosis in B16-F10 Cells*. Med Sci Monit Basic Res, 2022. **28**: p. e935139.
32. Slominski, A.T., et al., *On the role of classical and novel forms of vitamin D in melanoma progression and management*. J Steroid Biochem Mol Biol, 2018. **177**: p. 159-170.
33. Jin, T., et al., *Vitamin D inhibits the proliferation of Oral Squamous Cell Carcinoma by suppressing lncRNA LUCAT1 through the MAPK pathway*. J Cancer, 2020. **11**(20): p. 5971-5981.
34. Piotrowska, A., et al., *Vitamin D Enhances Anticancer Properties of Cediranib, a VEGFR Inhibitor, by Modulation of VEGFR2 Expression in Melanoma Cells*. Front Oncol, 2021. **11**: p. 763895.
35. Piotrowska, A., et al., *Vitamin D Modulates the Response of Patient-Derived Metastatic Melanoma Cells to Anticancer Drugs*. Int J Mol Sci, 2023. **24**(9).
36. Finamor, D.C., et al., *A pilot study assessing the effect of prolonged administration of high daily doses of vitamin D on the clinical course of vitiligo and psoriasis*. Dermatoendocrinol, 2013. **5**(1): p. 222-34.
37. Zabul, P., et al., *A Proposed Molecular Mechanism of High-Dose Vitamin D<sub>3</sub> Supplementation in Prevention and Treatment of Preeclampsia*. Int J Mol Sci, 2015. **16**(6): p. 13043-64.
38. Civitelli, R., et al., *Nongenomic activation of the calcium message system by vitamin D metabolites in osteoblast-like cells*. Endocrinology, 1990. **127**(5): p. 2253-62.
39. Sterling, T.M. and I. Nemere, *1,25-dihydroxyvitamin D<sub>3</sub> stimulates vesicular transport within 5 s in polarized intestinal epithelial cells*. J Endocrinol, 2005. **185**(1): p. 81-91.
40. Nemere, I., et al., *Identification and characterization of 1,25D<sub>3</sub>-membrane-associated rapid response, steroid (1,25D<sub>3</sub>-MARRS) binding protein*. J Steroid Biochem Mol Biol, 2004. **89-90**(1-5): p. 281-5.

41. Richard, C.L., et al., *Involvement of 1,25D3-MARRS (membrane associated, rapid response steroid-binding), a novel vitamin D receptor, in growth inhibition of breast cancer cells.* Exp Cell Res, 2010. **316**(5): p. 695-703.
42. Żmijewski, M.A., *Nongenomic Activities of Vitamin D.* Nutrients, 2022. **14**(23).
43. Nemere, I., et al., *Ribozyme knockdown functionally links a 1,25(OH)2D3 membrane binding protein (1,25D3-MARRS) and phosphate uptake in intestinal cells.* Proc Natl Acad Sci U S A, 2004. **101**(19): p. 7392-7.
44. Piotrowska, A., et al., *Vitamin D derivatives enhance cytotoxic effects of H2O2 or cisplatin on human keratinocytes.* Steroids, 2016. **110**: p. 49-61.
45. Wasiewicz, T., et al., *Antiproliferative Activity of Non-Calcemic Vitamin D Analogs on Human Melanoma Lines in Relation to VDR and PDIA3 Receptors.* Int J Mol Sci, 2018. **19**(9).
46. Hu, L., D.D. Bikle, and Y. Oda, *Reciprocal role of vitamin D receptor on  $\beta$ -catenin regulated keratinocyte proliferation and differentiation.* J Steroid Biochem Mol Biol, 2014. **144 Pt A**: p. 237-41.
47. A.M, O., et al., *Dissection of an Impact of VDR and RXRa on Genomic Activity of 1,25(OH)2D3 in A431 Squamous Cell Carcinoma.* 2023: SSRN.
48. Wang, Y., et al., *Disruption of Pdia3 gene results in bone abnormality and affects 1 $\alpha$ ,25-dihydroxy-vitamin D3-induced rapid activation of PKC.* J Steroid Biochem Mol Biol, 2010. **121**(1-2): p. 257-60.
49. den Dekker, E., et al., *The epithelial calcium channels, TRPV5 & TRPV6: from identification towards regulation.* Cell Calcium, 2003. **33**(5-6): p. 497-507.
50. Olszewska, A.M., et al., *Different impact of vitamin D on mitochondrial activity and morphology in normal and malignant keratinocytes, the role of genomic pathway.* Free Radic Biol Med, 2023. **210**: p. 286-303.
51. Santos, J.M., et al., *Vitamin D(3) decreases glycolysis and invasiveness, and increases cellular stiffness in breast cancer cells.* J Nutr Biochem, 2018. **53**: p. 111-120.
52. Zuo, S., et al., *Long Non-coding RNA MEG3 Activated by Vitamin D Suppresses Glycolysis in Colorectal Cancer via Promoting c-Myc Degradation.* Front Oncol, 2020. **10**: p. 274.
53. Ozaki, T., T. Yamashita, and S. Ishiguro, *ERp57-associated mitochondrial  $\mu$ -calpain truncates apoptosis-inducing factor.* Biochim Biophys Acta, 2008. **1783**(10): p. 1955-63.
54. Kondo, R., et al., *Downregulation of protein disulfide-isomerase A3 expression inhibits cell proliferation and induces apoptosis through STAT3 signaling in hepatocellular carcinoma.* Int J Oncol, 2019. **54**(4): p. 1409-1421.
55. Peron, M., et al., *Y705 and S727 are required for the mitochondrial import and transcriptional activities of STAT3, and for regulation of stem cell proliferation.* Development, 2021. **148**(17).
56. Sukumaran, P., et al., *Calcium Signaling Regulates Autophagy and Apoptosis.* Cells, 2021. **10**(8).
57. Patergnani, S., et al., *Various Aspects of Calcium Signaling in the Regulation of Apoptosis, Autophagy, Cell Proliferation, and Cancer.* Int J Mol Sci, 2020. **21**(21).
58. He, J., et al., *ERp57 modulates mitochondrial calcium uptake through the MCU.* FEBS Lett, 2014. **588**(12): p. 2087-94.
59. Benn, B.S., et al., *Active intestinal calcium transport in the absence of transient receptor potential vanilloid type 6 and calbindin-D9k.* Endocrinology, 2008. **149**(6): p. 3196-205.
60. Bianco, S.D., et al., *Marked disturbance of calcium homeostasis in mice with targeted disruption of the Trpv6 calcium channel gene.* J Bone Miner Res, 2007. **22**(2): p. 274-85.
61. Nemere, I., et al., *Identification of a membrane receptor for 1,25-dihydroxyvitamin D3 which mediates rapid activation of protein kinase C.* J Bone Miner Res, 1998. **13**(9): p. 1353-9.

62. Warwick, T., et al., *A hierarchical regulatory network analysis of the vitamin D induced transcriptome reveals novel regulators and complete VDR dependency in monocytes*. *Sci Rep*, 2021. **11**(1): p. 6518.
63. Nowak, J.I., et al., *PDIA3 modulates genomic response to 1,25-dihydroxyvitamin D(3) in squamous cell carcinoma of the skin*. *Steroids*, 2023. **199**: p. 109288.
64. Chen, J., et al., *Plasma membrane Pdia3 and VDR interact to elicit rapid responses to 1 $\alpha$ ,25(OH)(2)D(3)*. *Cell Signal*, 2013. **25**(12): p. 2362-73.
65. Nowak, J.I., et al., *Protein Disulfide Isomerase Family A Member 3 Knockout Abrogate Effects of Vitamin D on Cellular Respiration and Glycolysis in Squamous Cell Carcinoma*. *Nutrients*, 2023. **15**(21): p. 4529.



## **X. PUBLICATIONS**



## PDIA3 modulates genomic response to 1,25-dihydroxyvitamin D<sub>3</sub> in squamous cell carcinoma of the skin

Joanna I. Nowak<sup>a</sup>, Anna M. Olszewska<sup>a</sup>, Anna Piotrowska<sup>a</sup>, Kamil Myszczyński<sup>b</sup>, Paweł Domżański<sup>a</sup>, Michał A. Żmijewski<sup>a,\*</sup>

<sup>a</sup> Department of Histology, Medical University of Gdansk, 1a Dębinki, 80-211 Gdansk, Poland

<sup>b</sup> Centre of Biostatistics and Bioinformatics Analysis Medical University of Gdansk, 1a Debinki, 80-211 Gdansk, Poland

### ARTICLE INFO

#### Keywords:

PDIA3  
1,25-dihydroxyvitamin D<sub>3</sub>  
Squamous cell carcinoma  
Transcriptome

### ABSTRACT

An active form of vitamin D<sub>3</sub> (1,25-dihydroxyvitamin D<sub>3</sub>) acts through vitamin D receptor (VDR) initiating genomic response, but several studies described also non-genomic actions of 1,25-dihydroxyvitamin D<sub>3</sub>, implying the role of PDIA3 in the process. PDIA3 is a membrane-associated disulfide isomerase involved in disulfide bond formation, protein folding, and remodeling. Here, we used a transcriptome-based approach to identify changes in expression profiles in *PDIA3*-deficient squamous cell carcinoma line A431 after 1,25-dihydroxyvitamin D<sub>3</sub> treatment. *PDIA3* knockout led to changes in the expression of more than 2000 genes and modulated proliferation, cell cycle, and mobility of cells; suggesting an important regulatory role of PDIA3. *PDIA3*-deficient cells showed increased sensitivity to 1,25-dihydroxyvitamin D<sub>3</sub>, which led to decrease migration. 1,25-dihydroxyvitamin D<sub>3</sub> treatment altered also genes expression profile of A431Δ*PDIA3* in comparison to A431WT cells, indicating the existence of PDIA3-dependent genes. Interestingly, classic targets of VDR, including *CAMP* (Cathelicidin Antimicrobial Peptide), *TRPV6* (Transient Receptor Potential Cation Channel Subfamily V Member 6), were regulated differently by 1,25-dihydroxyvitamin D<sub>3</sub> in A431Δ*PDIA3*. Deletion of *PDIA3* impaired 1,25-dihydroxyvitamin D<sub>3</sub>-response of genes, such as *PTGS2*, *MMP12*, and *FOCAD*, which were identified as PDIA3-dependent. Additionally, response to 1,25-dihydroxyvitamin D<sub>3</sub> in cancerous A431 cells differed from immortalized HaCaT keratinocytes, used as non-cancerous control. Finally, silencing of *PDIA3* and 1,25-dihydroxyvitamin D<sub>3</sub>, at least partially reverse the expression of cancer-related genes in A431 cells, thus targeting *PDIA3* and use of 1,25-dihydroxyvitamin D<sub>3</sub> could be considered in a prevention and therapy of the skin cancer. Taken together, PDIA3 has a strong impact on gene expression and physiology, including genomic response to 1,25-dihydroxyvitamin D<sub>3</sub>.

**Abbreviations:** 1,25-MARRS, Membrane-associated, rapid response steroid-binding; ADAMTS, A disintegrin and metalloproteinase with thrombospondin motifs; ARK1, Aldo-Keto Reductase Family 1 Member; CAMKIIA, Calcium/Calmodulin Dependent Protein Kinase II Alpha; CAMP, Cathelicidin Antimicrobial Peptide; CDKN1A, Cyclin Dependent Kinase Inhibitor 1A; CDKN2A, Cyclin Dependent Kinase Inhibitor 2A; CORO1B, Coronin 1B; Cyp24A1, Cytochrome P450 Family 24 Subfamily A Member 1; DEG, Differentially expressed genes; EPSTI1, Epithelial Stromal Interaction 1; ERp57, Endoplasmic Reticulum Resident Protein 57; FOCAD, Focadhesin; FOXP1, Forkhead Box P1; GRP58, Glucose Regulated Protein, 58kDa; GSEA, Gene set enrichment analysis; HaCaT, Immortalized human keratinocyte cell line; HNSCC, Head and neck squamous cell carcinoma; ICAM1, Intercellular Adhesion Molecule 1; IFI44L, Interferon Induced Protein 44 Like; JUNB, JunB Proto-Oncogene, AP-1 Transcription Factor Subunit; MAF, MAF BZIP Transcription Factor; MAPK, Mitogen-Activated Protein Kinase; MKI67, Marker Of Proliferation Ki-67; MMP12, Matrix Metalloproteinase 12; NKAIN2, Sodium/Potassium Transporting ATPase Interacting 2; OSR2, Odd-Skipped Related Transcription Factor 2; PDIA3, Protein Disulfide Isomerase Family A Member 3; PERK, Protein Kinase RNA-Like ER Kinase; PKC, Protein Kinase C; PLA2, Phospholipase A2; PLAA, Phospholipase A2 Activating Protein; PLG, Plasminogen; PPI, Protein-protein interaction; PTGS2, Prostaglandin-Endoperoxide Synthase 2; RUNX2, RUNX Family Transcription Factor 2; RXRA, Retinoid X Receptor Alpha; SCC, Squamous Cell Carcinoma; SEMA3E, Semaphorin 3E; SERPINB7, Serpin Family B Member 7; TRPV6, Transient Receptor Potential Cation Channel Subfamily V Member 6; VDR, Vitamin D Receptor; VIM, Vimentin; ZNF185, Zinc Finger Protein 185 With LIM Domain.

\* Corresponding author.

E-mail addresses: [j.chorzepa@gumed.edu.pl](mailto:j.chorzepa@gumed.edu.pl) (J.I. Nowak), [anna.olszewska@gumed.edu.pl](mailto:anna.olszewska@gumed.edu.pl) (A.M. Olszewska), [annapiotrowska@gumed.edu.pl](mailto:annapiotrowska@gumed.edu.pl) (A. Piotrowska), [kamil.myszczyński@gumed.edu.pl](mailto:kamil.myszczyński@gumed.edu.pl) (K. Myszczyński), [pawel.domzalski@gumed.edu.pl](mailto:pawel.domzalski@gumed.edu.pl) (P. Domżański), [mzmijewski@gumed.edu.pl](mailto:mzmijewski@gumed.edu.pl) (M.A. Żmijewski).

<https://doi.org/10.1016/j.steroids.2023.109288>

Received 22 June 2023; Received in revised form 28 July 2023; Accepted 2 August 2023

Available online 5 August 2023

0039-128X/© 2023 The Author(s). Published by Elsevier Inc. This is an open access article under the CC BY license (<http://creativecommons.org/licenses/by/4.0/>).

## 1. Introduction

Protein Disulfide Isomerase Family A Member 3 (PDIA3), also known as ERp57 or GRP58, belongs to the oxidoreductase enzyme family (PDIs), which have thioredoxin-like (TRX-like) domains containing active sites [1]. PDIA3, among other proteins from the PDIs family, is involved in multiple processes, including: protein folding, disulfide bond formation, and remodeling [2]. PDIA3 is mainly localized in the endoplasmic reticulum (ER), but may also be found in different locations such as the nucleus or cell membrane [3]. PDIA3 has binding sites for other ER chaperones like calreticulin and calnexin to form complexes that are necessary for its catalytic redox activity [4]. Moreover, it plays a role in the activation of PERK in response to misfolded protein, leading to unfolded protein response [5]. PDIA3 was also identified as an alternative membrane-associated receptor for 1,25-dihydroxyvitamin D<sub>3</sub> (and named membrane-associated, rapid response steroid-binding protein – 1,25D3-MARRS) [6]. PDIA3 can form a complex with caveolin-1, activating downstream mediators like phospholipase A2-activating protein (PLAA). PDIA3/PLAA complex acts on phospholipase A2 (PLA2) together with Ca<sup>2+</sup>/calmodulin-dependent protein kinase II (CaMKII), leading to the activation of protein kinase C (PKC). CaMKII $\alpha$  is required not only for mediating the rapid actions of 1 $\alpha$ ,25(OH)<sub>2</sub>D<sub>3</sub> from PLAA to PLA2 but also for mediating the Ca<sup>2+</sup>-dependent actions [7,8].

In recent years the involvement of PDIA3 protein in many pathological processes such as neurodegenerative diseases [9,10], cardiac diseases, and cancer [11,12] has been shown. PDIA3 is known to be dysregulated in various types of cancer and its expression levels can serve as a prognostic marker. Depending on the affected tissue either high or low expression levels can correlate with poor prognosis. The knockout of *PDIA3* in mice is lethal, which emphasizes the importance of PDIA3 protein in cell functioning [13,14]. Knockdown or over-expression of *PDIA3* has a broad range of physiological effects such as apoptosis, proliferation, and motility [15–17].

Vitamin D directly or indirectly modulates the expression of around 3000 genes in the human genome including genes involved in cell differentiation, proliferation, and migration [18,19]. A broad range of studies has shown the anticancer effects of an active form of vitamin D in various types of cancers e.g. head and neck skin carcinoma, melanoma, or breast cancer [20–22]. Genomic activity of 1,25-dihydroxyvitamin D<sub>3</sub> is mediated through its nuclear receptor VDR (Vitamin D receptor), but numerous studies also describe the rapid, non-genomic activities, which involves PDIA3 protein as a membrane receptor for 1,25-dihydroxyvitamin D<sub>3</sub> [14,23,24].

In this study, the effects of 1,25-dihydroxyvitamin D<sub>3</sub> on biological features and gene expression in squamous cell carcinoma (SCC) cells line A431, in the presence or absence of PDIA3 protein was investigated. Bioinformatics was applied in order to compare transcriptomic profiles of A431 cell lines of immortalized human keratinocyte cell line (HaCaT) and head and neck squamous cell carcinoma (HNSCC) gene expression pattern available in a public database (TACCO) [25,26].

## 2. Results

### 2.1. Deletion of *PDIA3* in A431 cells affects response to 1,25-dihydroxyvitamin D<sub>3</sub> treatment

It is well established that deletion of *PDIA3* is lethal in mice, however, we were able to establish human knockout of *PDIA3* in human squamous cell carcinoma cell line A431 (A431 $\Delta$ *PDIA3*) using gene editing technology (CRISPR/Cas9). An analogous procedure was used to establish a stable cell line with impaired vitamin D receptor (*VDR*) expression (A431 $\Delta$ *VDR*, [27]), which was used as an additional control. In order to investigate the impact of *PDIA3* knockout on proliferation of A431 cells treated with an active form of vitamin D<sub>3</sub>, an SRB assay was performed. 1,25-dihydroxyvitamin D<sub>3</sub> at 100 nM concentration inhibited proliferation of A431 WT cells maximally about 18% with half

maximal effective concentration EC<sub>50</sub> = 39,355 nM after 24 h of incubation (Fig. 1A). For both A431 knockouts A431  $\Delta$ *VDR*, and A431  $\Delta$ *PDIA3*, only 10% of inhibition was observed. However, deletions of *VDR* or *PDIA3* sensitized cells to 1,25-dihydroxyvitamin D<sub>3</sub>, as judged from the decrease in EC<sub>50</sub> values (1,346 and 0,019 nM, respectively) (Fig. 1B, C). Interestingly, under given conditions prolonged incubation (72 h) effect of 100 nM 1,25-dihydroxyvitamin D<sub>3</sub> on proliferation was diminished (not shown). In previous studies, it was shown that in HaCaT cells 1,25-dihydroxyvitamin D<sub>3</sub> treatment reduced proliferation rate around 20% with EC<sub>50</sub> = 0,089 nM [28]. It was suggested that A431 cells are more resistant to 1,25-dihydroxyvitamin D<sub>3</sub> treatment. It was shown that 1,25-dihydroxyvitamin D<sub>3</sub> affected the distribution of A431 cells in different phases of the cell cycle, however, the effects were not statistically significant after incubation for only 24 h (Fig. 1D). Prolonged treatment of A431 cells for 72 h, significantly decreased the number of cells in the SubG1 and G1 phases of the cell cycle, regardless presence or absence of deletion of *VDR* or *PDIA3* gene. Moreover, 1,25-dihydroxyvitamin D<sub>3</sub> triggered cell cycle arrest in the S phase, and the result was the most prominent in A431  $\Delta$ *VDR* cells (Fig. 1E). In general, prolonged incubation with 1,25-dihydroxyvitamin D<sub>3</sub> resulted in limited accumulation of cells in subG1 representing dying cells and the effect was more pronounced in  $\Delta$ *PDIA3* cells (Fig. 1F). Next, to assess the impact of *PDIA3* deletion on 1,25-dihydroxyvitamin D<sub>3</sub> biological activity, expression of genes associated with proliferation and cell cycle, was analyzed by qPCR. Expression of proliferation marker *MKI67* was increased in *VDR* knockout cells, while in A431 *PDIA3* cells, was greatly reduced after 1,25-dihydroxyvitamin D<sub>3</sub> treatment (Fig. 1G). The expression of cycle inhibitors, *Cyclin Dependent Kinase Inhibitor 2A* (*CDKN2A*) and *Cyclin Dependent Kinase Inhibitor 1A* (*CDKN1A*), was increased significantly in A431 WT treated with 1,25-dihydroxyvitamin D<sub>3</sub>. Deletion of *VDR* moderately increased expression of *CDKN2A*, but not *CDKN1A*, while the effect of 1,25-dihydroxyvitamin D<sub>3</sub> treatment was not observed (Fig. 1H). In *PDIA3* deficient A431 cells no regulation of *CDKN2A* was observed after 1,25-dihydroxyvitamin D<sub>3</sub> treatment. Deletion of  $\Delta$ *PDIA3* effectively upregulated an expression of *CDKN1A*, but the effect was attenuated by 1,25-dihydroxyvitamin D<sub>3</sub> treatment (Fig. 1I). To study the physiological effects of *PDIA3* deletion on motility and migration of cells, a wound closure assay was recorded live, with use of Olympus cellVivo IX83 for 72 h. In A431 WT cells, a full closure of the artificial wound was achieved after 50 h. In agreement with other studies [21] 1,25-dihydroxyvitamin D<sub>3</sub> inhibited cell motility, as full wound closure was not achieved at the end of the experiment (72 h). Interestingly, the effect of 1,25-dihydroxyvitamin D<sub>3</sub> was abolished in A431 $\Delta$ *VDR* cells, but not in A431 $\Delta$ *PDIA3* cells. Surprisingly, the mobility of A431 $\Delta$ *PDIA3* cells was greatly reduced by *PDIA3* deletion, with a further decrease observed after 1,25-dihydroxyvitamin D<sub>3</sub> treatment (Fig. 1J, K).

### 2.2. *PDIA3* knockout largely affects the transcriptome of A431 squamous cell carcinoma cell line

Previously, we have described the effects of the knockout of vitamin D receptor – *VDR* or its co-receptor *RXR $\alpha$*  on 1,25-dihydroxyvitamin D<sub>3</sub> transcriptome in A431 SSC cells [27].

To establish the changes in expression profile after *PDIA3* knockout, differentially expressed genes (DEGs) from A431WT cells and A431 $\Delta$ *PDIA3* were compared. Unexpectedly, the deletion of *PDIA3* in A431 SCC cell line affected the expression of 2184 genes, of which 1027 were upregulated and 1157 were downregulated. Out of 1866 detected DEGs, 1766 belonged to well-characterized coding genes (890 upregulated and 976 downregulated), 66 represented long intergenic non-protein coding RNA (*LIN\_ID*) with 21 upregulated and 45 downregulated, and 252 were categorized as uncharacterized novel transcripts (116 upregulated and 136 downregulated) (Fig. 2A). None of the genes of uncertain functions were affected by *PDIA3* deletion. All DEGs in A431 $\Delta$ *PDIA3* cells with significantly altered expression, in

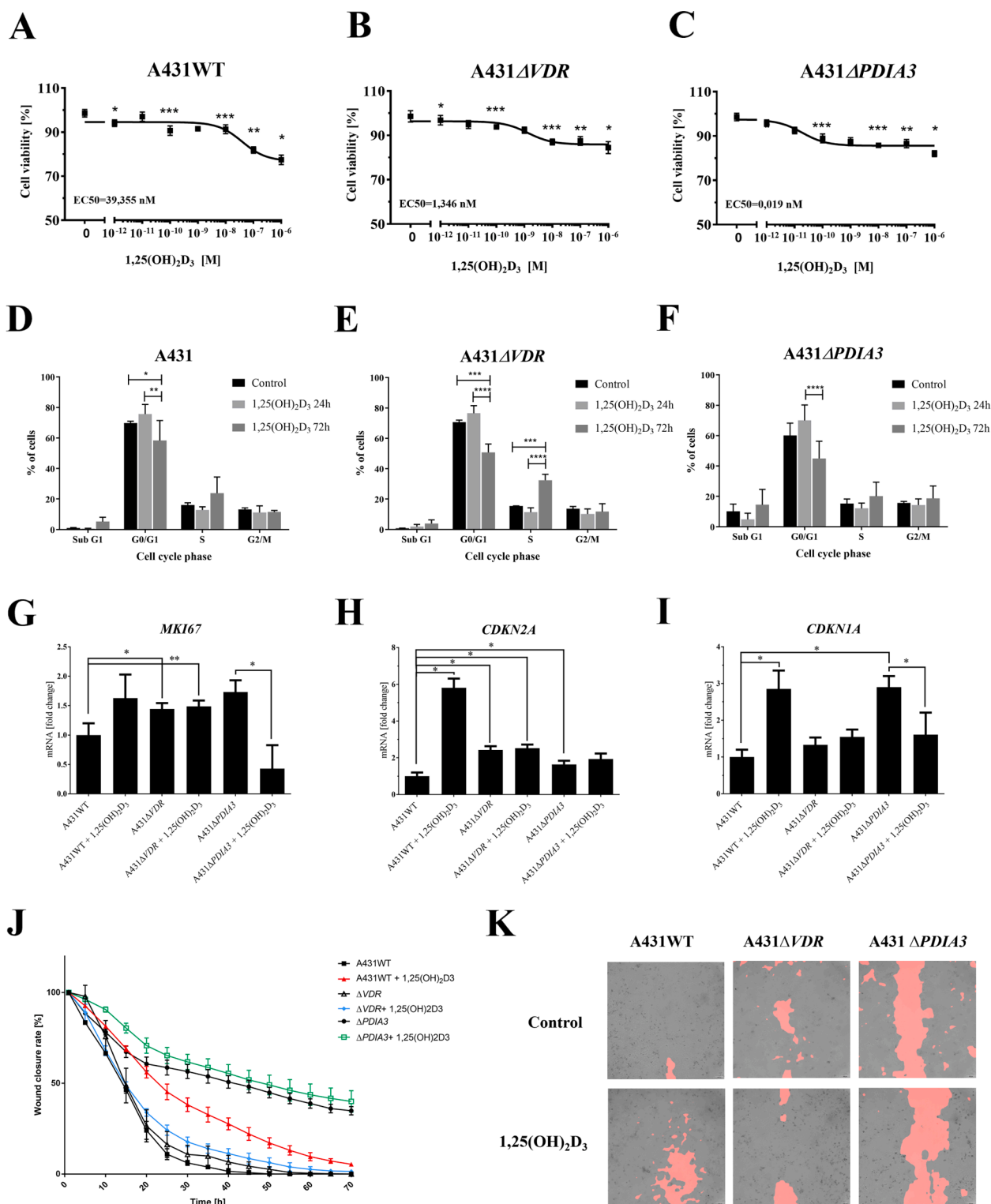


**Fig. 1.** Changes in biological actions of 1,25-dihydroxyvitamin D<sub>3</sub> in A431ΔPDIA3 squamous cell carcinoma. The effect of 1,25-dihydroxyvitamin D<sub>3</sub> on the proliferation of (A) A431WT, (B) A431ΔVDR, and (C) A431ΔPDIA3 human squamous cell carcinoma. The cell lines were treated with serial dilutions (10<sup>-6</sup>-10<sup>-12</sup>) of 1,25-dihydroxyvitamin D<sub>3</sub> for 24–72 h. Experiments were conducted in three independent experiments (n = 6 in each) ± SEM. Representative graphs for each cell line are shown. Statistical significance between plots was estimated using two-way ANOVA and presented as \*p < 0.05; \*\*p < 0.01, or \*\*\*p < 0.001. (D-F) The effect of 24–72 h incubation with 1,25-dihydroxyvitamin D<sub>3</sub> on the distribution of human squamous cell carcinoma sublines throughout the phases of the cell cycle. The data are presented as the mean ± standard deviation (n = 3). Statistical significance was estimated using two-way ANOVA followed by Tukey's multiple comparison tests and presented as \*p < 0.05; \*\*p < 0.01; \*\*\*p < 0.001, \*\*\*\*p < 0.0001. The results are representative of three experiments. Real-time PCR analysis of (G) MKI67, (H) CDKN2A, (I) CDKN1A mRNA expression levels in A431WT, A431ΔVDR and A431ΔPDIA3 cell lines. Results were normalized to none treated A431WT for all A431 sublines. (J) The effect of 72 h incubation with 1,25-dihydroxyvitamin D<sub>3</sub> on the migration rate in A431WT and A431ΔPDIA3 human squamous cell carcinoma cell lines. (K) Representative pictures of wound closure at 72 h. Statistical values were calculated with a one-way analysis of variance and Tukey's posthoc test and presented as \*p < 0.05; \*\*p < 0.01; \*\*\*p < 0.001, \*\*\*\*p < 0.0001.

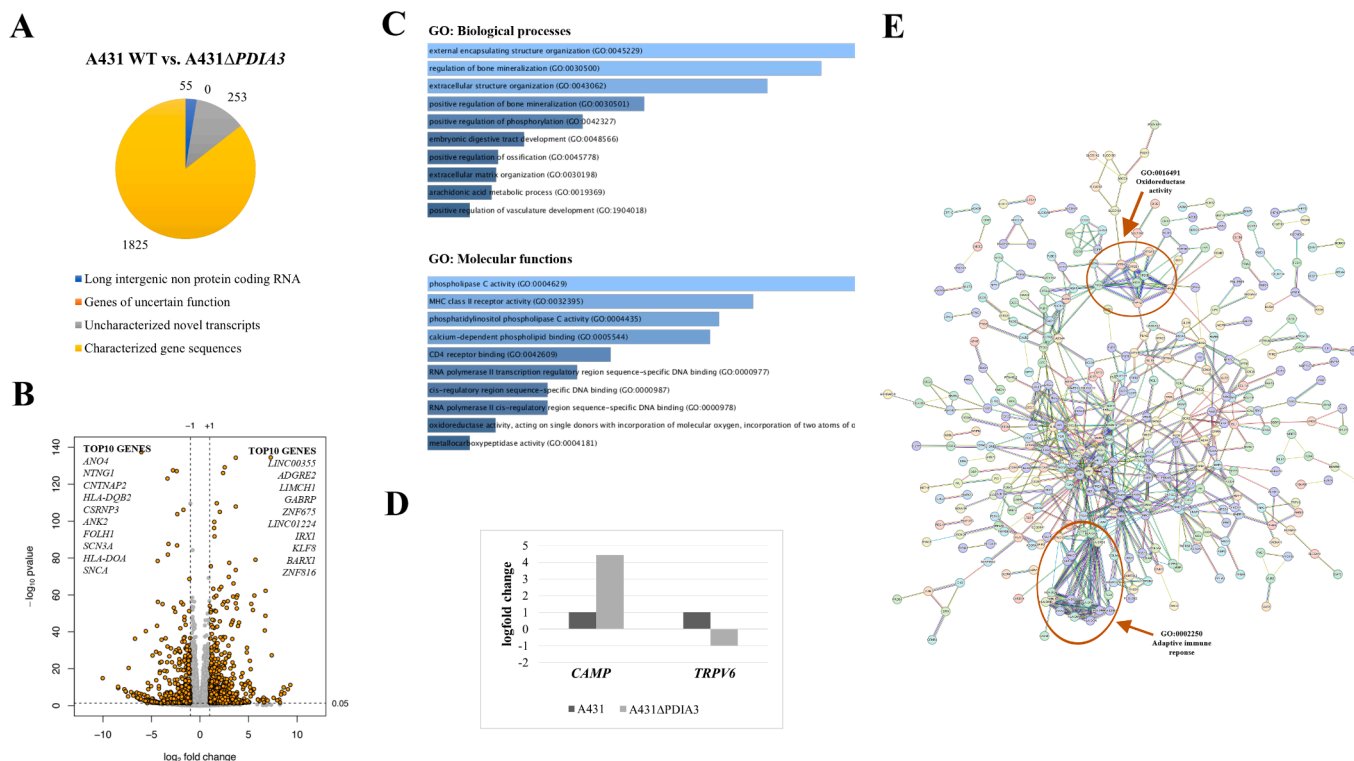


**Fig. 2.** Changes in gene expression in A431ΔPDIA3 human squamous carcinoma cells. **(A)** The amount of upregulated and downregulated DEGs after PDIA3 deletion. **(B)** Volcano plot of significantly upregulated and downregulated DEGs in A431ΔPDIA3 cells ( $|\log_2 FC| \geq 1$  and  $FDR < 0.01$ ). **(C)** Gene ontology enrichment analysis of DEGs expressed in A431ΔPDIA3 cells according to biological processes and molecular functions. **(D)** Changes in the expression levels of genes connected with the Vitamin D receptor as a transcription factor. **(E)** Protein-protein interaction network of differentially expressed proteins in A431ΔPDIA3 cells in comparison to A431WT cells. The network nodes represent proteins while the edges represent predicted functional associations. There are 5 types of associations presented: neighborhood (green), experimental (purple), text mining (yellow), database (light blue), and co-expression (black) evidence. (For interpretation of the references to colour in this figure legend, the reader is referred to the web version of this article.)

comparison to A431WT cells, were shown as a heatmap (Supplementary Fig. 2A). Volcano plot demonstrated DEGs with the most significant fold change and top ten (TOP10) upregulated and downregulated DEGs were listed in Fig. 2B. Gene ontology (GO) analysis showed significant enrichment of DEGs associated with cellular calcium-phosphorus signaling (bone mineralization, positive regulation of phosphorylation) in terms of biological processes and regarding to GO molecular functions: phospholipase C activity, MHC class II receptor activity, calcium-dependent phospholipid binding were considerably enriched (Fig. 2C).

Interestingly, detailed analyses of DEGs revealed that deletion of PDIA3 affects the expression of several classic targets for 1,25-dihydroxyvitamin D<sub>3</sub> transcriptional activity driven by VDR, including *Cytochrome P450 Family 24 Subfamily A Member 1 (CYP24A1)* [29], even in absence of the ligand. In addition, in A431ΔPDIA3 an increased expression of *Cathelicidin Antimicrobial Peptide (CAMP)* and a decrease of *Transient Receptor Potential Cation Channel Subfamily V Member (TRPV6)* were observed (Fig. 2D).

STRING online database [30] was used to perform network analysis of protein-protein interaction (PPI). Data revealed a dense interaction cluster between members of the Major Histocompatibility Complex Family and the second one between members of the Cytochrome P450 Family. Moreover, PPI analysis revealed interactions between proteins connected to cell adhesion (Fig. 2E).

### 2.3. Deletion of PDIA3 gene strongly influences response of A431 SCC cells to 1,25-dihydroxyvitamin D<sub>3</sub>

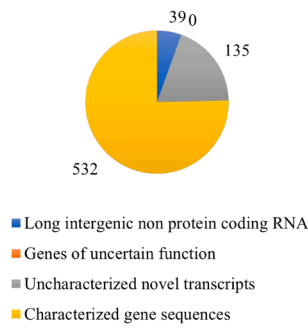
Next, the effects of 1,25-dihydroxyvitamin D<sub>3</sub> at 100 nM concentration on the transcriptome of A431ΔPDIA3 were studied after 24 h

incubation. The analysis revealed the presence of 704 DEGs of which 374 genes were upregulated and 331 downregulated. Among 704 DEGs, 532 were identified as genes of known function (295 upregulated and 275 downregulated); and 39 represented long intergenic non-protein coding RNA (LIN\_ID), with 25 upregulated and 14 downregulated. Finally, among DEGs, we detected 135 uncharacterized novel transcripts (79 upregulated and 56 downregulated). Contrary to A431WT cells [27] none of the genes of uncertain function were identified (LOC\_ID) (Fig. 3A). Lists of the TOP10 downregulated and upregulated DEGs found in A431ΔPDIA3 after incubation with 1,25-dihydroxyvitamin D<sub>3</sub> for 24 h were shown on the Volcano plot (Fig. 3B). Gene Ontology analysis revealed significant enrichment of DEGs in A431ΔPDIA3 cells after 24 h treatment with 1,25-dihydroxyvitamin D<sub>3</sub> in terms of biological processes (phosphorus metabolic processes, MAPK cascade, and positive regulation of the apoptotic process) and in terms of molecular functions categories (identical protein binding, protein kinase binding, and calcium ion binding) (Fig. 3C, D). Venn analysis (Fig. 3E, Supplementary Table S2) showed that knockout of PDIA3 alone affected 1880 coding genes (lncRNA and uncharacterized genes were excluded), of which 1611 were not affected by 1,25-dihydroxyvitamin D<sub>3</sub>. Among 1,25-dihydroxyvitamin D<sub>3</sub> dependent DEGs detected in both A431WT and A431ΔPDIA3, 59 were solely found in A431 WT cells, which suggested that the regulatory effect of 1,25-dihydroxyvitamin D<sub>3</sub> depended on PDIA3 expression. On the other hand, 191 DEGs were unique for A431ΔPDIA3 cells, while 168 genes were commonly regulated by 1,25-dihydroxyvitamin D<sub>3</sub> in A431WT and A431ΔPDIA3, thus their expression was not affected by PDIA3 presence. In A431ΔPDIA3 a group of 102 DEGs were identified as 1,25-dihydroxyvitamin D<sub>3</sub>-dependent and PDIA3-regulated, while 109 DEGs were affected by 1,25-dihydroxyvitamin D<sub>3</sub> in both cell lines, but also deletion of PDIA3 influenced their

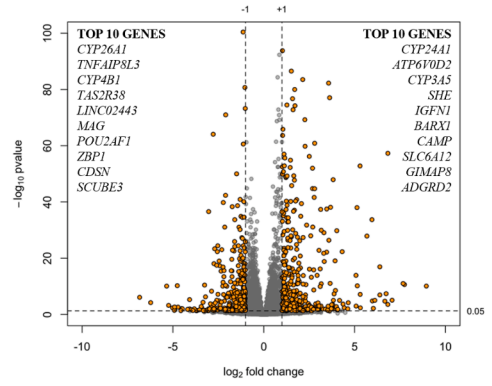


**A**

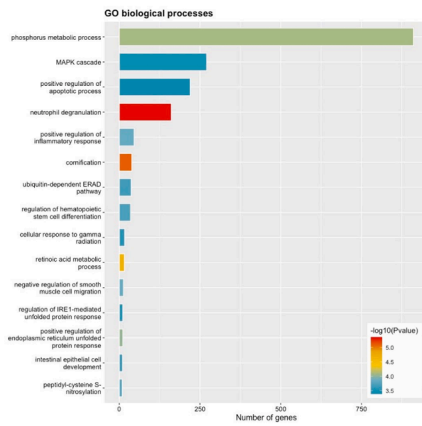
A431Δ*PDI*A3 NT vs. 1,25(OH)<sub>2</sub>D<sub>3</sub> 24h



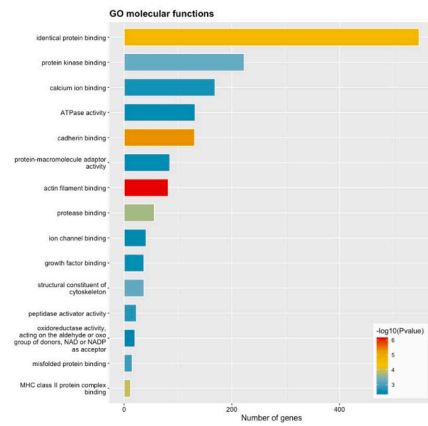
**B**



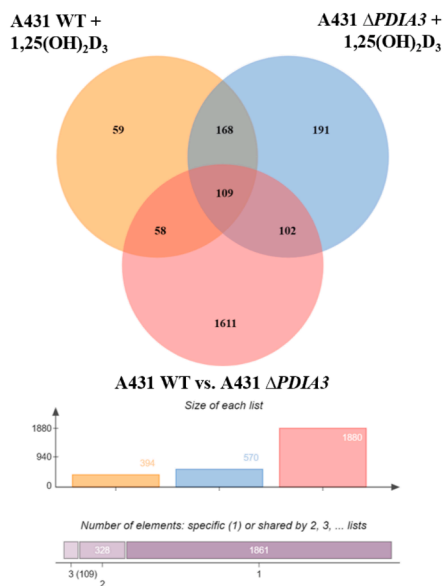
**C**



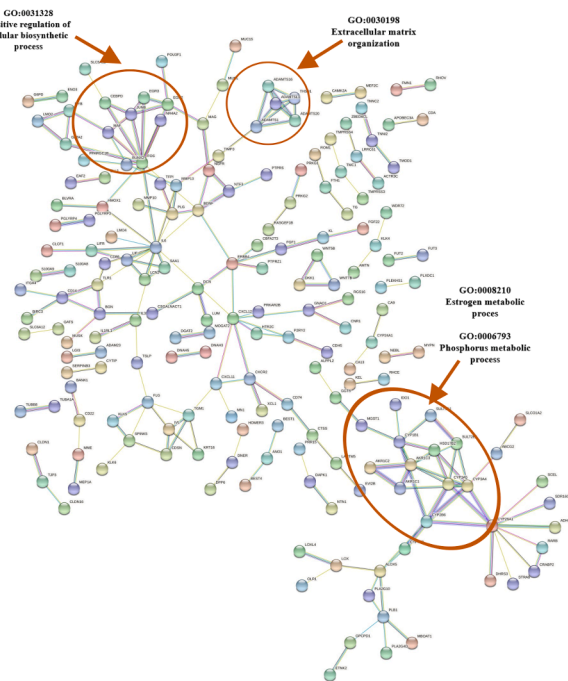
**D**



**E**



**F**



(caption on next page)

**Fig. 3.** Changes in gene expression in human squamous carcinoma cells with the *PDIA3* gene knockout treated with 1,25-dihydroxyvitamin D<sub>3</sub> for 24 h. **(A)** The number of regulated DEGs after 24 h 1,25-dihydroxyvitamin D<sub>3</sub> treatment in A431WT and A431Δ*PDIA3* cell lines. **(B)** Volcano plot of significantly upregulated and downregulated DEGs in A431Δ*PDIA3* cells treated with 1,25-dihydroxyvitamin D<sub>3</sub> ( $|\log_2 \text{FC}| \geq 1$  and  $\text{FDR} < 0.01$ ). List of the top ten most regulated genes in A431Δ*PDIA3* after 24 h 1,25-dihydroxyvitamin D<sub>3</sub> treatment. Gene ontology enrichment analysis of DEGs expressed in A431Δ*PDIA3* cells treated with 1,25-dihydroxyvitamin D<sub>3</sub> in terms of **(C)** biological processes and **(D)** molecular functions. **(E)** Venn diagram showing the distribution of DEGs between A431WT and A431Δ*PDIA3* cells treated with 1,25-dihydroxyvitamin D<sub>3</sub> and non-treated A431Δ*PDIA3*. **(F)** Protein-protein interaction network of differentially expressed proteins in A431Δ*PDIA3* cells in comparison to non-treated or treated with 1,25-dihydroxyvitamin D<sub>3</sub>. The network nodes represent proteins while the edges represent predicted functional associations. There are 5 types of associations presented: neighborhood (green), experimental (purple), text mining (yellow), database (light blue), and co-expression (black) evidence. (For interpretation of the references to colour in this figure legend, the reader is referred to the web version of this article.)

expression. Finally, 58 DEGs, which were found in A431Δ*PDIA3* cells were also modulated by 1,25-dihydroxyvitamin D<sub>3</sub>, but only in A431WT cells. Overall, amongst 117 *PDIA3*-dependent DEGs detected in A431WT cells, which were 1,25-dihydroxyvitamin D<sub>3</sub>-dependent, 98% were found to be also VDR-dependent, while around 80% RXR-dependent [27].

PPI network analysis revealed three major clusters of A431Δ*PDIA3* DEGs: the first one among positive regulators of the cellular biosynthetic process including Runt-related transcription factor 2 (RUNX2), JunB Proto-Oncogene (JUNB), MAF BZIP Transcription Factor (MAF). The second network was detected among the proteins involved in phosphorus metabolic processes including several cytochrome family

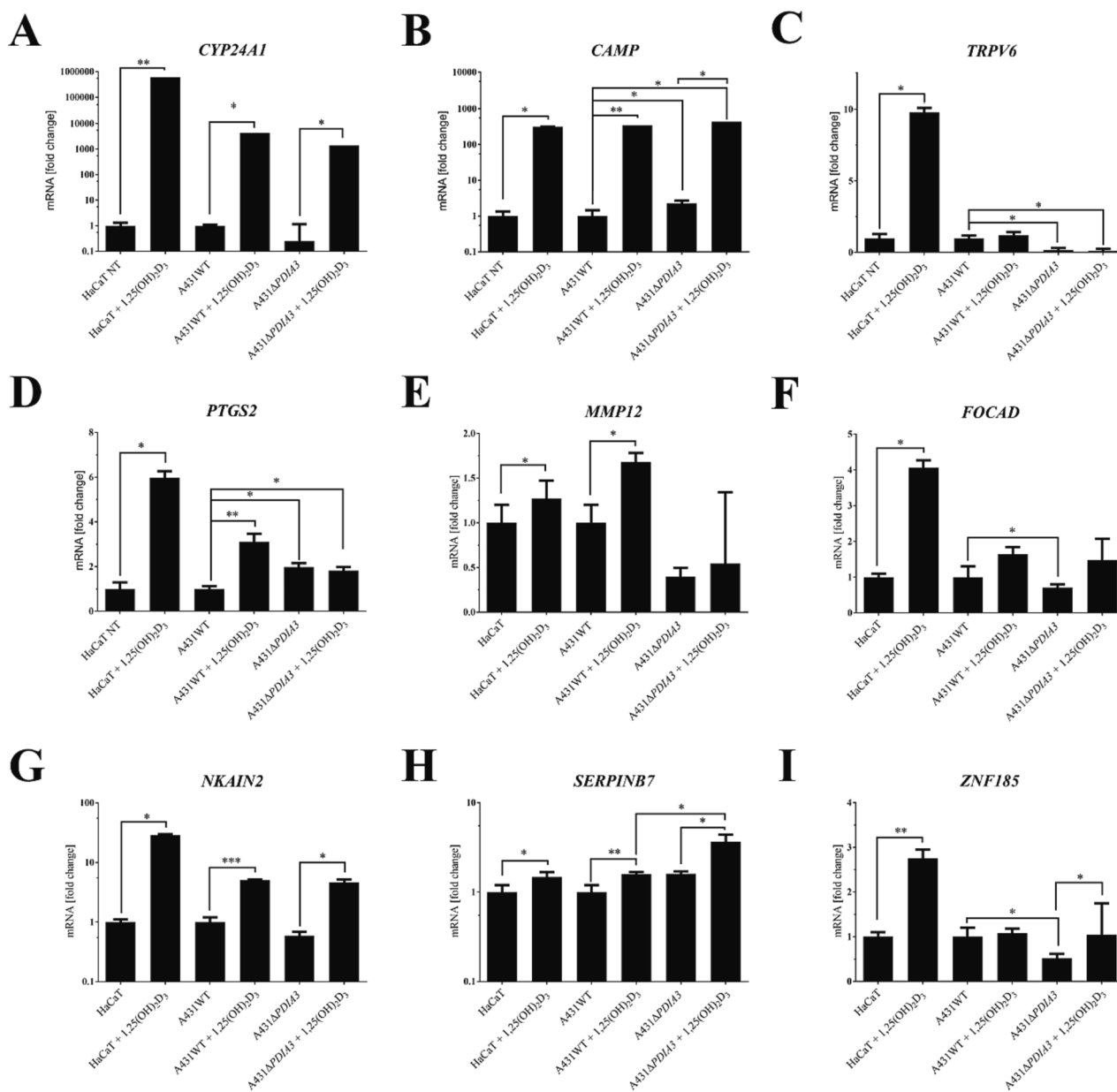


**Fig. 4.** Treatment with 1,25-dihydroxyvitamin D<sub>3</sub> changes the gene expression profile of A431Δ*PDIA3* squamous cell carcinoma cells. Real-time PCR analysis of **(A)** *CYP24A1*, **(B)** *CAMP*, **(C)** *TRPV6*, **(D)** *PTGS2*, **(E)** *MMP12*, **(F)** *FOCAD*, **(G)** *NKAIN2*, **(H)** *SERPINB7* and **(I)** *ZNF185* mRNA expression levels in HaCaT, A431WT and A431Δ*PDIA3* cell lines. Results were normalized separately to HaCaT NT for HaCaT cells and to A431 WT NT for all A431 sublines. Statistical values were calculated with a T-test and presented as \* $p < 0.05$ ; \*\* $p < 0.01$ ; \*\*\* $p < 0.001$ , \*\*\*\* $p < 0.0001$ .

members and proteins from the Aldo/keto reductase superfamily (AKR1C1-3). The list comprised members of the ADAMTS (a disintegrin and metalloproteinase with thrombospondin motifs) protein family and other proteins involved in extracellular pathway organization including Intercellular Adhesion Molecule 1 (ICAM1), Plasminogen (PLG), or Matrix Metalloproteinase (MMPs) proteins (Fig. 3F).

The transcriptomic results were confirmed by a qPCR evaluation of the expression of selected classic targets of VDR-dependent signaling including *Cytochrome P450 Family 24 Subfamily A Member 1 (CYP24A1)*, *Cathelicidin Antimicrobial Peptide (CAMP)*, *Transient Receptor Potential Cation Channel Subfamily V Member 6 (TRPV6)*, *Prostaglandin-Endoperoxide Synthase 2 (PTGS2)*, *Matrix Metalloproteinase 12 (MMP12)*, *Focadhesin (FOCAD)*, *Sodium/Potassium Transporting ATPase Interacting 2 (NKAIN2)*, *Serpin Family B Member 7 (SERPINB7)*, and *Zinc Finger Protein 185 With LIM Domain (ZNF185)*. The list was also supplemented with potential *PDI A3*-dependent and independent genes. Furthermore, human-immortalized HaCaT keratinocytes, which served as non-cancerous control, were included in the study. Interestingly, in HaCaT keratinocytes, treated with 1,25-dihydroxyvitamin D<sub>3</sub>, *CYP24A1* induction was significantly higher than in both A431 cell lines (Fig. 4A). The expression of *CAMP* was elevated after 1,25-dihydroxyvitamin D<sub>3</sub>

treatment in all cell lines (Fig. 4B). The expression of another classical target for 1,25-dihydroxyvitamin D<sub>3</sub> - *TRPV6*, which was upregulated in HaCaT cells after treatment, but this effect was not observed in both A431 sublines. Furthermore, the expression of *TRPV6* was almost completely attenuated in A431Δ*PDI A3* cells (Fig. 4C). Deletion of *PDI A3* increased expression of two genes (*CAMP*, *PTGS2*) in A431Δ*PDI A3* subline and a decrease of baseline expression of five genes (*CYP24A1*, *TRPV6*, *MMP12*, *FOCAD*, and *ZNF185*) in comparison to A431WT. In general, the expression of *PTGS2* (Fig. 4D), *MMP12* (Fig. 4E), and *FOCAD* (Fig. 4F) genes was induced by 1,25-dihydroxyvitamin D<sub>3</sub> in HaCaT and A431WT, but not in A431Δ*PDI A3*. Of note, overexpression of *PTGS2* was significantly higher in HaCaT cells treated with 1,25-dihydroxyvitamin D<sub>3</sub>, when compared to A431WT cells (6 vs. 2 folds, respectively). Further, those genes were assessed to be *PDI A3*-dependent. Expression of *NKAIN2* (Fig. 4G) and *SERPINB7* (Fig. 4H) was upregulated in all cell lines. Interestingly, the expression of *ZNF185* (Fig. 4I) was significantly reduced in cancerous cell lines compared to HaCaT cells. Moreover, expression of *ZNF185* was affected by 1,25-dihydroxyvitamin D<sub>3</sub> treatment only in HaCaT and A431Δ*PDI A3* cells, thus those genes were assessed to be *PDI A3*-independent.

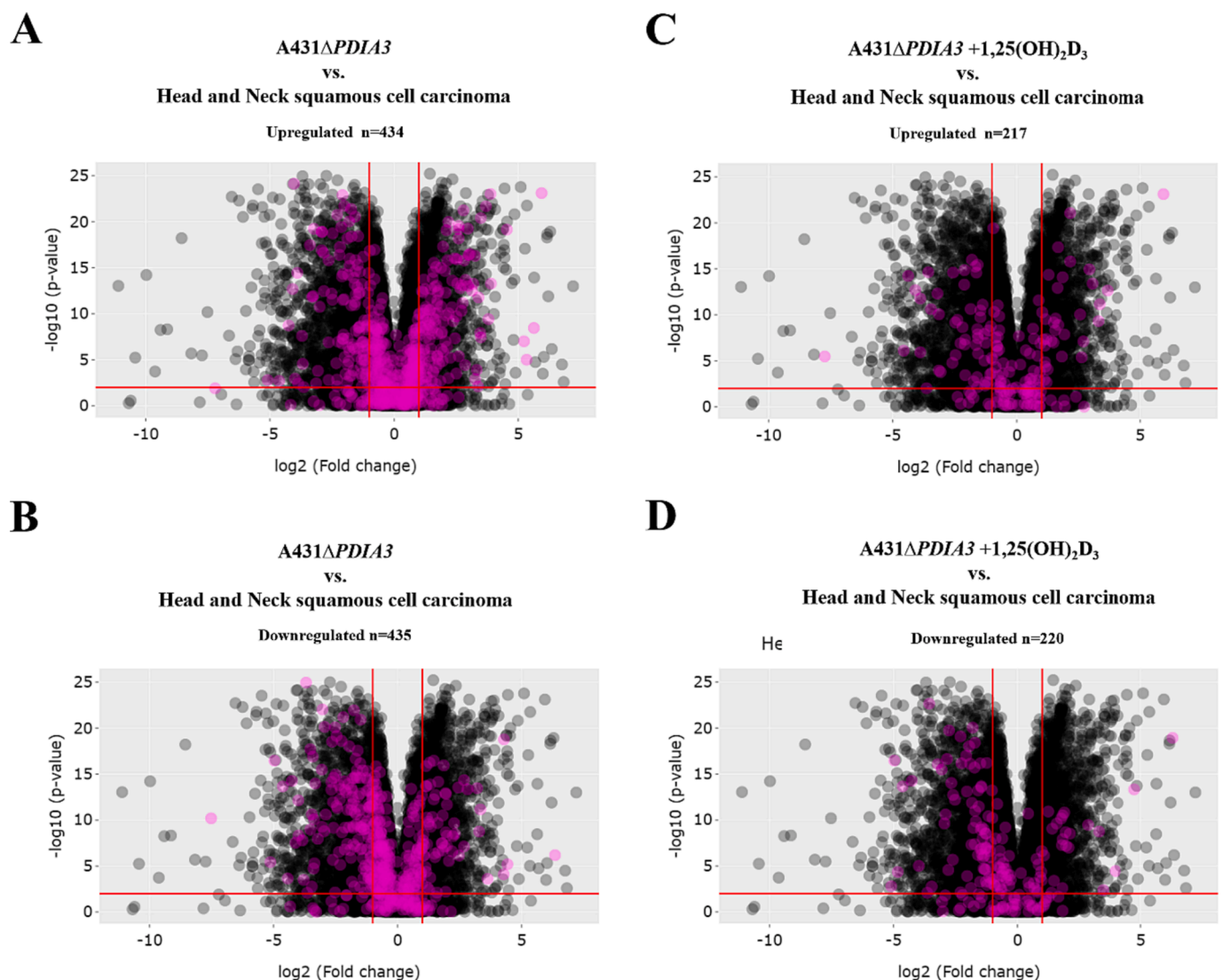


Fig. 5. Deletion of *PDI A3* in A431 squamous cell carcinoma affects the expression of common DEGs found in Head and Neck squamous cell carcinoma. Volcano plots of DEGs from A431 cell lines, the pink dots represent significantly (A) upregulated and (B) downregulated genes after *PDI A3* deletion or (C) upregulated and (D) downregulated genes after 1,25-dihydroxyvitamin D<sub>3</sub> treatment, and black dots represent gene expression profiles from Head and neck Squamous cell carcinoma obtained from TACCO database. (For interpretation of the references to colour in this figure legend, the reader is referred to the web version of this article.)



#### 2.4. Deletion of *PDIA3* in A431 squamous cell carcinoma affects the expression of common DEGs found in head and neck squamous cell carcinoma

Previously, we reported that treatment of A431 SCC cell line with 1,25-dihydroxyvitamin D<sub>3</sub>, at least partially reverse the expression of signature genes for Head and Neck squamous cell carcinoma (HNSCC) from the TACCO database [27]. Thus, here an impact of *PDIA3* knockout and 1,25-dihydroxyvitamin D<sub>3</sub> on the expression of the DEGs characteristic for HNSCC were evaluated. As the previous experiment showed changes in the expression of DEGs in A431 cell lines with *PDIA3* knockout (Fig. 5A) and after 24 h 1,25-dihydroxyvitamin D<sub>3</sub> treatment (Fig. 5B), the transcriptome of A431WT and A431Δ*PDIA3* was compared with publicly available head and neck squamous cell carcinoma database (TACCO database). Analysis revealed that from 1027 DEGs upregulated in A431Δ*PDIA3* cell line only 434 were commonly upregulated in HNSCC, while 377 were conversely expressed. Among DEGs that are downregulated after knockout of *PDIA3*, expression of 270 was increased and 435 decreased, when compared to the HNSCC expression pattern. 1,25-dihydroxyvitamin D<sub>3</sub> treatment upregulated 217 DEGs, among which 102 had the same expression pattern, and 115 were conversely expressed after 1,25-dihydroxyvitamin D<sub>3</sub> treatment. In the group of downregulated DEGs, 220 were identified in comparison to the TACCO database; 148 were downregulated and 72 were upregulated.

### 3. Discussion

The present study aimed to identify the transcriptional changes in squamous cell carcinoma cells after the knockout of *PDIA3* and its impact on response to 1,25-dihydroxyvitamin D<sub>3</sub>. To our knowledge, this is the first transcriptomic-based approach to study the contribution of *PDIA3* in the regulation of the genomic activity of 1,25-dihydroxyvitamin D<sub>3</sub>.

*PDIA3* is involved in a wide range of physiological processes, such as mediation of protein folding or modulation of store-operated Ca<sup>2+</sup> entry [31,32]. Most importantly, it was linked with rapid response to 1,25-dihydroxyvitamin D<sub>3</sub> [7,8]. Furthermore, dysregulation of *PDIA3* is associated with multiple types of cancers [11,33,34], thus our study was focused on squamous cell carcinoma cell line A431.

Here we are presenting data indicating, that deletion of either, the main receptor for vitamin D - *VDR* or potential modulator - *PDIA3* changed the response of A431 cells to 1,25-dihydroxyvitamin D<sub>3</sub> treatment, in terms of proliferation, cell cycle, and migration. This is in agreement with our previous studies showing that silencing of *VDR* correlates with reduced responsiveness to 1,25-dihydroxyvitamin D<sub>3</sub> in melanoma cells [35]. Moreover, others showed that inhibition of *VDR* expression induced hyperproliferation of cells [36]. It is also supported by an impact of deletion of *VDR* or *PDIA3* on the expression of cell cycle inhibitors: *CDKN1A* and *CDKN2A* observed here.

Recently, we have shown that deletion of *VDR* resulted in complete inhibition of the classic genomic pathway after incubation of A431Δ*VDR* cells with 1,25-dihydroxyvitamin D<sub>3</sub> for 24 h [27], and this results are in an agreement with other studies [37]. However, after prolonged incubation (72 h), 20 most downregulated DEGs were detected [27], suggesting activation of the secondary (alternative) pathway(s) activated by 1,25-dihydroxyvitamin D<sub>3</sub> [38,39]. Among those 20 genes, two were found to be *VDR*-independent and *PDIA3*-dependent (*Interferon Induced Protein 44 Like (IFI44L)* and *Epithelial Stromal Interaction 1 (EPSTI1)*). It was postulated that *PDIA3* is the major element of fast membrane signaling of 1,25-dihydroxyvitamin D<sub>3</sub> [8], activation of which may also affect the gene expression, as a secondary effect. Surprisingly, deletion of *PDIA3* in human SCC cell line A431, regardless of the 1,25-dihydroxyvitamin D<sub>3</sub>, changed the expression of more than 2000 genes, and affects cell physiology, including proliferation and cell mobility. This observation underlines the importance of

*PDIA3* and explains why its deletion in mice models is lethal [40]. Interestingly, *PDIA3* was found in various intracellular locations, including the nucleus [4,38,41,42], and its activity as a transcription factor was postulated [43,44]. Aureli and coworkers suggested that *PDIA3* regulates the expression of *MSH6*, *TMEM126A*, *LRBA*, and *ETS1* genes [43]. However, neither deletion of *PDIA3* nor 1,25-dihydroxyvitamin D<sub>3</sub> treatment affected the expression of those genes (and their direct targets) in our cellular model. On the other hand, deletion of *PDIA3* was found to impair biological processes, such as bone mineralization, regulation of bone formation, or calcium homeostasis [40]. For example, deletion of *PDIA3* in primary osteoblast cultures decreased baseline expression of *Odd-Skipped Related Transcription Factor 2 (OSR2)* gene - crucial for secondary palate growth and morphogenesis [45], which was shown to be induced by 1,25-dihydroxyvitamin D<sub>3</sub> [46]. Nonetheless, 1,25-dihydroxyvitamin D<sub>3</sub> treatment did not affect *OSR2* gene expression in A431 cells. Instead, we observed changes in the expression of genes connected with calcium homeostasis including *TRPV6* [47], which levels were significantly reduced in *PDIA3*-deficient cells. Furthermore, after 1,25-dihydroxyvitamin D<sub>3</sub> treatment of A431Δ*PDIA3* cells we observed changes in phosphorus metabolic process (*ACKR3*, *CALM1*, *CAMK2A*), MAPK cascade (*MAPK8*, *MAP2K2*, *MAPK13*) and positive regulation of apoptosis (*BCL2L11*, *BAX*, *BAD*). Taken together, data presented here indicate that *PDIA3* is essential for the maintenance of calcium-phosphorus homeostasis, which links its function with vitamin D signaling, but the effect seems to be cell-type specific. It is worth mentioning, that deletion of *PDIA3* in A431 cells, resulted in destabilization of cellular homeostasis triggering apoptosis, which additionally was enhanced by 1,25-dihydroxyvitamin D<sub>3</sub> (with up to 10% of apoptotic cells was observed). The latest study in melanoma cells has shown that 1,25-dihydroxyvitamin D<sub>3</sub> can induce apoptosis-related proteins such as caspase-3, caspase 8, and caspase-9 [48] although apoptosis seems to be not the mayor mechanism of 1,25-dihydroxyvitamin D<sub>3</sub> activity.

Among 24 classic target genes associated with *VDR* transcriptional activity, an expression of *CAMP* and *TRPV6* was significantly changed after *PDIA3* deletion. Cathelicidin antimicrobial peptide (*CAMP*) plays a critical role in innate immune response and its expression is regulated by *VDR* transcription factor in response to 1,25-dihydroxyvitamin D<sub>3</sub>. Consequently, our data indicated strong upregulation of *CAMP* expression in both, normal keratinocytes (HaCaT) and cancer cells (A431). It is also in agreement with previously published data showing a concentration-dependent increase in *CAMP* mRNA after 1,25-dihydroxyvitamin D<sub>3</sub> treatment [49,50]. *TRPV6* is a highly Ca<sup>2+</sup>-selective channel, which plays a role in maintaining Ca<sup>2+</sup> ion homeostasis [51], but also is essential for Ca<sup>2+</sup>-induced differentiation of human keratinocytes [52]. Furthermore, it was shown that 1,25-dihydroxyvitamin D<sub>3</sub> treatment in HaCaT cells increases *TRPV6* expression, which lines up with the previous study [52]. In A431 cells there was no increase in the expression of *TRPV6* after 1,25-dihydroxyvitamin D<sub>3</sub> treatment and *PDIA3* deletion resulted in almost complete attenuation of its expression. Those results suggest that squamous cell carcinoma cell line A431 is not sensitive to 1,25-dihydroxyvitamin D<sub>3</sub> induced expression of *TRPV6* and deletion of *PDIA3* deepens that effect.

Further, support of indirect involvement of *PDIA3* in 1,25-dihydroxyvitamin D<sub>3</sub> signaling came from the detailed transcriptomic analysis. The deletion of *PDIA3* affected the expression of 167 DEGs detected in A431 WT cells, treated with 1,25-dihydroxyvitamin D<sub>3</sub>. In addition, expression of the genes involved in classic 1,25-dihydroxyvitamin D<sub>3</sub> signaling, *CYP24A1* was altered (increased) by *PDIA3* knockout, but not *VDR*, while expression of *RXRA* was decreased. The *PDIA3* knockout also significantly changed the top-ranked expressed gene in Δ*PDIA3* cells after 1,25-dihydroxyvitamin D<sub>3</sub> treatment in comparison to A431WT [27]. An increase in the expression of DEGs connected to cell-matrix adhesion *Semaphorin 3E (SEMA3E)* and *Coronin 1B (CORO1B)* after *PDIA3* deletion may indicate a potential mechanism of inhibition of mobility of A431Δ*PDIA3* cells. Indeed, expression of *SEMA3E* was

inversely correlated with melanoma progression [53]. However, we also noted enhanced expression of *Vimentin (VIM)*, which is a marker of epithelial-mesenchymal transition after *PDIA3* deletion [54].

Venn analysis of all 1,25-dihydroxyvitamin D<sub>3</sub> regulated DEGs allowed us to distinguish *PDIA3*-dependent (*PTGS2*, *MMP12*, *FOCAD*) and -independent (*NKAIN2*, *SERPINB7*, *ZNF185*) genes. Cyclooxygenase-2 (*COX-2/PTGS2*) is a membrane-bound prostaglandin (PG)-endoperoxide synthase 2 enzyme responsible for the generation of prostanoids [55]. In our study, 1,25-dihydroxyvitamin D<sub>3</sub>, strongly stimulated the expression *PTGS2* gene in HaCaT cells, which confirmed previous reports [56]. Shirvani and coworkers showed that *PTGS2* is downregulated after 6 months-long vitamin D<sub>3</sub> supplementation [57]. Those differences might be explained by different models and experiment set up. In SSC cell line A431WT, the effect 1,25-dihydroxyvitamin D<sub>3</sub> treatment was partially attenuated, but still statistically significant, while in A431 cells with deletion of *PDIA3*, expression of *PTGS2* was not affected by the treatment. Those results suggested that *PTGS2* response to 1,25-dihydroxyvitamin D<sub>3</sub> is *PDIA3*-dependent, and our previous studies also indicated the involvement of *RXRA* in its expression [27]. The *MMP12* is a matrix metalloproteinase with a broad range of anti-tumor effects [58], such as a protective role in tumor progression [59] or generation of anti-angiogenic peptides [60]. In our study, we noted elevated expression of *MMP12* after 1,25-dihydroxyvitamin D<sub>3</sub> treatment in HaCaT cells and its upregulation was even greater in A431WT cells. However, the deletion of *PDIA3* completely abrogated the effects of 1,25-dihydroxyvitamin D<sub>3</sub> on *MMP12*, indicating the involvement of *PDIA3* in its expressional regulation. Interestingly, *MMP12* expression was shown to be *RXRA*-independent [27]. Focadhesin (*FOCAD*) functions as an anti-tumor protein, inhibiting cell proliferation and migration [61]. It was shown, that the loss of *FOCAD* expression correlated with enhanced aggressiveness and worsen clinical outcomes in glioma patients [62]. Our study indicates that in cancerous cells (A431WT and A431Δ*PDIA3*) effect of 1,25-dihydroxyvitamin D<sub>3</sub> treatment on expression of *FOCAD* was significantly reduced and *PDIA3*-dependent. Recently, we have shown that its expression is also *VDR*- and *RXRA*-dependent [27]. The Na<sup>+</sup>/K<sup>+</sup> transporting ATPase interacting 2 (*NKAIN2*) is a novel tumor suppressor identified in prostate cancer [63]. Our study showed, that 1,25-dihydroxyvitamin D<sub>3</sub>-dependent *NKAIN2* expression is reduced in cancerous cells (A431) compared to non-cancerous (HaCaT). Moreover, the effect of 1,25-dihydroxyvitamin D<sub>3</sub> on the expression of this gene depends solely on *VDR*. The expression of *SERPINB7*, which belong to serine protease inhibitors, was elevated by *PDIA3* deletion alone and furtherly stimulated by 1,25-dihydroxyvitamin D<sub>3</sub>. An overexpression of *SERPINB7*, along with other serpin family members, was associated with suppression of the invasiveness and motility of cancer cells [64]. In our previous study, [27] it was shown that 1,25-dihydroxyvitamin D<sub>3</sub> impact on *SERPINB7* expression is *VDR*/*RXRA*-dependent and our current study suggested also the involvement of *PDIA3*. The *ZNF185* is a zinc finger protein, highly expressed during keratinocytes differentiation. Interestingly, its downregulation was also described as a potential biomarker of squamous cell carcinoma [65]. Our results showed that 1,25-dihydroxyvitamin D<sub>3</sub> upregulates the expression of *ZNF185* in HaCaT keratinocytes, but not in SCC line A431. Interestingly, the deletion of *PDIA3* reintroduced, to some extent, the effect of 1,25-dihydroxyvitamin D<sub>3</sub>, on *ZNF185* expression. Thus, it seems, that *PDIA3* in cancerous cells has an inhibitory effect on 1,25-dihydroxyvitamin D<sub>3</sub>-induced expression of *ZNF185*.

In recent years, the *PDIA3* protein has emerged as a potential prognostic marker for various types of cancer [34,66,67]. Large-scale transcriptomic analysis of Head and Neck Squamous Cell Carcinomas (HNSCC) showed that overexpression of *PDIA3* correlates with poor prognosis [68,69]. In our study, around 39% of identified DEGs in A431Δ*PDIA3* cells (A431Δ*PDIA3* vs A431WT), showed the same expression trend as in HNSCC. Data presented here also demonstrated an impaired genomic response to 1,25-dihydroxyvitamin D<sub>3</sub> of cancer cells in comparison to HaCaT keratinocytes. Importantly, *PDIA3* knockout

radically changed the response of the cells to 1,25-dihydroxyvitamin D<sub>3</sub> treatment, not only on the genomic level but also by sensitizing cells to 1,25-dihydroxyvitamin D<sub>3</sub> as shown by proliferation assay. Thus, *PDIA3* is not only important for normal cellular physiology but also is necessary for the response and biological activities of 1,25-dihydroxyvitamin D<sub>3</sub>. For many years *PDIA3* has been considered a membrane receptor for 1,25-dihydroxyvitamin D<sub>3</sub> [6], however, the nature of the interaction of *PDIA3* with 1,25-dihydroxyvitamin D<sub>3</sub> still is under debate [70], because the crystal structure of the complex of *PDIA3* with 1,25-dihydroxyvitamin D<sub>3</sub> was not determined, yet. Data presented here, however, open new possibilities. It could be postulated that *PDIA3* affects directly or indirectly several intracellular pathways essential for genomic and/or nongenomic activity of vitamin D, modulating cellular response to this powerful secosteroid. Furthermore, it seems that *PDIA3* could be also considered as a target for anticancer therapy as well as a modulator of response to 1,25-dihydroxyvitamin D<sub>3</sub>.

## 4. Materials and methods

### 4.1. 1,25-dihydroxyvitamin D<sub>3</sub>

1,25-dihydroxyvitamin D<sub>3</sub> was purchased from Sigma-Aldrich. Stock solutions of 1,25-dihydroxyvitamin D<sub>3</sub> were dissolved in ethanol and stored at -20 °C. 1,25-dihydroxyvitamin D<sub>3</sub> at 100 nM concentration was used in all experiments (the concentration of solvent (ethanol) was < 0.05%).

### 4.2. Cell cultures

Immortalized human basal cell carcinoma cell line (A431) was obtained from Synthego Corporation (Menlo Park, CA, USA), and immortalized human keratinocyte cell line (HaCaT) was obtained from CLS (Cell Line Service, Eppelheim, Germany). Cells were cultured in DMEM high glucose medium (4.5 g/L) with the addition of 10% FBS and penicillin (10000 units/ml) and streptomycin (10 mg/ml) (Sigma-Aldrich; Merck KGaA). Cell cultures were performed in the incubator with 5% CO<sub>2</sub> at 37 °C. Before treatment with 1,25-dihydroxyvitamin D<sub>3</sub> medium was changed to DMEM with 2% charcoal-stripped FBS.

### 4.3. CRISPR/Cas9 knock-out cell lines

The knockout of *PDIA3* gene was introduced to the squamous cell carcinoma cell line A431 using CRISPR/Cas7 technology [71]. Specific guide RNAs (gRNAs) targeting the *PDIA3* gene have been designed with the use of Synthego tools (<https://www.synthego.com/guide/how-to-use-crispr/design-tool-tutorial>). After selecting the appropriate gRNA, a pool of knockout cells (with an editing efficiency of at least 50 %) was purchased from Synthego (Menlo Park, CA, USA). For clonal selection, cloning discs were used (Bel-Art SP SCIENCEWARE). Briefly, cells in low density were seeded, on 6-well plates, and the growth of single-cell colonies was monitored every third day. When the colonies were large enough, trypsin-immersed discs were placed on the colonies and then transferred along with the cells to 12-well plates. The next day cloning discs were removed from the plate. Cells adhere to the discs after trypsinization were transferred to the individual wells and cultured for screening. The introduction of the knockouts was verified by Sanger sequencing (Oligo.pl, Institute of Biochemistry and Biophysics, Poland), qPCR, and Western blot analysis. The detailed analyses of the *PDIA3* deletion in A431 SCC cell line were presented in **Supplementary Fig. 1**. The preparation and characterization of A431Δ*VDR* cells were described elsewhere [27].

### 4.4. Proliferation assay

The sulforhodamine B (SRB) assay was performed as described previously [28]. Shortly, the A431 wild-type (WT) cells or A431Δ*PDIA3*

cells were seeded on 96-well plates in DMEM medium supplemented with 2% FBS charcoal and cultured overnight. Then, cells were treated with serial dilution of 1,25-dihydroxyvitamin D<sub>3</sub> (10<sup>-6</sup>-10<sup>-12</sup>M) for 72 h. Cells were fixated with 10% trichloroacetic acid and stained with the solution of 0.4% SRB (Sigma-Aldrich; Merck KGaA) in acetic acid. Tris Base buffer was used to solubilize SRB dye. The absorbance was measured at 570 nm on an Epoch™ microplate spectrophotometer (BioTek Instruments, Inc., Winooski, VT, USA).

#### 4.5. Cell cycle analysis

The cell cycle analysis was based on the quantification of DNA content with flow cytometry as described previously [21]. Shortly, cells were treated with 1,25-dihydroxyvitamin D<sub>3</sub> for 24 or 72 h, at 100 nM concentration. Cells were harvested and fixated with 70% ethanol, then treated with ribonuclease, and finally stained with propidium iodide (PI, Sigma-Aldrich; Merck KGaA) at 37°C. The fluorescence of the PI-stained cells was measured by flow cytometry (FACS Calibur™; Becton, Dickinson and Company, Franklin, Lakes, NJ, USA). The results were analyzed using the CellQuest™ Pro Software version 6.0 (Becton, Dickinson, and Company).

#### 4.6. Wound healing assay

For motility assessment, A431-derived cell lines were seeded on 8 chamber slides. When cells reached 100% confluency mechanical wound was created by physical scraping with a pipette tip. Cells were treated with 1,25-dihydroxyvitamin D<sub>3</sub> at 100 nM concentration and migration of cells was observed for 72 h as live imaging with Olympus cell Vivo IX83. The cell-free area was calculated with Olympus cell Sens software with the use of TruAI technology.

#### 4.7. Immunoblotting

A431-derived cell lines were treated with 100 nM 1,25-dihydroxyvitamin D<sub>3</sub> for 4, 8, and 24 h. The medium was removed from the plate and cells were washed twice with PBS and were scratched from the plate. The solution was moved to an Eppendorf tube and centrifuged at 16,000 × g for 10 min. The received cell sediment was dissolved in 100 µl of RIPA buffer (ThermoFisher, Waltham, Massachusetts, USA). Concentration was determined by Bradford Assay. For SDS-PAGE electrophoresis 10% bottom gel and 5% upper gel were used. An equal amount of protein (20µg) was loaded into each well. Electrophoresis was run at 90–110 V in the Bio-Rad apparatus. Proteins were transferred to PVDF membranes with the use of the Trans-Blot Turbo system (Bio-Rad). After the transfer membranes were blocked in 5% milk dissolved in TBS-T. The membranes were incubated with primary antibodies anti-PDIA3/ERp57 (ThermoFisher, Waltham, Massachusetts, USA), anti-VDR (Santa Cruz Biotechnology, Dallas, Texas, USA), or anti-Cyp24A1 (Santa Cruz Biotechnology, Dallas, Texas, USA), overnight at 4 °C. Then, it was incubated with proper secondary peroxidase-conjugated antibodies (anti-rabbit antibody, Santa Cruz Biotechnology, Dallas, Texas, USA, or anti-Mouse antibody, Sigma-Aldrich, Saint Louis, Missouri, USA). For loading control membranes were stripped and reprobed using HRP conjugated anti-β-actin antibody (Santa Cruz Biotechnology, Dallas, Texas, USA). Bands were developed using enhanced chemiluminescence ECL Plus (Perkin Elmer, Waltham, Massachusetts, USA). Imaging was performed on ImageQuant LAS 500 (Cytivia, Mulhouse, France).

#### 4.8. Sample preparation for qPCR and RNA sequencing

A431 wild-type cells and A431 knock-out (ΔPDIA3) cells were seed on 6 well plates and treated with 100 µM 1,25-dihydroxyvitamin D<sub>3</sub> or solvent (0.05% ethanol) (Sigma-Aldrich, Saint Louis, Missouri, USA) for 24 h. RNA was extracted according to the manufacturer's instruction

with the use of ExtractMe total RNA kit (Blirt, Poland), and the concentrations were assessed with EPOCH Microplate Spectrophotometer (BioTek, USA).

#### 4.9. RNA sequencing

For RNAseq, the RNA purity and quality were assessed using the RNA ScreenTape assays on the 4200 TapeStation System (Agilent Technologies, Germany). The RNA samples with RIN (RNA Integrity Number) between 9,6–10 were sequenced in CeGaT (Tübingen, Germany). The amount of mRNA was 100 ng per sample. The library of RNA was prepared with the use of TruSeq stranded mRNA (Illumina), Q30 value greater than 91%, NovaSeq 6000, 2x 100 bp with usually 30–40 M sequenced raw fragments per sample. The initial quality control assessment confirmed that biological replicates and technical repeats were significantly clustered.

#### 4.10. Real-Time PCR

Real-time PCR was performed using a StepOnePlus™ Real-Time PCR System (Life Technologies Applied Biosystems, Grand Island, NY, USA) with an AMPLIFYME SG No-ROX Mix kit (Blirt, Poland). All primers were purchased from Merck, Germany. All PCR reactions were conducted with the primers grouped in the table (Supplementary Table S1). The amount of amplified product for each gene was compared to that of the reference gene (RPL37) using a comparative ΔΔCT method and presented as a fold change ± SD [21].

#### 4.11. Bioinformatics analyses

The raw reads were first quality-checked and cleaned up using FastQC [72] and Trimmomatic [73]. Principal Component Analysis (PCA) for data quality control and cell line disparities checks, were performed. It detected major clusters distinct from each other, for each experimental condition and treatment. FastQC box plots of quality scores per reading position, Phred score greater than 30 were also performed. Samples clustering based on a distance matrix created from rlog-transformed gene expression values was done [27]. RNA-seq data generated as part of this work are available without restriction. The data have been deposited in SRA under accession number PRJNA926032.

The reads were mapped to the human reference genome (GRCh38) using STAR [74]. Next, the mapped reads were counted with feature Counts 2.0.3 [75]. To compare transcriptomic profiles across samples PCA was conducted on rlog-transformed count values [76]. Differential gene expression analysis was conducted using DESeq2 [76]. The absolute value of log<sub>2</sub>fold change ≥ 1.0 and adjusted p-value < 0.05 were used as a criterion to identify differentially expressed genes. Gene ontology (GO) enrichment analysis was performed using the R package top GO [77] with Fisher's exact test to determine the functions of differentially expressed genes. Gene names were mapped to GO terms using the org.Hs.eg.db [78] package. Only GO terms with a p-value < 0.05 were considered significantly enriched.

The results of the analysis were visualized using the R package [79]. The search Tool for the Retrieval Interacting Genes (STRING) database was used to construct the network of differentially expressed genes and proteins [80].

#### 4.12. Statistical analysis

Statistical analysis was performed using GraphPad Prism version 7.05 (GraphPad Software, Inc., La Jolla, CA, USA). Data are presented as mean ± SD and were analyzed with a Student's *t*-test (for two groups) or one-way ANOVA analysis of variance with appropriate posthoc tests (for more than two groups) using Prism software. Statistically significant differences are illustrated with asterisks: \**p* < 0.05, \*\**p* < 0.01, \*\*\**p* < 0.001, or \*\*\*\**p* < 0.0001.



#### 4.13. Accession number

RNA-seq data generated as part of this work are available without restriction. The data have been deposited in Sequence Read Archive (SRA) under accession number PRJNA926032.

#### Founding

The study was supported by a National Science Center OPUS grant NCN grant 2017/25/B/NZ3/00431.

#### CRedit authorship contribution statement

**Joanna I. Nowak:** Conceptualization, Investigation, Methodology, Visualization, Writing – original draft. **Anna M. Olszewska:** Investigation. **Anna Piotrowska:** Investigation, Methodology, Visualization. **Kamil Myszczyński:** Investigation, Data curation, Validation, Visualization. **Paweł Domżański:** Investigation, Methodology. **Michał A. Żmijewski:** Conceptualization, Funding acquisition, Supervision, Validation, Writing – review & editing.

#### Declaration of Competing Interest

The authors declare that they have no known competing financial interests or personal relationships that could have appeared to influence the work reported in this paper.

#### Appendix A. Supplementary data

Supplementary data to this article can be found online at <https://doi.org/10.1016/j.steroids.2023.109288>.

#### References

- [1] L.E. Powell, P.A. Foster, Protein disulphide isomerase inhibition as a potential cancer therapeutic strategy, *Cancer Med.* 10 (8) (2021) 2812–2825.
- [2] C. Turano, E. Gaucchi, C. Grillo, S. Chichiarelli, ERp57/GRP58: a protein with multiple functions, *Cell. Mol. Biol. Lett.* 16 (2011) 539–563.
- [3] B.J. Grindler, B. Rohe, S.E. Safford, J.J. Bennett, M.C. Farach-Carson, Tumor necrosis factor- $\alpha$  treatment of HepG2 cells mobilizes a cytoplasmic pool of ERp57/1,25D<sub>3</sub>-MARRS to the nucleus, *J. Cell. Biochem.* 112 (2011) 2606–2615.
- [4] S. Chichiarelli, F. Altieri, G. Paglia, E. Rubini, M. Minacori, M. Eufemi, ERp57/PDIA3: new insight, *Cell. Mol. Biol. Lett.* 27 (2022) 12.
- [5] P. Kranz, F. Neumann, A. Wolf, F. Classen, M. Pomsch, T. Ocklenburg, J. Baumann, K. Janke, M. Baumann, K. Goepelt, H. Riffkin, E. Metzgen, U. Brockmeier, PDI is an essential redox-sensitive activator of PERK during the unfolded protein response (UPR), *Cell Death Dis.* 8 (8) (2017) e2986.
- [6] I. Nemere, Z. Schwartz, H. Pedrozo, V.L. Sylvia, D.D. Dean, B.D. Boyan, Identification of a membrane receptor for 1,25-dihydroxyvitamin D<sub>3</sub> which mediates rapid activation of protein kinase C, *J. Bone Miner. Res.* 13 (9) (1998) 1353–1359.
- [7] M. Doroudi, Z. Schwartz, B.D. Boyan, Membrane-mediated actions of 1,25-dihydroxy vitamin D<sub>3</sub>: a review of the roles of phospholipase A2 activating protein and Ca(2+)/calmodulin-dependent protein kinase II, *The Journal of Steroid Biochemistry and Molecular Biology* 147 (2015) 81–84.
- [8] J. Chen, M. Doroudi, J. Cheung, A.L. Grozier, Z. Schwartz, B.D. Boyan, Plasma membrane Pdia3 and VDR interact to elicit rapid responses to 1 $\alpha$ ,25(OH)<sub>2</sub>D<sub>3</sub>, *Cell. Signal.* 25 (12) (2013) 2362–2373.
- [9] L. Bargsted, C. Hetz, S. Matus, ERp57 in neurodegeneration and regeneration, *Neural Regen. Res.* 11 (2016) 232–233.
- [10] R. Ghemrawi, M. Khair, Endoplasmic Reticulum Stress and Unfolded Protein Response in Neurodegenerative Diseases, *Int. J. Mol. Sci.* 21 (17) (2020) 6127.
- [11] F.S. Ramos, L.T.R. Serino, C.M.S. Carvalho, R.S. Lima, C.A. Urban, I.J. Cavalli, E.M. S.F. Ribeiro, PDIA3 and PDIA6 gene expression as an aggressiveness marker in primary ductal breast cancer, *Genet. Mol. Res.* 14 (2) (2015) 6960–6967.
- [12] N.C. Pressinotti, H. Klocker, G. Schäfer, V.-D. Luu, M. Ruschhaupt, R. Kuner, E. Steiner, A. Poustka, G. Bartsch, H. Sültmann, Differential expression of apoptotic genes PDIA3 and MAP3K5 distinguishes between low- and high-risk prostate cancer, *Mol. Cancer* 8 (1) (2009).
- [13] N. Garbi, S. Tanaka, F. Momberg, G.J. Hämmerling, Impaired assembly of the major histocompatibility complex class I peptide-loading complex in mice deficient in the oxidoreductase ERp57, *Nat. Immunol.* 7 (1) (2006) 93–102.
- [14] I. Nemere, N. Garbi, G.J. Hämmerling, R.C. Khanal, Intestinal cell calcium uptake and the targeted knockout of the 1,25D<sub>3</sub>-MARRS (membrane-associated, rapid response steroid-binding) receptor/PDIA3/Erp57, *J. Biol. Chem.* 285 (41) (2010) 31859–31866.
- [15] M.H. Choe, J.W. Min, H.B. Jeon, D.-H. Cho, J.S. Oh, H.G. Lee, S.-G. Hwang, S. An, Y.-H. Han, J.-S. Kim, ERp57 modulates STAT3 activity in radioresistant laryngeal cancer cells and serves as a prognostic marker for laryngeal cancer, *Oncotarget* 6 (5) (2015) 2654–2666.
- [16] K.e. Wang, H. Li, R. Chen, Y. Zhang, X.-X. Sun, W. Huang, H. Bian, Z.-N. Chen, Combination of CALR and PDIA3 is a potential prognostic biomarker for non-small cell lung cancer, *Oncotarget* 8 (57) (2017) 96945–96957.
- [17] H. Takata, M. Kudo, T. Yamamoto, J. Ueda, K. Ishino, W.-X. Peng, R. Wada, N. Taniai, H. Yoshida, E. Uchida, Z. Naito, Increased expression of PDIA3 and its association with cancer cell proliferation and poor prognosis in hepatocellular carcinoma, *Oncol. Lett.* 12 (6) (2016) 4896–4904.
- [18] J. Wierzbicka, A. Piotrowska, M.A. Żmijewski, The renaissance of vitamin D, *Acta Biochim. Pol.* 61 (2014) 679–686.
- [19] A. Piotrowska, J. Wierzbicka, M.A. Żmijewski, Vitamin D in the skin physiology and pathology, *Acta Biochim. Pol.* 63 (2016) 17–29.
- [20] Segovia-Mendoza M, García-Quiroz J, Díaz L, García-Becerra R. Combinations of Calcitriol with Anticancer Treatments for Breast Cancer: An Update. *Int J Mol Sci.* 2021;22.
- [21] A. Piotrowska, F.P. Beserra, J.M. Wierzbicka, J.I. Nowak, M.A. Żmijewski, Vitamin D Enhances Anticancer Properties of Cediranib, a VEGFR Inhibitor, by Modulation of VEGFR2 Expression in Melanoma Cells, *Front. Oncol.* 11 (2021), 763895.
- [22] A.S.W. Oak, GEORGETA Bocheva, TAE-KANG Kim, A.A. Brożyna, ZORICA Janjetovic, MOHAMMAD Athar, R.C. Tuckey, A.T. Slominski, Noncalcemic Vitamin D Hydroxyderivatives Inhibit Human Oral Squamous Cell Carcinoma and Down-regulate Hedgehog and WNT/ $\beta$ -Catenin Pathways, *Anticancer Res* 40 (5) (2020) 2467–2474.
- [23] C.S. Hii, A. Ferrante, The Non-Genomic Actions of Vitamin D, *Nutrients* 8 (2016) 135.
- [24] I. Nemere, S.E. Safford, B. Rohe, M.M. DeSouza, M.C. Farach-Carson, Identification and characterization of 1,25D<sub>3</sub>-membrane-associated rapid response, steroid (1,25D<sub>3</sub>-MARRS) binding protein, *J. Steroid Biochem. Mol. Biol.* 89–90 (2004) 281–285.
- [25] P.H. Chou, W.C. Liao, K.W. Tsai, K.C. Chen, J.S. Yu, T.W. Chen, TACCO, a Database Connecting Transcriptome Alterations, Pathway Alterations and Clinical Outcomes in Cancers, *Sci. Rep.* 9 (2019) 3877.
- [26] Z. Tang, B. Kang, C. Li, T. Chen, Z. Zhang, GEPIA2: an enhanced web server for large-scale expression profiling and interactive analysis, *Nucleic Acids Res.* 47 (2019) W556–W560.
- [27] A. M. Olszewska, J. I. Nowak, K. Myszczyński, A. Slominski, M. A. Żmijewski, Dissection of an Impact of VDR and RXRa on Genomic Activity of 1,25(OH)<sub>2</sub>D<sub>3</sub> in A431 Squamous Cell Carcinoma. doi:<https://doi.org/10.2139/ssrn.4474791>.
- [28] A. Piotrowska, J. Wierzbicka, T. Ślebioda, M. Woźniak, R.C. Tuckey, A. T. Slominski, M.A. Żmijewski, Vitamin D derivatives enhance cytotoxic effects of H<sub>2</sub>O<sub>2</sub> or cisplatin on human keratinocytes, *Steroids* 110 (2016) 49–61.
- [29] A.T. Slominski, T.K. Kim, Z. Janjetovic, A.A. Brożyna, M.A. Żmijewski, H. Xu, et al., Differential and Overlapping Effects of 20,23(OH)<sub>2</sub>D<sub>3</sub> and 1,25(OH)<sub>2</sub>D<sub>3</sub> on Gene Expression in Human Epidermal Keratinocytes: Identification of aHR as an Alternative Receptor for 20,23(OH)<sub>2</sub>D<sub>3</sub>, *Int. J. Mol. Sci.* 19 (2018).
- [30] C. von Mering, M. Huynen, D. Jaeggi, S. Schmidt, P. Bork, B. Snel, STRING: a database of predicted functional associations between proteins, *Nucleic Acids Res.* 31 (2003) 258–261.
- [31] D. Prins, J. Groenendyk, N. Touret, M. Michalak, Modulation of STIM1 and capacitative Ca<sup>2+</sup> entry by the endoplasmic reticulum luminal oxidoreductase ERp57, *EMBO Rep.* 12 (11) (2011) 1182–1188.
- [32] M. Torres, D.B. Medinas, J.M. Matamala, U. Woelblier, V.H. Cornejo, T. Solda, C. Andreu, P. Rozas, S. Matus, N. Muñoz, C. Vergara, L. Cartier, C. Soto, M. Molinari, C. Hetz, The Protein-disulfide Isomerase ERp57 Regulates the Steady-state Levels of the Prion Protein, *J. Biol. Chem.* 290 (39) (2015) 23631–23645.
- [33] M. Chiavari, G.M.P. Ciotti, F. Canonico, F. Altieri, P.M. Lacial, G. Graziani, P. Navarra, L. Lisi, PDIA3 Expression in Glioblastoma Modulates Macrophage/Microglia Pro-Tumor Activation, *Int. J. Mol. Sci.* 21 (21) (2020) 8214.
- [34] M.A. Diaz Cruz, S. Karlsson, F. Szekeres, M. Faresjö, D. Lund, D. Larsson, Differential expression of protein disulfide-isomerase A3 isoforms, PDIA3 and PDIA3N, in human prostate cancer cell lines representing different stages of prostate cancer, *Molecular Biology Reports* 48 (3) (2021) 2429–2436.
- [35] T. Wasiewicz, A. Piotrowska, J. Wierzbicka, A. Slominski, M. Żmijewski, Antiproliferative Activity of Non-Calcemic Vitamin D Analogs on Human Melanoma Lines in Relation to VDR and PDIA3 Receptors, *Int. J. of Molecular Sciences* 19 (9) (2018) 2583.
- [36] L. Hu, D.D. Bikle, Y. Oda, Reciprocal role of vitamin D receptor on  $\beta$ -catenin regulated keratinocyte proliferation and differentiation, *J. Steroid Biochem. Mol. Biol.* 144 (2014) 237–241.
- [37] T. Warwick, M.H. Schulz, S. Günther, R. Gilsbach, A. Neme, C. Carlberg, R. P. Brandes, S. Seuter, A hierarchical regulatory network analysis of the vitamin D induced transcriptome reveals novel regulators and complete VDR dependency in monocytes, *Sci. Rep.* 11 (1) (2021).
- [38] M.A. Żmijewski, Nongenomic Activities of Vitamin D, *Nutrients* 14 (23) (2022) 5104.
- [39] M.A. Żmijewski, C. Carlberg, Vitamin D receptor(s): In the nucleus but also at membranes? *Experimental Dermatology* 29 (9) (2020) 876–884.
- [40] Y. Wang, A. Nizkorodov, K. Riemenscheider, C.S.D. Lee, R. Olivares-Navarrete, Z. Schwartz, B.D. Boyan, P.J. Marie, Impaired bone formation in Pdia3 deficient mice, *PLoS One* 9 (11) (2014) e112708.
- [41] A. Hettinghouse, R. Liu, C.J. Liu, Multifunctional molecule ERp57: From cancer to neurodegenerative diseases, *Pharmacol. Ther.* 181 (2018) 34–48.

- [42] S.T.T. Lam, C.J. Lim, Cancer Biology of the Endoplasmic Reticulum Lectin Chaperones Calreticulin, Calnexin and PDIA3/ERp57, *Prog. Mol. Subcell. Biol.* 59 (2021) 181–196.
- [43] C. Aureli, E. Gaucci, V. Arcangeli, C. Grillo, M. Eufemi, S. Chichiarelli, ERp57/PDIA3 binds specific DNA fragments in a melanoma cell line, *Gene* 524 (2) (2013) 390–395.
- [44] C. Grillo, C. D'Ambrosio, V. Consalvi, R. Chiaraluce, A. Scaloni, M. Maceroni, M. Eufemi, F. Altieri, DNA-binding activity of the ERp57 C-terminal domain is related to a redox-dependent conformational change, *J. Biol. Chem.* 282 (14) (2007) 10299–10310.
- [45] Y. Lan, C.E. Ovit, E.S. Cho, K.M. Maltby, Q. Wang, R. Jiang, Odd-skipped related 2 (Osr2) encodes a key intrinsic regulator of secondary palate growth and morphogenesis, *Development* 131 (2004) 3207–3216.
- [46] L. Verlinden, C. Kriebitzsch, G. Eelen, M. Van Camp, C. Leyssens, B.K. Tan, I. Beullens, A. Verstuyf, The odd-skipped related genes Osr1 and Osr2 are induced by 1,25-dihydroxyvitamin D3, *J. Steroid Biochem. Mol. Biol.* 136 (2013) 94–97.
- [47] J.W. Pike, L.A. Zella, M.B. Meyer, J.A. Fretz, S. Kim, Molecular actions of 1,25-dihydroxyvitamin D3 on genes involved in calcium homeostasis, *J. Bone Miner. Res.* 22 (Suppl 2) (2007) V16–V19.
- [48] E.K. Sutedja, D. Amarassaphira, H. Goenawan, Y. Susanti Pratiwi, N. Sylviana, B. Setiabudiawan, O. Suwarsa, R. Tina Dewi Judistiani, U. Supratman, R. Lesmana, Calcitriol Inhibits Proliferation and Potentially Induces Apoptosis in B16-F10 Cells, *Med. Sci. Monit. Basic Res.* 28 (2022) e935139.
- [49] J. García-Quiroz, R. García-Becerra, N. Santos-Martínez, E. Avila, F. Larrea, L. Díaz, Calcitriol stimulates gene expression of cathelicidin antimicrobial peptide in breast cancer cells with different phenotype, *J. Biomed. Sci.* 23 (2016) 78.
- [50] G. Weber, J.D. Heilborn, C.I. Chamorro Jimenez, A. Hammarsjö, H. Törmä, M. Stähle, Vitamin D induces the antimicrobial protein hCAP18 in human skin, *J. Invest Dermatol. United States* 124 (5) (2005) 1080–1082.
- [51] E. den Dekker, J.G. Hoenderop, B. Nilius, R.J. Bindels, The epithelial calcium channels, TRPV5 & TRPV6: from identification towards regulation, *Cell Calcium* 33 (2003) 497–507.
- [52] V. Lehen'kyi, B. Beck, R. Polakowska, M. Charveron, P. Bordat, R. Skryma, N. Prevarskaya, TRPV6 is a Ca<sup>2+</sup> entry channel essential for Ca<sup>2+</sup>-induced differentiation of human keratinocytes, *J. Biol. Chem.* 282 (31) (2007) 22582–22591.
- [53] I. Roodink, G. Kats, L. van Kempen, M. Grunberg, C. Maass, K. Verrijp, J. Raats, W. Leenders, Semaphorin 3E expression correlates inversely with Plexin D1 during tumor progression, *Am. J. Pathol.* 173 (6) (2008) 1873–1881.
- [54] S. Li, X. Zhao, S. Chang, Y. Li, M. Guo, Y. Guan, ERp57-small interfering RNA silencing can enhance the sensitivity of drug-resistant human ovarian cancer cells to paclitaxel, *Int. J. Oncol.* 54 (2019) 249–260.
- [55] Baber SR, Hyman AL, Kadowitz PJ. Role of COX-1 and -2 in prostanoid generation and modulation of angiotensin II responses. *Am J Physiol Heart Circ Physiol.* 2003; 285:H2399-410.
- [56] A. Ravid, O. Shenker, E. Buchner-Maman, C. Rotem, R. Koren, Vitamin D Induces Cyclooxygenase 2 Dependent Prostaglandin E2 Synthesis in HaCaT Keratinocytes, *Journal of Cellular Physiology* 231 (4) (2016) 837–843.
- [57] A. Shirvani, T.A. Kalajian, A. Song, M.F. Holick, Disassociation of Vitamin D's Calcemic Activity and Non-calcemic Genomic Activity and Individual Responsiveness: A Randomized Controlled Double-Blind Clinical Trial, *Sci. Rep.* 9 (2019) 17685.
- [58] N. Dandachi, N.J. Kelly, J.P. Wood, C.L. Burton, J.E. Radder, A.S. Leme, A. D. Gregory, S.D. Shapiro, Macrophage Elastase Induces TRAIL-mediated Tumor Cell Death through Its Carboxy-Terminal Domain, *Am. J. Respir. Crit. Care Med.* 196 (3) (2017) 353–363.
- [59] Houghton AM, Grisolano JL, Baumann ML, Kobayashi DK, Hautamaki RD, Nehring LC, et al. Macrophage elastase (matrix metalloproteinase-12) suppresses growth of lung metastases. *Cancer Res.* 2006;66:6149-55.
- [60] L.A. Cornelius, L.C. Nehring, E. Harding, M. Bolanowski, H.G. Welgus, D. K. Kobayashi, et al., Matrix metalloproteinases generate angiostatin: effects on neovascularization, *J. Immunol.* 161 (1998) 6845–6852.
- [61] A. Brockschmidt, D. Trost, H. Peterziel, K. Zimmermann, M. Ehrler, H. Grassmann, et al., KIAA1797/FOCAD encodes a novel focal adhesion protein with tumour suppressor function in gliomas, *Brain* 135 (2012) 1027–1041.
- [62] F. Brand, A. Förster, A. Christians, M. Bucher, C.M. Thomé, M.S. Raab, M. Westphal, T. Pietsch, A. von Deimling, G. Reifenberger, P. Claus, B. Hentschel, M. Weller, R.G. Weber, FOCAD loss impacts microtubule assembly, G2/M progression and patient survival in astrocytic gliomas, *Acta Neuropathol.* 139 (1) (2020) 175–192.
- [63] X. Mao, F. Luo, L.K. Boyd, B. Zhou, Y. Zhang, E. Stankiewicz, J. Marzec, N. Vasiljevic, Y. Yu, N. Feng, J. Xu, A. Lorincz, Y. Jiang, C. Chelala, G. Ren, D. M. Berney, S.-C. Zhao, Y.-J. Lu, NKAIN2 functions as a novel tumor suppressor in prostate cancer, *Oncotarget* 7 (39) (2016) 63793–63803.
- [64] R.H. Chou, H.C. Wen, W.G. Liang, S.C. Lin, H.W. Yuan, C.W. Wu, et al., Suppression of the invasion and migration of cancer cells by SERPINB family genes and their derived peptides, *Oncol. Rep.* 27 (2012) 238–245.
- [65] A. Smirnov, A.M. Lena, A. Cappello, E. Panatta, L. Anemona, S. Bischetti, M. Annicchiarico-Petruzzelli, A. Mauriello, G. Melino, E. Candi, ZNF185 is a p63 target gene critical for epidermal differentiation and squamous cell carcinoma development, *Oncogene* 38 (10) (2019) 1625–1638.
- [66] J. Zhang, H. Li, H. Li, D. Lin, X. Wang, K. Wang, V. Indio, Expression and Prognostic Significance of PDIA3 in Cervical Cancer, *Int J Genomics.* 2022 (2022) 1–25.
- [67] H. Zhang, Y. Zhou, Q. Cheng, Z. Dai, Z. Wang, F. Liu, F. Fan, B. Cui, H. Cao, PDIA3 correlates with clinical malignant features and immune signature in human gliomas, *Aging (Albany NY)* 12 (15) (2020) 15392–15413.
- [68] Y. He, F. Shao, W. Pi, C. Shi, Y. Chen, D. Gong, B. Wang, Z. Cao, K. Tang, M. Zhao, Largescale Transcriptomics Analysis Suggests Over-Expression of BGH3, MMP9 and PDIA3 in Oral Squamous Cell Carcinoma, *PLoS One* 11 (1) (2016) e0146530.
- [69] S.V. Puram, I. Tirosh, A.S. Parikh, A.P. Patel, K. Yizhak, S. Gillespie, C. Rodman, C. L. Luo, E.A. Mroz, K.S. Emerick, D.G. Deschler, M.A. Varvares, R. Mylvaganam, O. Rozenblatt-Rosen, J.W. Rocco, W.C. Faquin, D.T. Lin, A. Regev, B.E. Bernstein, Single-Cell Transcriptomic Analysis of Primary and Metastatic Tumor Ecosystems in Head and Neck Cancer, *Cell* 171 (7) (2017) 1611–1624.e24.
- [70] E. Gaucci, D. Raimondo, C. Grillo, L. Cervoni, F. Altieri, G. Nittari, M. Eufemi, S. Chichiarelli, Analysis of the interaction of calcitriol with the disulfide isomerase ERp57, *Sci. Rep.* 6 (1) (2016).
- [71] Y. Ma, L. Zhang, X. Huang, Genome modification by CRISPR/Cas9, *FEBS J.* 281 (23) (2014) 5186–5193.
- [72] Andrews, S. K. F., Seconds-Pichon, A., Biggins, F., and Wingett, S. FastQC: a quality control tool for high throughput sequence data. <https://www.bioinformatics.babraham.ac.uk/projects/fastqc>. 2015.
- [73] Bolger AM, Lohse M, Usadel B. Trimmomatic: a flexible trimmer for Illumina sequence data. *Bioinformatics.* 2014;30:2114-20.
- [74] Dobin A, Davis CA, Schlesinger F, Drenkow J, Zaleski C, Jha S, et al. STAR: ultrafast universal RNA-seq aligner. *Bioinformatics.* 2013;29:15-21.
- [75] Liao Y, Smyth GK, Shi W. featureCounts: an efficient general purpose program for assigning sequence reads to genomic features. *Bioinformatics.* 2014;30:923-30.
- [76] M.I. Love, W. Huber, S. Anders, Moderated estimation of fold change and dispersion for RNA-seq data with DESeq2, *Genome Biol.* 15 (2014) 550.
- [77] Alexa A RJ. *topGO: Enrichment Analysis for Gene Ontology*. R package version 2.48.0. 2022.
- [78] M C. *org.Hs.eg.db: Genome wide annotation for Human*. R package version 3.8.2. 2019.
- [79] Team, C. R. R: A Language and Environment for Statistical Computing. <https://www.R-project.org2021>.
- [80] D. Szklarczyk, A.L. Gable, D. Lyon, A. Junge, S. Wyder, J. Huerta-Cepas, et al., STRING v11: protein-protein association networks with increased coverage, supporting functional discovery in genome-wide experimental datasets, *Nucleic Acids Res.* 47 (2019) D607–D613.

## Article

# Protein Disulfide Isomerase Family A Member 3 Knockout Abrogate Effects of Vitamin D on Cellular Respiration and Glycolysis in Squamous Cell Carcinoma

Joanna I. Nowak <sup>1</sup>, Anna M. Olszewska <sup>1</sup>, Oliwia Król <sup>2</sup> and Michał A. Żmijewski <sup>1,\*</sup>

<sup>1</sup> Department of Histology, Medical University of Gdansk, 1a Dębinki, 80-211 Gdansk, Poland; j.chorzepa@gumed.edu.pl (J.I.N.); anna.olszewska@gumed.edu.pl (A.M.O.)

<sup>2</sup> Department of Biochemistry, Medical University of Gdansk, 80-211 Gdansk, Poland; oliwia.krol@gumed.edu.pl

\* Correspondence: mzmijewski@gumed.edu.pl; Tel.: +48-583-491455

**Abstract:** PDIA3 is an endoplasmic reticulum disulfide isomerase, which is involved in the folding and trafficking of newly synthesized proteins. PDIA3 was also described as an alternative receptor for the active form of vitamin D (1,25(OH)<sub>2</sub>D<sub>3</sub>). Here, we investigated an impact of PDIA3 in mitochondrial morphology and bioenergetics in squamous cell carcinoma line A431 treated with 1,25(OH)<sub>2</sub>D<sub>3</sub>. It was observed that PDIA3 deletion resulted in changes in the morphology of mitochondria including a decrease in the percentage of mitochondrial section area, maximal diameter, and perimeter. The 1,25(OH)<sub>2</sub>D<sub>3</sub> treatment of A431ΔPDIA3 cells partially reversed the effect of PDIA3 deletion increasing aforementioned parameters; meanwhile, in A431WT cells, only an increase in mitochondrial section area was observed. Moreover, PDIA3 knockout affected mitochondrial bioenergetics and modulated STAT3 signaling. Oxygen consumption rate (OCR) was significantly increased, with no visible effect of 1,25(OH)<sub>2</sub>D<sub>3</sub> treatment in A431ΔPDIA3 cells. In the case of Extracellular Acidification Rate (ECAR), an increase was observed for glycolysis and glycolytic capacity parameters in the case of non-treated A431WT cells versus A431ΔPDIA3 cells. The 1,25(OH)<sub>2</sub>D<sub>3</sub> treatment had no significant effect on glycolytic parameters. Taken together, the presented results suggest that PDIA3 is strongly involved in the regulation of mitochondrial bioenergetics in cancerous cells and modulation of its response to 1,25(OH)<sub>2</sub>D<sub>3</sub>, possibly through STAT3.

**Keywords:** PDIA3; squamous cell carcinoma; mitochondria bioenergetic; vitamin D

**Citation:** Nowak, J.I.; Olszewska, A.M.; Król, O.; Żmijewski, M.A. Protein Disulfide Isomerase Family A Member 3 Knockout Abrogate Effects of Vitamin D on Cellular Respiration and Glycolysis in Squamous Cell Carcinoma. *Nutrients* **2023**, *15*, 4529. <https://doi.org/10.3390/nu15214529>

Academic Editor: Paweł Pludowski

Received: 4 October 2023

Revised: 20 October 2023

Accepted: 23 October 2023

Published: 25 October 2023



**Copyright:** © 2023 by the authors. Licensee MDPI, Basel, Switzerland. This article is an open access article distributed under the terms and conditions of the Creative Commons Attribution (CC BY) license (<https://creativecommons.org/licenses/by/4.0/>).

## 1. Introduction

Protein disulfide isomerases are key oxidoreductase enzymes that play a role in the proper folding and assembling of proteins and their complexes [1]. An oxidoreductase family member, PDIA3 protein, has a broad range of functions from promoting protein folding in ER [2,3], participating in signal transduction through STAT3 in the nucleus [4,5], to pro-apoptotic activities in mitochondria [6]. Moreover, it was shown that PDIA3 can be localized in the mitochondria-associated membranes (MAMs) region of the endoplasmic reticulum closely associated with mitochondria [7,8]. Several studies have shown that PDIA3 functions as a chaperone to STAT3 protein and can modulate its transcriptional activity by regulating phosphorylation at the Y705 site [4,5,9,10]. On the other hand, phosphorylation of STAT3 at S727 residue alone targets the import of this transcription factor into mitochondria [11]. Moreover, it was suggested, that PDIA3 can suppress mitochondrial bioenergetic functions by inhibiting phosphorylation of the S727 site [12]. PDIA3 has been also linked to various diseases from neurodegenerative to cancer [13]. It was postulated that PDIA3 can be treated as a chemoprevention target and prognostic marker in cancer patients [14,15].

An active form of vitamin D,  $1,25(\text{OH})_2\text{D}_3$ , is a steroid hormone that regulates calcium–phosphorus homeostasis along with various cellular processes [16,17]. Canonically, vitamin D acts through the complex of its receptors: VDR and RXR, regulating the expression of hundreds of genes in the human genome [18,19]. However, not all effects of  $1,25(\text{OH})_2\text{D}_3$  can be related to the genomic action of VDR–RXR heterodimer [20,21]. Consequently, PDIA3 was identified as a membrane-bound receptor for the active form of vitamin D ( $1,25\text{D}_3$ -MARRS), responsible for non-genomic responses to the hormone [22–24]. It was shown that PDIA3 can form a complex with caveolin-1 and subsequently activated phospholipase A2-activating protein (PLAA) [25,26]. Thus, leading to the rapid action of  $1,25(\text{OH})_2\text{D}_3$  via PKC [27]. Our recent studies have shown that genomic activity of  $1,25(\text{OH})_2\text{D}_3$  strictly depends on VDR and only partially on RXR $\alpha$  [28], while deletion of *PDIA3* significantly modulates the response [29]. Moreover, it was postulated that VDR can regulate the transcription of mitochondrial genes and directly interact with mitochondrial DNA [30]. However, several studies have shown the direct effects of  $1,25(\text{OH})_2\text{D}_3$  on ion transport [31,32], including activity of mitochondrial membrane potassium channels [33]. Finally, pre-incubation with  $1,25(\text{OH})_2\text{D}_3$  significantly deepened the effect of anti-cancer drugs on the mitochondrial respiration of patient-derived melanoma cells [34].

In our previous study, we established that PDIA3 is involved in  $1,25(\text{OH})_2\text{D}_3$  action in the manner of gene expression profile and range of phenotypic effects, such as proliferation or migration [29]. Here, the impact of *PDIA3* deletion on mitochondrial morphology and bioenergetics in squamous cell carcinoma (A431) and its potential role in the action of vitamin D on mitochondria were investigated for the first time.

## 2. Materials and Methods

### 2.1. The $1,25(\text{OH})_2\text{D}_3$

The  $1,25(\text{OH})_2\text{D}_3$  was purchased from Sigma-Aldrich (St. Louis, MO, USA). Stock solutions of  $1,25(\text{OH})_2\text{D}_3$  were dissolved in ethanol and stored at  $-20\text{ }^\circ\text{C}$ . At 100 nM concentration,  $1,25(\text{OH})_2\text{D}_3$  was used in all experiments (the concentration of solvent (ethanol) was  $<0.05\%$ ).

### 2.2. Cell Cultures

Immortalized human basal cell carcinoma cell line (A431) was obtained from Synthego Corporation (Menlo Park, CA, USA). *PDIA3* knockout cell line was obtained with CRISPR/Cas9 technology as previously described [29]. The early passages 6 to 15 (after clonal selection) were used and deletion of *PDIA3* was routinely confirmed via Western blot. Cells were cultured in DMEM high glucose medium (4.5 g/L) with the addition of 10% FBS, penicillin (10,000 units/mL), and streptomycin (10 mg/mL) (Sigma-Aldrich; Merck KGaA). Cell cultures were performed in the incubator with 5%  $\text{CO}_2$  at  $37\text{ }^\circ\text{C}$ . Before treatment with  $1,25(\text{OH})_2\text{D}_3$ , medium was changed to DMEM with 2% charcoal-stripped FBS.

### 2.3. Transmission Electron Microscopy (TEM)

The A431 $\Delta$ *PDIA3* cells were seeded onto a Petri dish (10 cm; VWR, Gdansk, Poland) at a density of  $1 \times 10^6$  cells/plate standard medium and after 24 h treated with 100 nM  $1,25(\text{OH})_2\text{D}_3$ . Consequently, the cells were fixed in 2.5% glutaraldehyde in 0.1 mM sodium-cacodylate buffer, scratched, and centrifuged. The cell pellets were then postfixed in 2% osmium tetroxide, dehydrated in ethanol, and infiltrated with a mixture of propylene. The pelleted cells were subsequently embedded to polymerize. Ultrathin sections (70 nm) were cut and, after dehydration, stained with uranyl acetate (Plano GmbH, Wetzlar, Germany) and lead citrate (Electron Microscopy Sciences, Hatfield, PA, USA). Samples were analyzed with an electron microscope (JEOL JEM-1200 EXII, University Park, PA, USA) at an acceleration voltage of 80 kV. Mitochondria from EM photos were counted in cellSens Olympus Software v 4.1.

#### 2.4. Seahorse Analysis

The effects of 1,25(OH)<sub>2</sub>D<sub>3</sub> on the mitochondrial function of A431  $\Delta$ PDIA3 were measured using the Seahorse Mito Stress Test following the manufacturer's protocol. Briefly,  $2 \times 10^4$  cells/well were seeded on a Seahorse plate and after 24 h treated with 100 nM 1,25(OH)<sub>2</sub>D<sub>3</sub> for 24 h. All essential compounds were diluted to final concentrations of 1  $\mu$ M for Oligomycin, 1  $\mu$ M for Carbonyl cyanide 4-(trifluoromethoxy) phenylhydrazone (FCCP), and 1  $\mu$ M for Antimycin A/Rotenone, and cells were prepared according to Seahorse protocols. The experiment was run with Seahorse XF24 (Agilent Technologies, Santa Clara, CA, USA). After the Seahorse analysis, the cells were lysed with modified RIPA buffer supplemented with Roche (Basel, Switzerland) protease and phosphatase inhibitors cocktail (Roche, Basel, Switzerland), and protein concentration was measured with bicinchoninic acid assay (Thermo Fisher Scientific, Waltham, MA, USA) for data normalization. Each experiment was repeated at least three times, independently. The data were analyzed with Wave software version 1.1.1.3 (Agilent Technologies, Santa Clara, CA, USA), and the Student's *t*-test was used to compare the mean fluorescence values between different experimental conditions. Basal respiration was calculated after subtraction of non-mitochondrial respiration (remaining OCR after Antimycin A addition). ATP-linked OCR was derived as the difference between basal and Antimycin A-inhibited OCR. Proton leak was calculated as the difference between OCR following Oligomycin A inhibition and OCR following Antimycin A inhibition. Maximal respiration was measured following the addition of FCCP. Spare capacity was calculated based on the difference between basal respiration and maximal respiration.

#### 2.5. Fluorescent Probes

For fluorometric measurements, cells were seeded in 8-well chambers (MoBiTec Molecular Biology, Goettingen, Germany) at a density of 200,000 cells/well and incubated overnight (37 °C, 5% CO<sub>2</sub>). The next day, the medium was removed and cells were incubated with diluted to a final concentration of 2  $\mu$ M JC-1 (Thermo Fisher Scientific, Waltham, MA, USA) or 100 nM MitoGreen (Thermo Fisher Scientific, Waltham, MA, USA) probes for 20 min. Then, solution containing fluorescent probe was replaced with 100 nM 1,25(OH)<sub>2</sub>D<sub>3</sub> medium solution, and cells were grown for 24 h with live imaging under a microscope Olympus cell Vivo IX83 (Tokyo, Japan). For JC-1 (Thermo Fisher Scientific, Waltham, MA, USA) the ratio of red/green fluorescence intensity was analyzed with cellSens Olympus software version 4.1. For MitoGreen calculation, fluorescence intensity measurements were normalized against cell numbers before being expressed as percentages of control values.

#### 2.6. Western Blotting

A431-derived cell lines were treated with 100 nM 1,25(OH)<sub>2</sub>D<sub>3</sub> for 4, 8, and 24 h. The medium was removed from the plate, and cells were washed twice with PBS and were scratched from the plate. The solution was moved to an Eppendorf tube and centrifuged at  $16,000 \times g$  for 10 min. The received cell sediment was dissolved in 100  $\mu$ L of RIPA buffer (Thermo Fisher, Waltham, MA, USA). Concentration was determined by a modified Bradford Assay. For SDS-PAGE electrophoresis, 10% bottom gel and 5% upper gel were used. An equal amount of protein (20  $\mu$ g) was loaded into each well. Electrophoresis was run at 90–110 V in the Bio-Rad apparatus. Proteins were transferred to PVDF membranes with the use of the Trans-Blot Turbo system (Bio-Rad, Hercules, CA, USA). After, the transfer membranes were blocked in 5% milk dissolved in TBS-T. The membranes were incubated with primary antibodies anti-STAT3 (Abclonal, Woburn, MA, USA), anti-pSTAT3 (Y705) (Abclonal, Woburn, MA, USA), or anti-pSTAT3 (S727) (Abclonal, Woburn, MA, USA), overnight at 4 °C. For loading control, membranes were stripped and re-probed with anti- $\beta$ -actin antibodies (Abclonal, Woburn, MA, USA). Then, they were incubated with proper



secondary fluorescent antibodies (AlexaFluor® 790 or AlexaFluor® 680 from Jackson ImmunoResearch, West Grove, PA, USA). Bands were visualized with Odyssey Clx system, and densitometry of bands was performed with Image Studio Software Version 5.2.

### 2.7. Immunofluorescence Staining

A431 cell lines were seeded in 8-well imaging chambers (MoBiTec Molecular Biology, Germany) at a density of 200,000 cells/well, incubated overnight (37 °C, 5% CO<sub>2</sub>). The next day, cells were treated with 1,25(OH)<sub>2</sub>D<sub>3</sub> in DMEM medium supplemented with 2% charcoal-stripped FBS and 100 U/mL penicillin/streptomycin. After incubation time (4, 8, 24 h), cells were rinsed three times with PBS and fixed with 4% (*v/v*) formaldehyde solution, then washed three times with PBS, and permeabilized with 0.1% Triton X-100, blocked with 10% BSA in PBS for 1 h at RT and incubated with primary antibodies at 4 °C overnight (anti-STAT3, Abclonal, Woburn, MA 01801, United States). Following, the cells were rinsed three times with PBS, incubated with secondary antibodies for 1 h at RT (Alexa Fluor 488 anti-rabbit, Invitrogen, Waltham, MA, USA), then rinsed again with PBS, incubated with DAPI solution, and mounted with DAKO fluorescence mounting medium (S3025, Agilent Technologies, Santa Clara, CA, USA). The cells were visualized using fluorescence microscopy (Olympus Cell-Vivo IX 83, Japan) with camera ORCA-FLASH 4.0 and 60X objective (Hamamatsu, Shizuoka, Japan).

### 2.8. Bioinformatic Analysis

Transcriptomic data from a previous study were used to define mitochondrial genes expressed in A431Δ*PDIA3* cells after 1,25(OH)<sub>2</sub>D<sub>3</sub> treatment [29]. Venn analysis was performed with the online available tool [35].

### 2.9. Statistical Analysis

Statistical analysis was performed using GraphPad Prism version 7.05 (GraphPad Software, Inc., La Jolla, CA, USA). Data are presented as mean ± SD and were analyzed with a Student's *t*-test (for two groups) or one-way ANOVA with appropriate post hoc tests (for more than two groups). Statistically significant differences are illustrated with asterisks: \* *p* < 0.05, \*\* *p* < 0.01, \*\*\* *p* < 0.001, or \*\*\*\* *p* < 0.0001.

## 3. Results

### 3.1. Deletion of *PDIA3* and 1,25(OH)<sub>2</sub>D<sub>3</sub> Treatment Affect Morphology of Mitochondria

The knockout of *PDIA3* in the A431 squamous cell carcinoma cell line was generated with the use of CRISPR/Cas9 technology as previously described [29]. The effects of *PDIA3* deletion and 1,25(OH)<sub>2</sub>D<sub>3</sub> treatment on the morphology of mitochondria were investigated using transmission electron microscopy (TEM) (Figure 1A). A knockout of the *PDIA3* gene resulted in a twofold decrease in volume of mitochondria in comparison to wild type A431 (A431WT) cells, as shown by the percentage of the mitochondria section in whole cells observed using TEM. The treatment of A431WT or A431Δ*PDIA3* with 1,25(OH)<sub>2</sub>D<sub>3</sub> for 24 h resulted in a significant increase in the percentage of the mitochondria section (Figure 1B), but also in a reduction in the mitochondria diameter (Figure 1C) and perimeter (Figure 1D). The 1,25(OH)<sub>2</sub>D<sub>3</sub> treatment of A431Δ*PDIA3* cells partially reversed the effect of *PDIA3* deletion by increasing the aforementioned parameters, but there was no visible effect on A431WT cells. Interestingly, the elongation factor was not impaired by *PDIA3* deletion, but was decreased by 1,25(OH)<sub>2</sub>D<sub>3</sub> treatment in the absence of *PDIA3* (Figure 1E). Further investigation with use of fluorescence probes revealed that 1,25(OH)<sub>2</sub>D<sub>3</sub> treatment noticeably affected mitochondrial surface area and mitochondrial membrane potential in A431Δ*PDIA3* cells; however, the effect was not statistically significant (Figure 2A,B).

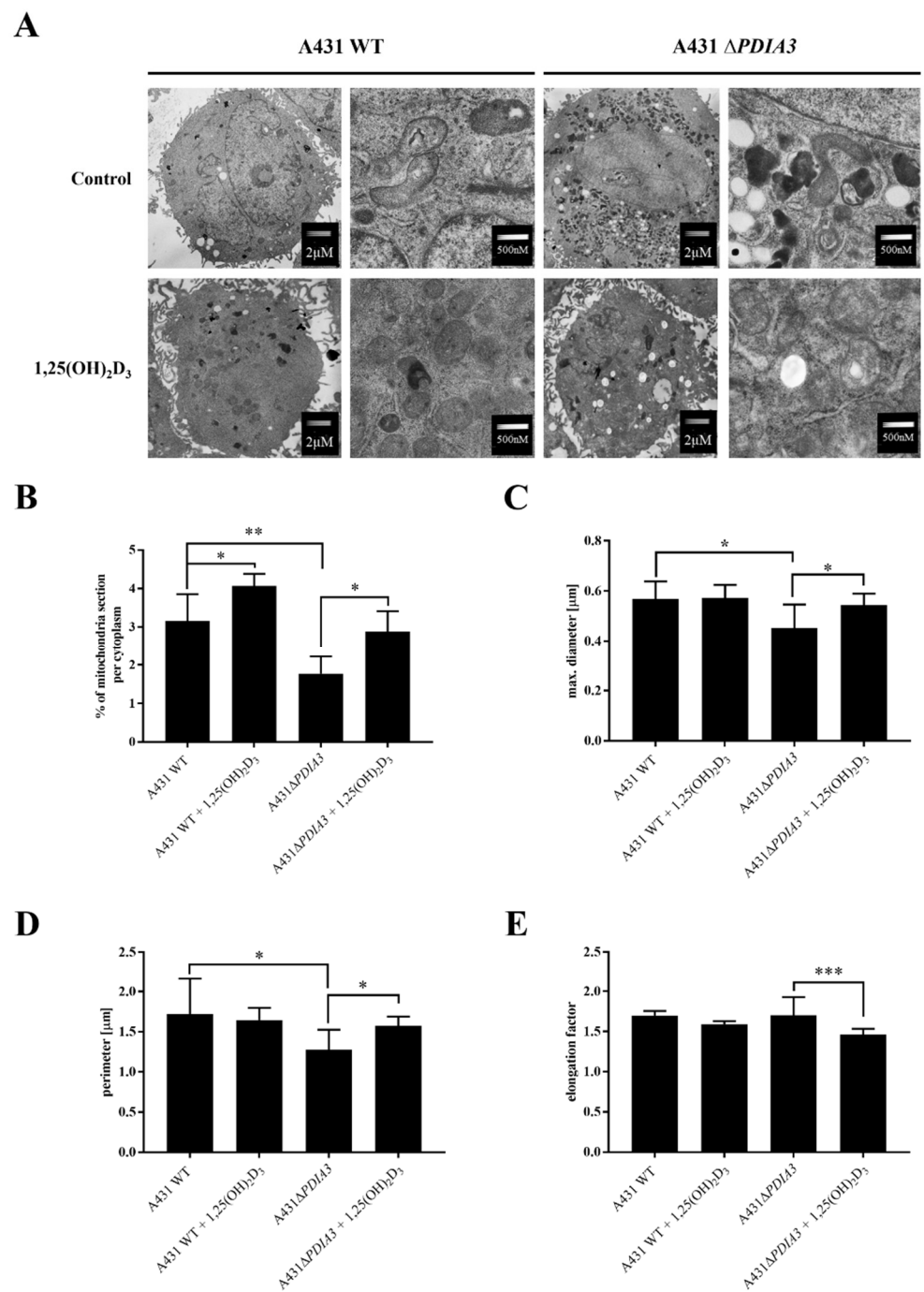


**Figure 1.** The 1,25(OH)<sub>2</sub>D<sub>3</sub> treatment and PDIA3 deletion affect the morphology of mitochondria. (A) EM micrographs representing morphology of mitochondria of A431WT and A431 $\Delta$ PDIA3 cells non-treated/treated with 1,25(OH)<sub>2</sub>D<sub>3</sub> at two different magnifications. (B) Percentage of mitochondria section through the cytoplasm of A431WT and  $\Delta$ PDIA3 cells after 1,25(OH)<sub>2</sub>D<sub>3</sub> treatment. Assessment of another mitochondrial parameter of A431 strains like (C) maximal diameter and (D) perimeter. Data are expressed as mean  $\pm$  SEM. \*  $p < 0.05$ , \*\*  $p < 0.005$ , \*\*\*  $p < 0.001$  (E).

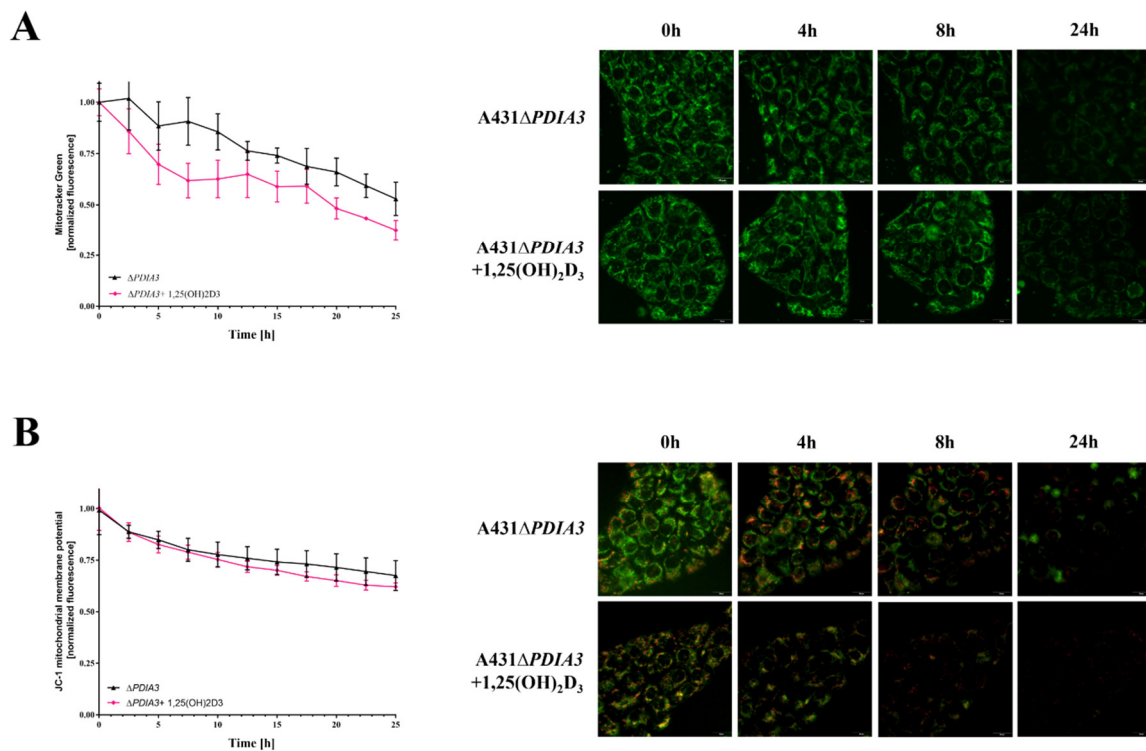


**Figure 2.** Mitochondrial surface area and membrane potential in *PDIA3* knockout A431 cell line after  $1,25(OH)_2D_3$  treatment. **(A)** The mitochondrial surface area in A431 $\Delta PDIA3$  cells stained with MitoTracker Green dye imaged with live microscopy Olympus cell Vivo IX83. **(B)** Mitochondrial membrane potential in A431  $\Delta PDIA3$  cells stained with JC-1 fluorescence probe with the use of live microscopy Olympus cell Vivo IX83.

### 3.2. *PDIA3* Inhibits Mitochondrial Functions and Affects the Response to $1,25(OH)_2D_3$ Treatment

The effect of  $1,25(OH)_2D_3$  treatment on mitochondrial bioenergetics in A431WT and A431 $\Delta PDIA3$  was determined using the Seahorse XF24. An oxygen consumption rate (OCR) was monitored in real-time with the following addition of Oligomycin, FCCP, Rotenone, and Antimycin. It was observed that in A431 $\Delta PDIA3$ , the OCR, expressed in pmoles/min/mg of protein, is significantly higher than in A431WT cells, and  $1,25(OH)_2D_3$  treatment did not affect those results (Figure 3A). Overall, it was shown that deletion of *PDIA3* enhances all parameters of oxidative phosphorylation; however, despite the clear trends, some results did not reach statistical significance. To increase the strength of comparison, data for treated and non-treated cells were combined, and the effect of *PDIA3* on cellular bioenergetics was reanalyzed (Figure 3). In a case of basal respiration (Figure 3B) and ATP-linked respiration (Figure 3D), a statistically significant increase was observed after deletion of *PDIA3*, and for  $1,25(OH)_2D_3$  treated cells decrease in A431WT and increase in A431 $\Delta PDIA3$  was observed (Figure 3B). Further *PDIA3* deletion increased maximal respiration, but this parameter was not affected by  $1,25(OH)_2D_3$  treatment (Figure 3C). Interestingly, for non-mitochondrial oxygen consumption, a threefold increase in A431 $\Delta PDIA3$  cells was observed, with no further effect of  $1,25(OH)_2D_3$  (Figure 3E). Similarly, an increase in proton leakage was observed, but with adverse trends in A431WT and A431 $\Delta PDIA3$  cells after  $1,25(OH)_2D_3$  addition (decrease in A431WT and increase in A431 $\Delta PDIA3$ ; Figure 3F). A mitochondrial spare capacity was increased twofold in A431 $\Delta PDIA3$  cells in comparison to wild-type cells. No effect of  $1,25(OH)_2D_3$  treatment on this parameter was observed (Figure 3G). Next, the impact of *PDIA3* knockout and/or  $1,25(OH)_2D_3$  treatment on glycolysis was investigated using glycolytic stress tests. The Extracellular Acidification Rate (ECAR) was measured in real-time by adding glucose to the medium on Seahorse XF24. Significant changes in the ECAR were observed between the

30th and 70th minute of the assay in the case of non-treated A431WT cells versus A431 $\Delta$ *PDIA3* cells (Figure 4A). Deletion of *PDIA3* gene enhanced levels of glycolysis and other parameters (Figure 4B,E), except for glycolytic capacity and reserve (Figure 4C,D). In general, treatment of A431WT cells with 1,25(OH) $_2$ D $_3$  resulted in a decrease in glycolysis (Figure 4B), glycolytic capacity (Figure 4C), glycolytic reserve (Figure 4D), and non-glycolytic acidification (Figure 4E), but the results were marginally statistically significant. The tendency was not so pronounced in A431 $\Delta$ *PDIA3* cells.

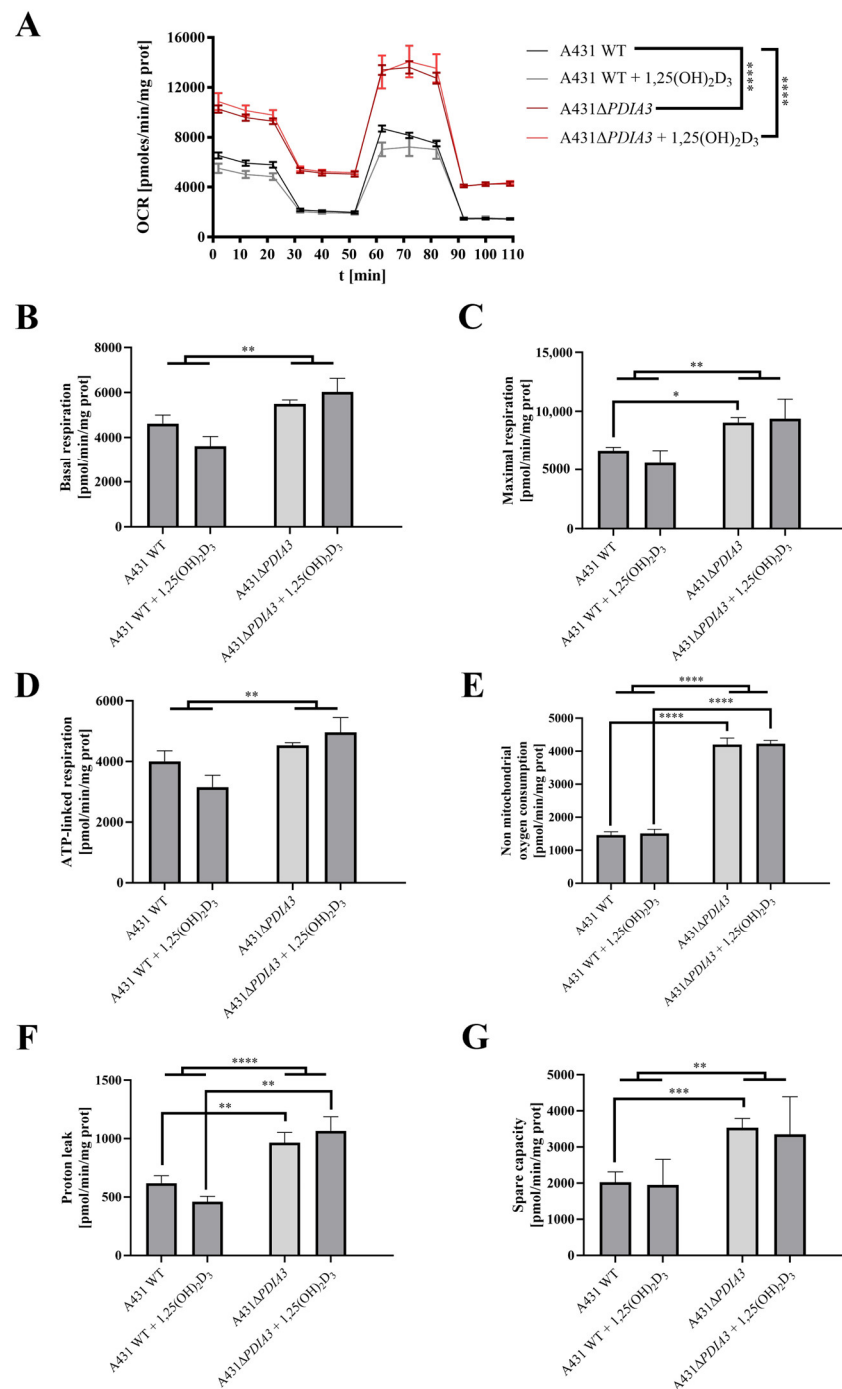


**Figure 3.** *PDIA3* deletion increases mitochondrial bioenergetics and abolishes the effect of 1,25(OH) $_2$ D $_3$  treatment in A431 cells. (A) Representative traces of mitochondrial oxygen consumption rate of A431WT and A431 $\Delta$ *PDIA3* cells after 24 h of 1,25(OH) $_2$ D $_3$  treatment. Mitochondrial respiration parameters: (B) basal respiration, (C) maximal respiration, (D) ATP-linked respiration, (E)

non-mitochondrial oxygen consumption, (F) proton leak, and (G) spare capacity. Data are expressed as mean  $\pm$  SEM. \*  $p < 0.05$ , \*\*  $p < 0.005$ , \*\*\*  $p < 0.001$ , and \*\*\*\*  $p < 0.0001$ .

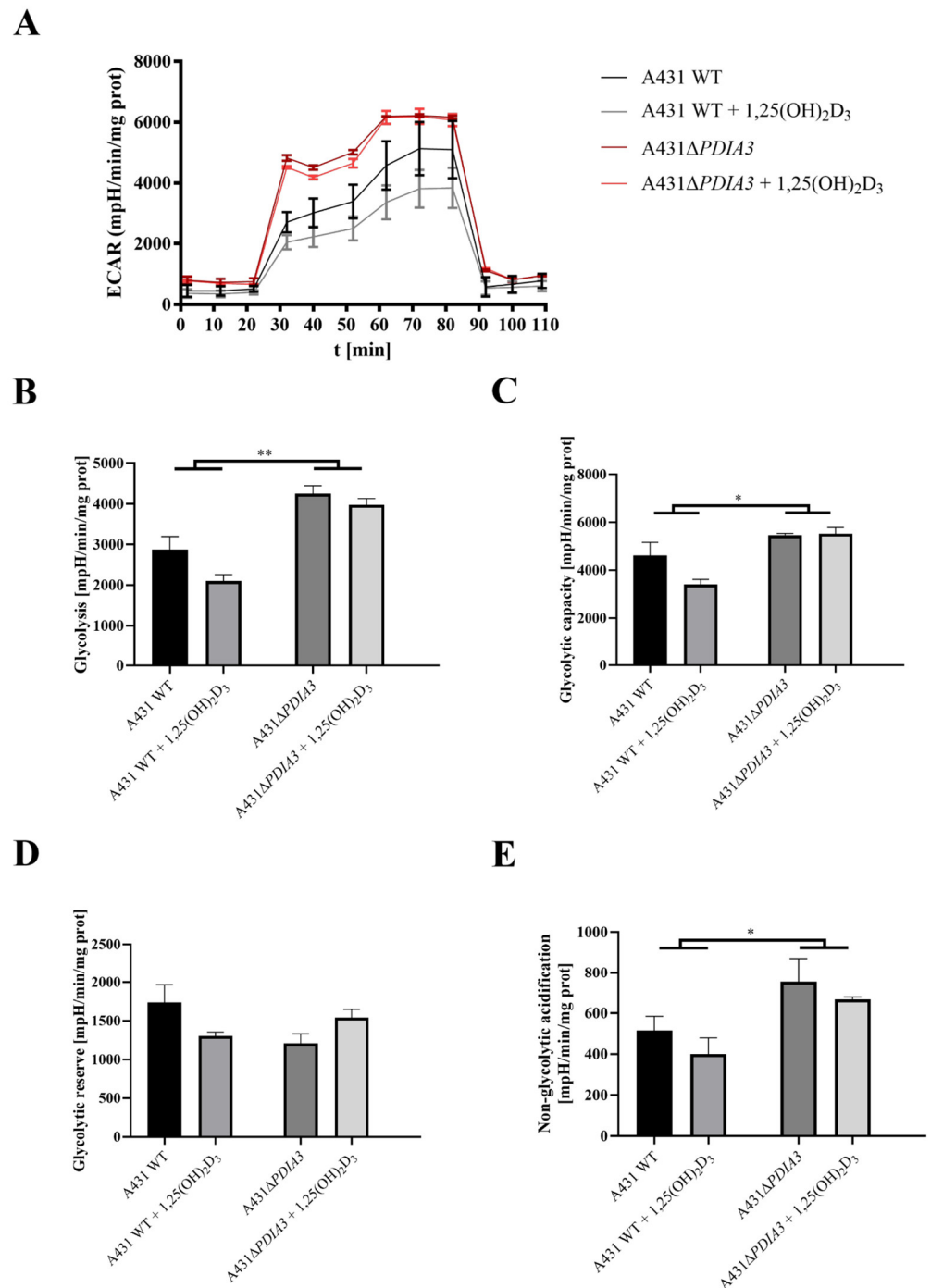


**Figure 4.** *PDIA3* deletion disrupts glycolytic functions and response to 1,25(OH)<sub>2</sub>D<sub>3</sub> treatment of A431 strains. (A) Representative traces of mitochondrial Extracellular Acidification Rate of A431WT and A431Δ*PDIA3* cells after 24 h of 1,25(OH)<sub>2</sub>D<sub>3</sub> treatment. Mitochondrial glycolytic parameters: (B) glycolysis, (C) glycolytic capacity, (D) glycolytic reserve, and (E) non-glycolytic acidification. Data are expressed as mean  $\pm$  SEM. \*  $p < 0.05$ , \*\*  $p < 0.005$ .

### 3.3. *PDIA3* Knockout Affects the Expression of Mitochondrial Genes

In previous work, the effects of 24 h incubation with 1,25(OH)<sub>2</sub>D<sub>3</sub> at 100 nM concentration on the transcriptome of A431Δ*PDIA3* were studied [29]. To assess the impact of

*PDIA3* on the expression of the genes related to mitochondria, a previously obtained dataset of differentially expressed genes (DEGs; false discovery rate (FDR) = 0.05) from *A431ΔPDIA3* non-treated and 1,25(OH)<sub>2</sub>D<sub>3</sub>-treated cells was used. The dataset was compared with mitochondria-associated genes (mtDEGs) from MitoCarta 3.0 database [36] via Venn analysis [35] (Supplementary Table S1), followed by gene ontology (GO) analysis [37]. The data are deposited in Sequence Read Archive (SRA) under accession number PRJNA926032. Venn analysis revealed 5831 DEGs expressed after *PDIA3* deletion in *A431* cells and 4372 DEGs after treatment of *A431ΔPDIA3* cells with 1,25(OH)<sub>2</sub>D<sub>3</sub>. Among those, 302 mtDEGs identified in *A431ΔPDIA3* were affected solely by *PDIA3* deletion, while 149 mtDEGs were changed by 1,25(OH)<sub>2</sub>D<sub>3</sub> treatment (Figure 5A). Interestingly, 111 mtDEGs were commonly regulated after *PDIA3* deletion and 1,25(OH)<sub>2</sub>D<sub>3</sub> treatment. GO analysis of molecular processes revealed that deletion of *PDIA3* in *A431* cells alone mainly affected cellular respiration (GO:0045333), aerobic electron transport chain (GO:0019646), and mitochondrial ATP synthesis (GO:0042775) (Figure 5B). Curiously, the 1,25(OH)<sub>2</sub>D<sub>3</sub> treatment of knockout cells changed entirely different molecular processes linked to mitochondrial transcription/translation, such as mitochondrial translation (GO:0032543), mitochondrial gene expression (GO:0140053), and mitochondrial transport (GO:0006839) (Figure 5C). mtDEGs affected by both deletion of *PDIA3* and 1,25(OH)<sub>2</sub>D<sub>3</sub> treatment were connected with mitochondrion organization (GO:0007005), glutamate (GO:0006536), and dicarboxylic acid (GO:0043648) metabolic processes (Figure 5D).

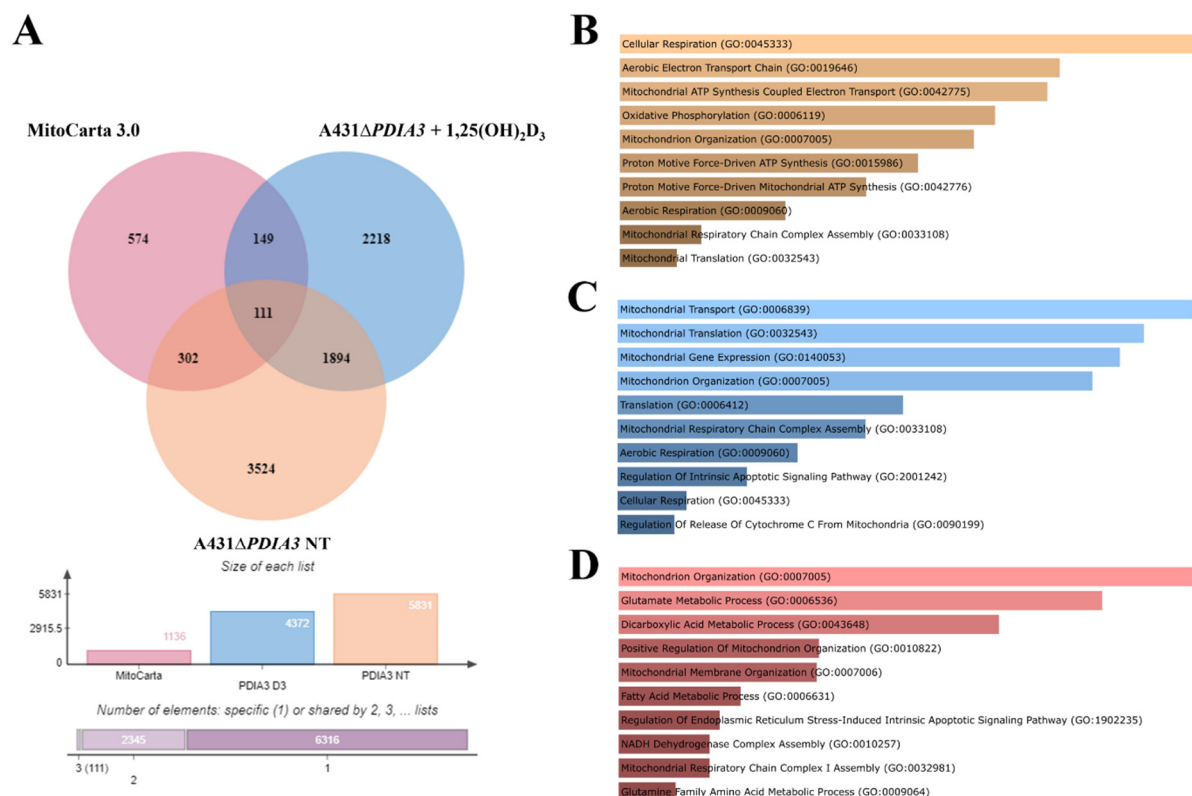


**Figure 5.** *PDIA3* deletion alters the expression of mitochondrial genes after 1,25(OH)<sub>2</sub>D<sub>3</sub> treatment in *A431* cells. (A) Comparison of mitochondrial genes from MitoCarta 3.0, *A431*WT, and *A431ΔPDIA3* cells treated with 1,25(OH)<sub>2</sub>D<sub>3</sub>. Gene ontology of mtDEGs from *A431ΔPDIA3* in terms of (B) biological process, (C) molecular functions and (D) cellular components.

### 3.4. *PDIA3* or *VDR* Deletion Disrupts *STAT3* Signaling Changing Response to 1,25(OH)<sub>2</sub>D<sub>3</sub>

As *STAT3*–*PDIA3* interaction is widely described in the context of cell signaling, including regulation of cellular respiratory [4,12,38], it was checked whether 1,25(OH)<sub>2</sub>D<sub>3</sub>



can affect this signaling and, if so, how PDIA3 is involved in the process. To elucidate an impact of 1,25(OH)<sub>2</sub>D<sub>3</sub> on STAT3 translocation into the nucleus, immunofluorescent staining was performed (Figure 6A). In the case of A431WT cells, we observed translocation of STAT3 into the nucleus after 1,25(OH)<sub>2</sub>D<sub>3</sub> treatment, with the highest intensity ratio after 8 h of incubation. Deletion of the *VDR* (vitamin D receptor) decreased the basal signal, both nuclear and cytoplasm, resulting in a higher nucleus/cytoplasm ratio for STAT3, but the effect of 1,25(OH)<sub>2</sub>D<sub>3</sub> treatment was not observed. Interestingly, deletion of PDIA3 did not change basal intensity for STAT3, but similarly to A431Δ*VDR* cells, there was no visible effect of 1,25(OH)<sub>2</sub>D<sub>3</sub> treatment (Figure 6B). Secondly, levels of STAT3 protein and its two phosphorylation sites (Ser727, Tyr705) were examined using Western blot analysis (Figure 6C). The amount of total STAT3 increased in time, with the highest level observed after 8 h of incubation of A431WT cells with 1,25(OH)<sub>2</sub>D<sub>3</sub>. The deletion of *VDR* increased the initial level of STAT3 and abrogated an increase induced by 1,25(OH)<sub>2</sub>D<sub>3</sub> treatment. Similarly, *PDIA3* deletion slightly increased the basal amount of STAT3 with no effect from 1,25(OH)<sub>2</sub>D<sub>3</sub> treatment. Finally, phosphorylation of STAT3 at the Y705 site occurred after 4 h of treatment solely in A431WT cells treated with 1,25(OH)<sub>2</sub>D<sub>3</sub>. Interestingly, the STAT3 phosphorylation at the S727 site, which is lined to mitochondria, was strongly increased by both knockouts in A431 cells (A431Δ*VDR* and A431Δ*PDIA3*) and further amplified by treatment with 1,25(OH)<sub>2</sub>D<sub>3</sub> for 4 h.

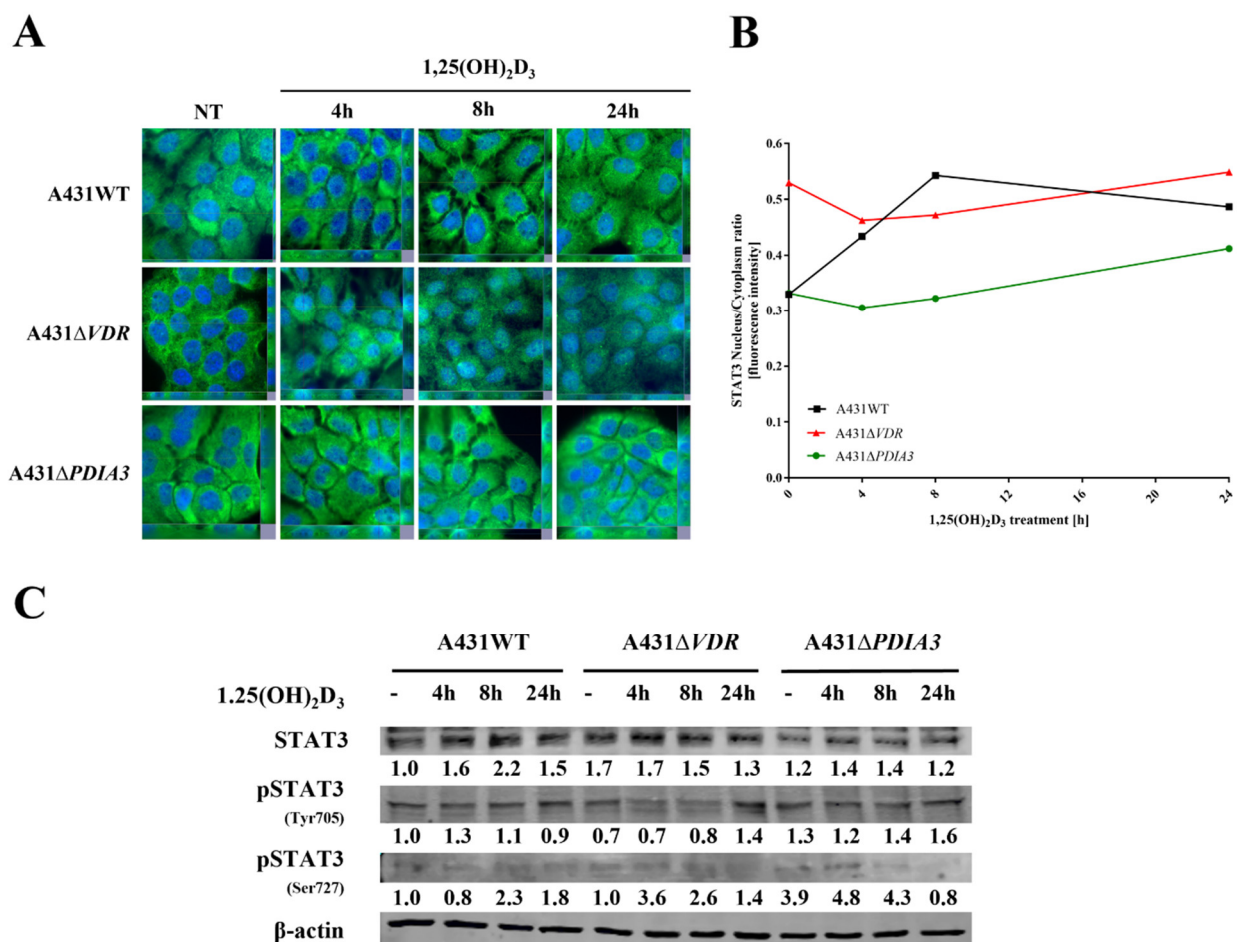


**Figure 6.** *PDIA3* deletion affects STAT3 signaling in A431 squamous cell carcinoma. (A) Fluorescence images of A431 cell lines treated with 1,25(OH)<sub>2</sub>D<sub>3</sub> for 4, 8, or 24 h and stained with anti-STAT3 antibody and DAPI. (B) STAT3 nucleus/cytoplasm ratio in A431 sublines. (C) Analysis of protein levels of STAT3, pSTAT3 (Y705), and pSTAT3 (S727) in A431WT and *VDR* or *PDIA3*-deficient knockout cell lines.

#### 4. Discussion

PDIA3 is a pleiotropic member of the oxidoreductase enzyme family, which is involved in a broad range of cellular processes, including protein folding and assembly, through the formation and remodeling of disulfide bridges [39]. PDIA3 has been strongly associated with various types of cancer as a prognostic biomarker (primary ductal breast cancer, prostate cancer, glioblastoma) and its overexpression is associated with poor outcomes of patients [15,40–42]. Thus, this study focused on a squamous cell carcinoma cell line with deletion of *PDIA3* (A431Δ*PDIA3*) as a model. In our previous study, we showed that deletion of *PDIA3* not only affects cellular physiology, but also plays an indispensable role in biological activities of 1,25(OH)<sub>2</sub>D<sub>3</sub> including genomic response [29]. Previously, we observed that *PDIA3* deletion alone modulates expression of nearly 2000 genes, among which, 269 were 1,25(OH)<sub>2</sub>D<sub>3</sub>-regulated. Furthermore, *PDIA3* knockout changed the expression of 1,25(OH)<sub>2</sub>D<sub>3</sub>-dependent genes, suggesting its role as a modulator of genomic response. The present study aimed to assess the impact of PDIA3 on morphology and bioenergetics of mitochondria and its role in 1,25(OH)<sub>2</sub>D<sub>3</sub> action on mitochondria in squamous cell carcinoma A431 cell line. To our knowledge, this is the first study investigating the role of PDIA3 in the mitochondrial activity of 1,25(OH)<sub>2</sub>D<sub>3</sub>. Hence, we are presenting data indicating that the deletion of *PDIA3* affects the morphology of the A431 cells, especially mitochondria. Knockout of *PDIA3* led to the decrease in total mitochondria surface and size within the cell, and 1,25(OH)<sub>2</sub>D<sub>3</sub> treatment reversed the effect of deletion to some extent. Interestingly, after *PDIA3* deletion we did not observe any statistically significant change in mitochondrial potential, even though vitamin D analogues have previously been shown to abolish the effects of hydrogen peroxide on mitochondrial membrane potential in immortalized HaCaT keratinocytes, thus protecting mitochondria against oxidative damage, but the effect was time-dependent [43]. Furthermore, it seems that the effect on mitochondrial membrane potential might be cell-type dependent.

As the deletion of *PDIA3* was shown to affect cellular responses to 1,25(OH)<sub>2</sub>D<sub>3</sub> treatment [29] and here we observed changes in the morphology of mitochondria, we decided to assess the impact of that deletion on mitochondria bioenergetics in A431 cells. All of the respiratory parameters of A431 cells were considerably elevated after *PDIA3* deletion. The presented data are in line with results published by Keasey et al., who showed that PDIA3 inhibits respiratory function in endothelial cells and *C. elegans* [12]. Previously, PDIA3 was localized within mitochondria, where it associates with mitochondrial μ-calpain, possibly playing a significant role in apoptotic signaling [44]. Moreover, PDIA3 was colocalized with STAT3 [45], suggesting its role in the modulation of STAT3 signaling within cells [46]. As those results suggested the possible involvement of PDIA3 in the modulation of 1,25(OH)<sub>2</sub>D<sub>3</sub>-induced STAT3 signaling, we analyzed levels of STAT3 protein together with its two phosphorylation sites at Tyr705 and Ser727. Our results suggest that VDR together with PDIA3 are necessary for the regulation of both phosphorylation sites via 1,25(OH)<sub>2</sub>D<sub>3</sub>. In our recent work [29], we identified the cyclooxygenase-2 coding gene (*PTGS2*) as a PDIA3-dependent gene. Interestingly, the expression of *PTGS2* is known to be regulated by STAT3 [47]. Consequently, we observed that *PDIA3* deletion abrogated the induction of the expression of *PTGS2* via 1,25(OH)<sub>2</sub>D<sub>3</sub> [29]. Here, we are presenting results indicating impaired STAT3 phosphorylation at site Y705 in *PDIA3* or *VDR* knockouts, suggesting that both proteins are necessary for the regulation of nuclear STAT3 phosphorylation. The enhanced oxygen consumption rate after *PDIA3* deletion is further supported by increased phosphorylation of STAT3 at S727 residue in A431Δ*PDIA3* cells. This observation is consistent with previous studies showing that PDIA3 can inhibit STAT3 phosphorylation and thereby influence mitochondrial bioenergetics [12]. Recently, Peron and coworkers showed that phosphorylation is needed for mito-STAT3 to exert its mitochondrial functions [48]. Here, for the first time, it was shown that phosphorylation of STAT3 at Tyr705 and Ser727 can be induced by 1,25(OH)<sub>2</sub>D<sub>3</sub> and depend on the presence of both VDR and PDIA3.



Interestingly, we observed that the lack of PDIA3 abrogated the effects of 1,25(OH)<sub>2</sub>D<sub>3</sub> on energy production parameters, suggesting its involvement in cellular bioenergetics. Furthermore, an increase in glycolytic parameters was acknowledged after *PDIA3* deletion while 1,25(OH)<sub>2</sub>D<sub>3</sub> treatment decreased glycolysis in wild-type A431 cells, but no effect was observed in A431Δ*PDIA3*. This is in agreement with other studies showing reduced glycolysis after vitamin D treatment in breast cancer cells [49] and colorectal cancer [50].

Recently, we showed that *PDIA3* deletion alters the expression of more than 2000 genes and modulates genomic response to 1,25(OH)<sub>2</sub>D<sub>3</sub> [29]. Here, we focused on genes related to mitochondria. However, we did not identify any PDIA3-dependent mtDEGs, which were also regulated by 1,25(OH)<sub>2</sub>D<sub>3</sub>, even though deletion of *PDIA3* alone changed the basal expression of mtDEGs, regulating different processes connected with cellular respiration. In a recent work [28], it was shown that 1,25(OH)<sub>2</sub>D<sub>3</sub> affects differently morphology and bioenergetics of cancerous and non-cancerous cells through genomic pathways regulated by VDR and partially by RXRA [44]. However, it is clear that PDIA3 somehow modulates the response of cancerous cells to 1,25(OH)<sub>2</sub>D<sub>3</sub> treatment in terms of mitochondrial morphology and bioenergetic; therefore, it supports our previous finding that PDIA3 possibly functions as a modulator of genomic response to 1,25(OH)<sub>2</sub>D<sub>3</sub>. Interestingly, Gezen-Ak and coworkers suggested that VDR affects directly mitochondrial DNA expression after 1,25(OH)<sub>2</sub>D<sub>3</sub> treatment [30], opening new possibilities for the direct impact of 1,25(OH)<sub>2</sub>D<sub>3</sub> and VDR on mitochondria; however, the presence of VDR in mitochondria is still under debate [20]. It was also postulated that VDR and PDIA3 are located at the cell membrane and are responsible for the trafficking of vitamin D and activation of fast membrane responses to this powerful secosteroid (see [20] for further discussion). However, the nature of VDR and PDIA3 interaction still remains to be solved.

Taken together, we have shown that *PDIA3* deletion affects mitochondria morphology and bioenergetics most likely through STAT3 regulation, as well as mitochondrial response to 1,25(OH)<sub>2</sub>D<sub>3</sub>. As we did not identify any PDIA3-dependent mtDEGs, we suggest that the main effects of 1,25(OH)<sub>2</sub>D<sub>3</sub> are genomic actions mediated by VDR and partially by RXRA [28]. As PDIA3 was found also in mitochondria, the direct impact on mitochondrial structure and function cannot be excluded [12,44,51]. Data presented here broaden our knowledge about the role of PDIA3 in 1,25(OH)<sub>2</sub>D<sub>3</sub> activities on mitochondria and open new perspectives to further explore topics of PDIA3-STAT3 regulation in 1,25(OH)<sub>2</sub>D<sub>3</sub> action. A potential limitation of this study was the use of the A431 squamous cell carcinoma cell line, rather than primary keratinocytes; however, primary cell lines are not suitable for producing stable knockouts. Moreover, our previous studies showed that the effects of 1,25(OH)<sub>2</sub>D<sub>3</sub> on cancer cell physiology, including mitochondrial function, were more pronounced in A431 cells compared to HaCaT keratinocytes. Most importantly, 1,25(OH)<sub>2</sub>D<sub>3</sub> treatment at least partially reversed the expression of cancer-related genes [28,29] and modulated mitochondrial activity as shown here.

**Supplementary Materials:** The following supporting information can be downloaded at: <https://www.mdpi.com/article/10.3390/nu15214529/s1>, Table S1. Venn analysis of MitoCarta 3.0, A431Δ*PDIA3* NT and A431Δ*PDIA3* + 1,25(OH)<sub>2</sub>D<sub>3</sub>.

**Author Contributions:** M.A.Ž. designed and coordinated the project. M.A.Ž., J.I.N. and A.M.O. planned and designed experiments. J.I.N., A.M.O. and O.K. performed experiments. J.I.N., A.M.O. and M.A.Ž. analyzed data. J.I.N. wrote the manuscript together with M.A.Ž. All authors have read and agreed to the published version of the manuscript.

**Funding:** The study was supported by a National Science Center OPUS Program under contracts 2017/25/B/NZ3/00431.

**Institutional Review Board Statement:** Not applicable.

**Informed Consent Statement:** Not applicable.

**Data Availability Statement:** The data presented in this study are available on request from the corresponding author.

**Conflicts of Interest:** The authors declare no conflict of interest.

### Abbreviations

PDIA3	Protein Disulfide Isomerase Family A Member 3
OCR	Oxygen consumption rate
ECAR	Extracellular Acidification Rate
STAT3	Signal Transducer And Activator Of Transcription 3
VDR	Vitamin D receptor
RXRA	Retinoid X Receptor Alpha
PLAA	Phospholipase A2 Activating Protein
PKC	Protein Kinase C
TEM	Transmission electron microscopy
mtDEGs	mitochondria-associated differently expressed genes
GO	Gene ontology

### References

- Ferrari, D.M.; Söling, H.D. The protein disulphide-isomerase family: Unravelling a string of folds. *Biochem. J.* **1999**, *339*, 1–10.
- Hughes, E.A.; Cresswell, P. The thiol oxidoreductase ERp57 is a component of the MHC class I peptide-loading complex. *Curr. Biol.* **1998**, *8*, 709–712.
- Morrice, N.A.; Powis, S.J. A role for the thiol-dependent reductase ERp57 in the assembly of MHC class I molecules. *Curr. Biol.* **1998**, *8*, 713–716.
- Eufemi, M.; Coppari, S.; Altieri, F.; Grillo, C.; Ferraro, A.; Turano, C. ERp57 is present in STAT3-DNA complexes. *Biochem. Biophys. Res. Commun.* **2004**, *323*, 1306–1312.
- Chichiarelli, S.; Gaucci, E.; Ferraro, A.; Grillo, C.; Altieri, F.; Cocchiola, R.; Arcangeli, V.; Turano, C.; Eufemi, M. Role of ERp57 in the signaling and transcriptional activity of STAT3 in a melanoma cell line. *Arch. Biochem. Biophys.* **2010**, *494*, 178–183.
- Zhao, G.; Lu, H.; Li, C. Proapoptotic activities of protein disulfide isomerase (PDI) and PDIA3 protein, a role of the Bcl-2 protein Bak. *J. Biol. Chem.* **2015**, *290*, 8949–8963.
- Hayashi, T.; Rizzuto, R.; Hajnoczky, G.; Su, T.P. MAM: More than just a housekeeper. *Trends Cell Biol.* **2009**, *19*, 81–88.
- Paillusson, S.; Stoica, R.; Gomez-Suaga, P.; Lau, D.H.W.; Mueller, S.; Miller, T.; Miller, C.C.J. There's Something Wrong with my MAM; the ER-Mitochondria Axis and Neurodegenerative Diseases. *Trends Neurosci.* **2016**, *39*, 146–157.
- Aureli, C.; Gaucci, E.; Arcangeli, V.; Grillo, C.; Eufemi, M.; Chichiarelli, S. ERp57/PDIA3 binds specific DNA fragments in a melanoma cell line. *Gene* **2013**, *524*, 390–395.
- Choe, M.H.; Min, J.W.; Jeon, H.B.; Cho, D.H.; Oh, J.S.; Lee, H.G.; Hwang, S.G.; An, S.; Han, Y.H.; Kim, J.S. ERp57 modulates STAT3 activity in radioresistant laryngeal cancer cells and serves as a prognostic marker for laryngeal cancer. *Oncotarget* **2015**, *6*, 2654–2666.
- Tammineni, P.; Anugula, C.; Mohammed, F.; Anjaneyulu, M.; Lerner, A.C.; Sepuri, N.B. The import of the transcription factor STAT3 into mitochondria depends on GRIM-19, a component of the electron transport chain. *J. Biol. Chem.* **2013**, *288*, 4723–4732.
- Keasey, M.P.; Razskazovskiy, V.; Jia, C.; Peterknecht, E.D.; Bradshaw, P.C.; Hagg, T. PDIA3 inhibits mitochondrial respiratory function in brain endothelial cells and *C. elegans* through STAT3 signaling and decreases survival after OGD. *Cell Commun. Signal* **2021**, *19*, 119.
- Hettinghouse, A.; Liu, R.; Liu, C.J. Multifunctional molecule ERp57: From cancer to neurodegenerative diseases. *Pharmacol. Ther.* **2018**, *181*, 34–48.
- Ménoret, A.; Drew, D.A.; Miyamoto, S.; Nakanishi, M.; Vella, A.T.; Rosenberg, D.W. Differential proteomics identifies PDIA3 as a novel chemoprevention target in human colon cancer cells. *Mol. Carcinog.* **2014**, *53* (Suppl. 1), E11–E22.
- Tu, Z.; Ouyang, Q.; Long, X.; Wu, L.; Li, J.; Zhu, X.; Huang, K. Protein Disulfide-Isomerase A3 Is a Robust Prognostic Biomarker for Cancers and Predicts the Immunotherapy Response Effectively. *Front. Immunol.* **2022**, *13*, 837512.
- Wierzbicka, J.; Piotrowska, A.; Żmijewski, M.A. The renaissance of vitamin D. *Acta Biochim. Pol.* **2014**, *61*, 679–686.
- Piotrowska, A.; Wierzbicka, J.; Żmijewski, M.A. Vitamin D in the skin physiology and pathology. *Acta Biochim. Pol.* **2016**, *63*, 17–29.
- Slominski, A.T.; Kim, T.K.; Janjetovic, Z.; Brożyna, A.A.; Żmijewski, M.A.; Xu, H.; Sutter, T.R.; Tuckey, R.C.; Jetten, A.M.; Crossman, D.K. Differential and Overlapping Effects of 20,23(OH)<sub>2</sub>D3 and 1,25(OH)<sub>2</sub>D3 on Gene Expression in Human Epidermal Keratinocytes: Identification of AhR as an Alternative Receptor for 20,23(OH)<sub>2</sub>D3. *Int. J. Mol. Sci.* **2018**, *19*, 3072.
- Hausler, M.R.; Jurutka, P.W.; Mizwicki, M.; Norman, A.W. Vitamin D receptor (VDR)-mediated actions of 1 $\alpha$ ,25(OH)<sub>2</sub> vitamin D: Genomic and non-genomic mechanisms. *Best Pract. Res. Clin. Endocrinol. Metab.* **2011**, *25*, 543–559.
- Żmijewski, M.A. Nongenomic Activities of Vitamin D. *Nutrients* **2022**, *14*, 5104.
- Zmijewski, M.A.; Carlberg, C. Vitamin D receptor(s): In the nucleus but also at membranes? *Exp. Dermatol.* **2020**, *29*, 876–884.



22. Nemere, I.; Schwartz, Z.; Pedrozo, H.; Sylvia, V.L.; Dean, D.D.; Boyan, B.D. Identification of a membrane receptor for 1,25-dihydroxyvitamin D<sub>3</sub> which mediates rapid activation of protein kinase C. *J. Bone Miner. Res.* **1998**, *13*, 1353–1359.
23. Boyan, B.D.; Sylvia, V.L.; McKinney, N.; Schwartz, Z. Membrane actions of vitamin D metabolites 1 $\alpha$ ,25(OH)<sub>2</sub>D<sub>3</sub> and 24R,25(OH)<sub>2</sub>D<sub>3</sub> are retained in growth plate cartilage cells from vitamin D receptor knockout mice. *J. Cell Biochem.* **2003**, *90*, 1207–1223.
24. Richard, C.L.; Farach-Carson, M.C.; Rohe, B.; Nemere, I.; Meckling, K.A. Involvement of 1,25D<sub>3</sub>-MARRS (membrane associated, rapid response steroid-binding), a novel vitamin D receptor, in growth inhibition of breast cancer cells. *Exp. Cell Res.* **2010**, *316*, 695–703.
25. Chen, J.; Doroudi, M.; Cheung, J.; Grozier, A.L.; Schwartz, Z.; Boyan, B.D. Plasma membrane Pdia3 and VDR interact to elicit rapid responses to 1 $\alpha$ ,25(OH)<sub>2</sub>D<sub>3</sub>. *Cell Signal.* **2013**, *25*, 2362–2373.
26. Doroudi, M.; Schwartz, Z.; Boyan, B.D. Membrane-mediated actions of 1,25-dihydroxy vitamin D<sub>3</sub>: A review of the roles of phospholipase A<sub>2</sub> activating protein and Ca<sup>2+</sup>/calmodulin-dependent protein kinase II. *J. Steroid Biochem. Mol. Biol.* **2015**, *147*, 81–84.
27. Schwartz, N.; Verma, A.; Bivens, C.B.; Schwartz, Z.; Boyan, B.D. Rapid steroid hormone actions via membrane receptors. *Biochim. Biophys. Acta* **2016**, *1863*, 2289–2298.
28. Olszewska, A.M.; Nowak, J.I.; Myszczyński, K.; Slominski, A.; Zmijewski, M.A. Dissection of an Impact of Vdr and Rxra on Genomic Activity of 1,25(OH)<sub>2</sub>D<sub>3</sub> in A431 Squamous Cell Carcinoma. *JSBMB* **2023**, submitted. Available online: [https://papers.ssrn.com/sol3/papers.cfm?abstract\\_id=4474791](https://papers.ssrn.com/sol3/papers.cfm?abstract_id=4474791) (accessed on 4 October 2023).
29. Nowak, J.I.; Olszewska, A.M.; Piotrowska, A.; Myszczyński, K.; Domżałski, P.; Żmijewski, M.A. PDIA3 modulates genomic response to 1,25-dihydroxyvitamin D<sub>3</sub> in squamous cell carcinoma of the skin. *Steroids* **2023**, *199*, 109288.
30. Gezen-Ak, D.; Alaylıoğlu, M.; Yurttas, Z.; Çamoğlu, T.; Şengül, B.; İşler, C.; Yaşar Kına, Ü.; Keskin, E.; Atasoy, İ.L.; Kafardar, A.M.; et al. Vitamin D receptor regulates transcription of mitochondrial DNA and directly interacts with mitochondrial DNA and TFAM. *J. Nutr. Biochem.* **2023**, *116*, 109322.
31. Sterling, T.M.; Nemere, I. 1,25-dihydroxyvitamin D<sub>3</sub> stimulates vesicular transport within 5 s in polarized intestinal epithelial cells. *J. Endocrinol.* **2005**, *185*, 81–91.
32. Tunsophon, S.; Nemere, I. Protein kinase C isotypes in signal transduction for the 1,25D<sub>3</sub>-MARRS receptor (ERp57/PDIA3) in steroid hormone-stimulated phosphate uptake. *Steroids* **2010**, *75*, 307–313.
33. Olszewska, A.M.; Sieradzan, A.K.; Bednarczyk, P.; Szewczyk, A.; Żmijewski, M.A. Mitochondrial potassium channels: A novel calcitriol target. *Cell Mol Biol Lett* **2022**, *27*, 3.
34. Piotrowska, A.; Zaucha, R.; Król, O.; Żmijewski, M.A. Vitamin D Modulates the Response of Patient-Derived Metastatic Melanoma Cells to Anticancer Drugs. *Int. J. Mol. Sci.* **2023**, *24*, 8037.
35. Bardou, P.; Mariette, J.; Escudié, F.; Djemiel, C.; Klopp, C. jvenn: An interactive Venn diagram viewer. *BMC Bioinform.* **2014**, *15*, 293.
36. Rath, S.; Sharma, R.; Gupta, R.; Ast, T.; Chan, C.; Durham, T.J.; Goodman, R.P.; Grabarek, Z.; Haas, M.E.; Hung, W.H.W.; et al. MitoCarta3.0: An updated mitochondrial proteome now with sub-organelle localization and pathway annotations. *Nucleic Acids Res.* **2021**, *49*, D1541–D1547.
37. Xie, Z.; Bailey, A.; Kuleshov, M.V.; Clarke, D.J.B.; Evangelista, J.E.; Jenkins, S.L.; Lachmann, A.; Wojciechowicz, M.L.; Kropiwnicki, E.; Jagodnik, K.M.; et al. Gene Set Knowledge Discovery with Enrichr. *Curr. Protoc.* **2021**, *1*, e90.
38. Wegrzyn, J.; Potla, R.; Chwae, Y.J.; Sepuri, N.B.; Zhang, Q.; Koeck, T.; Derecka, M.; Szczepanek, K.; Szelag, M.; Gornicka, A.; et al. Function of mitochondrial Stat3 in cellular respiration. *Science* **2009**, *323*, 793–797.
39. Turano, C.; Gaucci, E.; Grillo, C.; Chichiarelli, S. ERp57/GRP58: A protein with multiple functions. *Cell Mol. Biol. Lett.* **2011**, *16*, 539–563.
40. Diaz Cruz, M.A.; Karlsson, S.; Szekeres, F.; Faresjö, M.; Lund, D.; Larsson, D. Differential expression of protein disulfide-isomerase A3 isoforms, PDIA3 and PDIA3N, in human prostate cancer cell lines representing different stages of prostate cancer. *Mol. Biol. Rep.* **2021**, *48*, 2429–2436.
41. Ramos, F.S.; Serino, L.T.; Carvalho, C.M.; Lima, R.S.; Urban, C.A.; Cavalli, I.J.; Ribeiro, E.M. PDIA3 and PDIA6 gene expression as an aggressiveness marker in primary ductal breast cancer. *Genet. Mol. Res.* **2015**, *14*, 6960–6967.
42. Chiavari, M.; Ciotti, G.M.P.; Canonico, F.; Altieri, F.; Lacal, P.M.; Graziani, G.; Navarra, P.; Lisi, L. PDIA3 Expression in Glioblastoma Modulates Macrophage/Microglia Pro-Tumor Activation. *Int. J. Mol. Sci.* **2020**, *21*, 8214.
43. Piotrowska, A.; Wierzbička, J.; Ślebioda, T.; Woźniak, M.; Tuckey, R.C.; Slominski, A.T.; Żmijewski, M.A. Vitamin D derivatives enhance cytotoxic effects of H<sub>2</sub>O<sub>2</sub> or cisplatin on human keratinocytes. *Steroids* **2016**, *110*, 49–61.
44. Ozaki, T.; Yamashita, T.; Ishiguro, S. ERp57-associated mitochondrial  $\mu$ -calpain truncates apoptosis-inducing factor. *Biochim. Biophys. Acta* **2008**, *1783*, 1955–1963.
45. Kondo, R.; Ishino, K.; Wada, R.; Takata, H.; Peng, W.X.; Kudo, M.; Kure, S.; Kaneya, Y.; Tani, N.; Yoshida, H.; et al. Downregulation of protein disulfide-isomerase A3 expression inhibits cell proliferation and induces apoptosis through STAT3 signaling in hepatocellular carcinoma. *Int. J. Oncol.* **2019**, *54*, 1409–1421.
46. Coe, H.; Jung, J.; Groenendyk, J.; Prins, D.; Michalak, M. ERp57 modulates STAT3 signaling from the lumen of the endoplasmic reticulum. *J. Biol. Chem.* **2010**, *285*, 6725–6738.
47. Carpenter, R.L.; Lo, H.W. STAT3 Target Genes Relevant to Human Cancers. *Cancers* **2014**, *6*, 897–925.
48. Peron, M.; Dinarello, A.; Meneghetti, G.; Martorano, L.; Betto, R.M.; Facchinello, N.; Tesoriere, A.; Tiso, N.; Martello, G.; Argenton, F. Y705 and S727 are required for the mitochondrial import and transcriptional activities of STAT3, and for regulation of stem cell proliferation. *Development* **2021**, *148*, dev199477.

49. Santos, J.M.; Khan, Z.S.; Munir, M.T.; Tarafdar, K.; Rahman, S.M.; Hussain, F. Vitamin D<sub>3</sub> decreases glycolysis and invasiveness, and increases cellular stiffness in breast cancer cells. *J. Nutr. Biochem.* **2018**, *53*, 111–120.
50. Zuo, S.; Wu, L.; Wang, Y.; Yuan, X. Long Non-coding RNA MEG3 Activated by Vitamin D Suppresses Glycolysis in Colorectal Cancer via Promoting c-Myc Degradation. *Front. Oncol.* **2020**, *10*, 274.
51. He, J.; Shi, W.; Guo, Y.; Chai, Z. ERp57 modulates mitochondrial calcium uptake through the MCU. *FEBS Lett.* **2014**, *588*, 2087–2094.

**Disclaimer/Publisher's Note:** The statements, opinions and data contained in all publications are solely those of the individual author(s) and contributor(s) and not of MDPI and/or the editor(s). MDPI and/or the editor(s) disclaim responsibility for any injury to people or property resulting from any ideas, methods, instructions or products referred to in the content.

## Article

# VDR and PDIA3 Are Essential for Activation of Calcium Signaling and Membrane Response to 1,25(OH)<sub>2</sub>D<sub>3</sub> in Squamous Cell Carcinoma Cells

Joanna I. Nowak<sup>1</sup>, Anna M. Olszewska<sup>1</sup>, Justyna M. Wierzbicka<sup>1</sup>, Magdalena Gebert<sup>2</sup>, Rafał Bartoszewski<sup>3</sup>   
and Michał A. Żmijewski<sup>1,\*</sup> 

<sup>1</sup> Department of Histology, Medical University of Gdansk, 80-211 Gdansk, Poland; j.chorzepa@gumed.edu.pl (J.I.N.); anna.olszewska@gumed.edu.pl (A.M.O.); justyna.wierzbicka@gumed.edu.pl (J.M.W.)

<sup>2</sup> Department of Medical Laboratory Diagnostics-Fahrenheit Biobank BBMRI.pl, Medical University of Gdansk, 80-134 Gdansk, Poland; magdalena.gebert@gumed.edu.pl

<sup>3</sup> Department of Biophysics, Faculty of Biotechnology, University of Wrocław, 50-383 Wrocław, Poland; rafal.bartoszewski@uwr.edu.pl

\* Correspondence: mzmijewski@gumed.edu.pl

**Abstract:** The genomic activity of 1,25(OH)<sub>2</sub>D<sub>3</sub> is mediated by vitamin D receptor (VDR), whilst non-genomic is associated with protein disulfide isomerase family A member 3 (PDIA3). Interestingly, our recent studies documented that PDIA3 is also involved, directly or indirectly, in the modulation of genomic response to 1,25(OH)<sub>2</sub>D<sub>3</sub>. Moreover, PDIA3 was also shown to regulate cellular bioenergetics, possibly through the modulation of STAT signaling. Here, the role of VDR and PDIA3 proteins in membrane response to 1,25(OH)<sub>2</sub>D<sub>3</sub> and calcium signaling was investigated in squamous cell carcinoma A431 cell line with or without the deletion of *VDR* and *PDIA3* genes. Calcium influx was assayed by Fura-2AM or Fluo-4AM, while calcium-regulated element (NFAT) activation was measured using a dual luciferase assay. Further, the levels of proteins involved in membrane response to 1,25(OH)<sub>2</sub>D<sub>3</sub> in A431 cell lines were analyzed via Western blot analysis. The deletion of either *PDIA3* or *VDR* resulted in the decreased baseline levels of Ca<sup>2+</sup> and its responsiveness to 1,25(OH)<sub>2</sub>D<sub>3</sub>; however, the effect was more pronounced in A431Δ*PDIA3*. Furthermore, the knockout of either of these genes disrupted 1,25(OH)<sub>2</sub>D<sub>3</sub>-elicited membrane signaling. The data presented here indicated that the VDR is essential for the activation of calcium/calmodulin-dependent protein kinase II alpha (CAMK2A), while PDIA3 is required for 1,25(OH)<sub>2</sub>D<sub>3</sub>-induced calcium mobilization in A431 cells. Taken together, those results suggest that both VDR and PDIA3 are essential for non-genomic response to this powerful secosteroid.

**Keywords:** PDIA3; 1,25-dihydroxy vitamin D<sub>3</sub> signaling; VDRE; NFAT; Ca<sup>2+</sup> signaling



**Citation:** Nowak, J.I.; Olszewska, A.M.; Wierzbicka, J.M.; Gebert, M.; Bartoszewski, R.; Żmijewski, M.A. VDR and PDIA3 Are Essential for Activation of Calcium Signaling and Membrane Response to 1,25(OH)<sub>2</sub>D<sub>3</sub> in Squamous Cell Carcinoma Cells. *Cells* **2024**, *13*, 11. <https://doi.org/10.3390/cells13010011>

Academic Editors: Federica Saponaro and Giulia Battafarano

Received: 2 November 2023

Revised: 6 December 2023

Accepted: 18 December 2023

Published: 20 December 2023



**Copyright:** © 2023 by the authors. Licensee MDPI, Basel, Switzerland. This article is an open access article distributed under the terms and conditions of the Creative Commons Attribution (CC BY) license (<https://creativecommons.org/licenses/by/4.0/>).

## 1. Introduction

The classical signaling of 1,25(OH)<sub>2</sub>D<sub>3</sub> is mediated by the nuclear vitamin D receptor (VDR). This nuclear receptor for vitamin D, together with its co-receptor protein, retinoid X receptor (RXR), forms heterodimers, forming a powerful transcription factor. The VDR-RXR dimer upon ligand binding is translocated into the nucleus, where it binds to vitamin D response elements (VDRE) in the regulatory region of the vitamin D target genes and modulates their expression [1,2]. One of the principal activities of 1,25(OH)<sub>2</sub>D<sub>3</sub> is the regulation of calcium-phosphate homeostasis [3,4].

However, not all the effects of 1,25(OH)<sub>2</sub>D<sub>3</sub> can be attributed to genomic response; thus, the idea of alternative signaling pathways with potential membrane-bound receptor for this secosteroid has emerged [5]. The presence of such a pathway, for example, explained the rapid influx of calcium ions induced with 1,25(OH)<sub>2</sub>D<sub>3</sub> [6,7]. Eventually,

Nemere and coworkers described a  $1,25\text{D}_3$ -membrane-associated, rapid response steroid-binding protein ( $1,25\text{D}_3$ -MARRS), which was also known as protein disulfide isomerase family A member 3 (PDIA3) [8]. PDIA3 is an endoplasmic reticulum (ER) protein involved in protein folding, together with other chaperones like calnexin or calreticulin [9]. Outside of ER, PDIA3 was localized within the cell membrane, nucleus, cytoplasm, or mitochondria [10]. Importantly, this protein was proven to be involved in a rapid uptake of calcium and phosphate in intestine cells induced by  $1,25(\text{OH})_2\text{D}_3$  [11,12]. Thus, PDIA3 is strongly linked to calcium homeostasis. Lately, it has been shown that PDIA3 knockout in squamous cell carcinoma alters the expression of the genes connected to the regulation of bone mineralization, phospholipase C activity, and calcium-dependent phospholipid binding [13]. Moreover, it was shown that the partial silencing of *PDIA3* (*PDIA3*<sup>+/-</sup>) in mice model impaired skeletal development, while deletion was lethal [14–16].

PDIA3 was shown to interact with the phospholipase A2-activating protein (PLAA), subsequently leading to the activation of phospholipase A2 (PLA2) and the mediation of the non-genomic rapid response to  $1,25(\text{OH})_2\text{D}_3$ . As a result, calcium is released to the cytoplasm, followed by the activation of protein kinase C (PKC) or calcium/calmodulin-dependent protein kinase II (CaMKII). Thus, this leads to the induction of downstream signaling such as mitogen-activated protein kinases (MAPK) pathways and other transcription factors (STAT1-3, NF- $\kappa$ B). It has been shown that the disruption of PDIA3 protein attenuated PKA, PKC signaling, and calcium influx [11,14,17–19]. Recently, it has been shown that PDIA3 influences STAT3 expression in the *C. elegans* model, regulating cellular respiration [20]. Additionally, it has been shown that PDIA3 modulates STAT3 signaling induced by  $1,25(\text{OH})_2\text{D}_3$  [21].

In our latest studies, we investigated the impact of deletion of either *VDR* or *PDIA3* on gene expression profile and non-genomic effects of  $1,25(\text{OH})_2\text{D}_3$  in A431 squamous cell carcinoma, showing that PDIA3 is involved in genomic responses to  $1,25(\text{OH})_2\text{D}_3$  [13,22]. Moreover, we have shown that the deletion of *PDIA3* abrogates the effects of  $1,25(\text{OH})_2\text{D}_3$  on cellular bioenergetics, possibly through STAT3 signaling [21]. In this study, the effects of knockout of *PDIA3* and *VDR* on the  $1,25(\text{OH})_2\text{D}_3$  membrane's non-genomic signaling were investigated.

## 2. Materials and Methods

### 2.1. $1,25(\text{OH})_2\text{D}_3$

The active form of vitamin D ( $1,25(\text{OH})_2\text{D}_3$ ) was purchased from Sigma-Aldrich (Merck KGaA, Darmstadt, Germany).  $1,25(\text{OH})_2\text{D}_3$  was dissolved in ethanol and stored at  $-20\text{ }^\circ\text{C}$ . A 100 nM concentration was used in all experiments, as it was proven to have the most potent activity for proliferation as well as for photoprotection in other research [13,23,24].

### 2.2. Cell Cultures

Immortalized human basal cell carcinoma cell line (A431) was purchased from Synthego Corporation (Menlo Park, CA, USA). *PDIA3* and *VDR* knock-out cell lines were obtained with CRISPR/Cas9 technology, as described previously [13]. For cell cultures, DMEM high glucose medium (4.5 g/L) was used. Additionally, the medium was supplemented with 10% fetal bovine serum (FBS), penicillin (10,000 units/mL), and streptomycin (10 mg/mL) (Sigma-Aldrich; Merck KGaA, Darmstadt, Germany). A431 cell lines were cultured in the incubator with 5%  $\text{CO}_2$  at  $37\text{ }^\circ\text{C}$ . For experimental conditions, the medium was changed to DMEM supplemented with 2% charcoal-stripped FBS.

### 2.3. Measurement of Intracellular Calcium Concentration

A431 cell lines were seeded onto 96-well plates in DMEM medium supplemented with charcoal-stripped FBS and antibiotics. To test the effects of *VDR* and *PDIA3* deletion on calcium influx, cells were incubated with  $1\text{ }\mu\text{M}$  Fura-2AM solution (Sigma-Aldrich; Merck KGaA, Darmstadt, Germany) in HBSS for 1 h. Afterwards, incubation cells were rinsed

with medium. The fluorescence intensity of the cells was measured using a plate reader at  $\lambda_{\text{ex}}$  355 nm and  $\lambda_{\text{em}}$  495 nm for 16 min.

A431 cell lines were seeded onto an 8-well chamber slide in DMEM medium supplemented with charcoal-stripped FBS and antibiotics. To test the effects of *VDR* and *PDIA3* deletion on calcium influx, cells were incubated with 1  $\mu\text{M}$  Fluo-4AM solution (Sigma-Aldrich; Merck KGaA, Darmstadt, Germany) in Hank's Balanced Salt solution (HBSS) (PAN Biotech, Aidenbach, Germany) for 30 min. Cells were rinsed with HBSS and left in medium. The intensity of fluorescence was observed with the use of live microscopy on Olympus Cell-Vivo IX 83 (Olympus, Tokyo, Japan).

#### 2.4. Luciferase Reporter Assay

The human VDRE and NFAT firefly luciferase reporter constructs were purchased from Qiagen (Hilden, Germany). To test the effects of the deletion of either *VDR* or *PDIA3* on VDRE and NFAT elements, A431 cells were seeded onto 96-well polystyrene, white/clear flat bottom plates (30,000 cells/per well) and transfected with the constructs using Lipofectamin 2000 (Thermo Fisher Scientific, Waltham, MA, USA). After 24 h transfected cells were treated with 100 nM  $1,25(\text{OH})_2\text{D}_3$  for 4, 8, or 24 h. Then, cells were lysed using luciferase assay lysis buffer (Promega, Madison, WI, USA), and the firefly-*Renilla* luciferase activities were measured using the Dual-Luciferase Reporter Assay (Promega, Madison, WI, USA) according to the manufacturer's protocol using GloMax-Multi + Detection System (Promega, Madison, WI, USA). Results were normalized to non-treated cells for all A431 sublines, separately.

#### 2.5. Western Blot

Squamous cell carcinoma cell lines were treated with 100 nM  $1,25(\text{OH})_2\text{D}_3$  for 4, 8, and 24 h. After a given time (4 h, 8 h, and 24 h), the medium was removed and cells were washed twice with PBS. Next, A431 cells were scratched from the plate in cooled PBS, and the suspension was moved to an Eppendorf tube and centrifuged for 10 min at  $16,000\times g$ . The cell pellet was resuspended in RIPA buffer (Thermo Fisher Scientific, Waltham, MA, USA) with the addition of phosphatase and protease inhibitors (Sigma-Aldrich; Merck KGaA, Darmstadt, Germany). To measure the concentration of lysates, modified Bradford Assay was used according to manufacturer protocol (Bio-Rad, Hercules, CA, USA). Amounts of 10% bottom gel and 5% upper gel were used for SDS-PAGE electrophoresis. An equal amount of lysates (20  $\mu\text{g}$ ) was loaded into each well, and gels were resolved at 90–110 V in the Bio-Rad apparatus (Bio-Rad, Hercules, CA, USA). A Trans-Blot Turbo system was used for protein transfer to PVDF membranes (Bio-Rad, Hercules, CA, USA). Then, membranes were blocked in 5% milk dissolved in TBS-T. The membranes were incubated with specific primary antibodies: anti-PLAA, anti-PLC $\gamma$ , anti-PKC $\alpha$ , anti-ERK1/2, anti-phosphoERK1/2 (Thr202/Tyr204), anti-Caveolin 1, anti-Caveolin 3, anti-CAMK2A, anti-phosphoCAMK2A (T286), and anti-TRPV6 (Abclonal, Woburn, MA, USA), overnight at 4  $^{\circ}\text{C}$ . Proper secondary fluorescent antibodies conjugated with AlexaFluor<sup>®</sup> 790 or AlexaFluor<sup>®</sup> 680 were used (Jackson ImmunoResearch, Cambridgeshire, UK). As a loading control, anti- $\beta$ -actin antibodies (Abclonal, Woburn, MA, USA) were used. Results were visualized with the Odyssey Clx system and calculated with the use of Image Studio Software Ver 5.2 (both LI-COR Biosciences, Lincoln, NE, USA).

#### 2.6. Bioinformatic Analysis

As described in a previous study [13,22], data quality and cell line disparity were checked. To identify differentially expressed genes, the absolute value of log2fold change  $\geq 1.0$  and adjusted *p*-value  $< 0.05$  were used. To see whether the expression of selected genes was regulated by either the deletion of *PDIA3* or  $1,25(\text{OH})_2\text{D}_3$  treatment, the heat maps were prepared. Data showed the clustering of RNA-seq expression data and technical repeats within the groups. The RNA-seq data have been deposited in Sequence Read Archive (SRA) under accession number PRJNA926032.



### 2.7. Statistical Analysis

GraphPad Prism version 7.05 was used for the statistical analysis of obtained data (GraphPad Software, Inc., La Jolla, CA, USA). Results are presented as mean  $\pm$  SD and were analyzed either with Student's *t*-test or one-way ANOVA analysis of variance with appropriate post hoc tests. Statistical significance is illustrated as asterisks: \*  $p < 0.05$ , \*\*  $p < 0.01$ , \*\*\*  $p < 0.001$ , or \*\*\*\*  $p < 0.0001$ .

## 3. Results

### 3.1. Deletion of *PDIA3* Modulates the Expression of Calcium-Associated Genes in A431 Cells

Previously, it was shown that deletion of the *PDIA3* gene in the A431 squamous cell carcinoma line (A431 $\Delta$ *PDIA3*) affected expression of more than 1800 genes, including genes modulated by 1,25(OH)<sub>2</sub>D<sub>3</sub> treatment [13]. Here, the expression of calcium-associated genes and ER-related genes was evaluated. Thirty calcium-associated genes were found amongst differently expressed genes (DEGs) in the A431 $\Delta$ *PDIA3* cell line, including 12 upregulated and 18 downregulated genes (Figure 1A). All of those DEGs associated with calcium were further affected by 1,25(OH)<sub>2</sub>D<sub>3</sub> treatment, and 14 were upregulated and 16 downregulated in the *PDIA3* knockout cell line (Figure 1B). Further, those 30 calcium-associated DEGs disrupted by *PDIA3* deletion were analyzed in terms of the biological process using gene ontology. The analysis revealed their involvement in biological processes related to the positive regulation of mitochondrial calcium ion concentration, mitochondrial calcium ion homeostasis, the negative regulation of endoplasmic reticulum calcium ion concentration, and the positive regulation of calcium ion transport (Figure 1C).

### 3.2. Deletion of *PDIA3* Decreases Calcium Levels after 1,25(OH)<sub>2</sub>D<sub>3</sub> Treatment and Consequently Disrupts the Activity of Calcium-Regulated Nuclear Factor of Activated T-Cells (NFAT) in A431 Cells

Subsequent experiments were focused on changes in levels of intracellular calcium induced by 1,25(OH)<sub>2</sub>D<sub>3</sub>. To verify an impact of *PDIA3* on calcium homeostasis, intracellular levels of calcium were measured with the use of two fluorescence probes (Fura-2AM and Fluo-4AM) via fluorescent measurement using plate reader or live microscopy on Olympus Cell-Vivo IX 83, respectively (Figure 2). In A431 knockout cell lines, the baseline level of intracellular calcium measured with Fluo-4AM probe was decreased in comparison to A431WT cells. The effect was less pronounced for A431 $\Delta$ *VDR* cells. Curiously, in the case of A431 $\Delta$ *PDIA3* cells, there was a decrease in fluorescence after 1,25(OH)<sub>2</sub>D<sub>3</sub> addition (Figure 2A,B). Those results are further supported by data acquired with a Fura-2AM probe, indicating a role of *PDIA3* in calcium mobilization and 1,25(OH)<sub>2</sub>D<sub>3</sub>-induced calcium influx. An addition of 100 nM 1,25(OH)<sub>2</sub>D<sub>3</sub> elicited an influx of calcium ions into the A431 cells; however, the increase in both cell lines, A431 $\Delta$ *VDR* and A431 $\Delta$ *PDIA3*, was significantly smaller in comparison to A431WT cells. A431 $\Delta$ *PDIA3* cells were characterized by the lowest baseline calcium level and 1,25(OH)<sub>2</sub>D<sub>3</sub>-induced calcium influx. Additionally, lower concentrations of 1,25(OH)<sub>2</sub>D<sub>3</sub> (1 nM and 10 nM) were tested with a similar effect (Supplementary Figure S1), suggesting that even low concentrations of 1,25(OH)<sub>2</sub>D<sub>3</sub> are sufficient for the activation of calcium influx in A431 cells. This is in agreement with previous studies where calcium uptake was triggered by even lower, picomolar concentrations of 1,25(OH)<sub>2</sub>D<sub>3</sub> (0.13 nM [7] or 0.3 nM [25]). Calimycin (calcium ionophore) was used as a positive control of calcium influx. Interestingly, a calimycin-induced influx of calcium ions was also slightly affected by either *VDR* or *PDIA3* deletion in A431 cells and the effect was more pronounced in  $\Delta$ *PDIA3* cells (Figure 2C,D). In our recent publication, it was shown that *PDIA3* deletion impacts the expression of the well-known calcium channel TRPV6 [13]. Here, the level of the mentioned protein was checked after the deletion of *VDR* or *PDIA3* and 1,25(OH)<sub>2</sub>D<sub>3</sub> treatment. In A431WT cells 1,25(OH)<sub>2</sub>D<sub>3</sub> treatment increased levels of TRPV6 protein. The same effect was observed for A431 $\Delta$ *VDR* cells, but the increase was slightly reduced in comparison to the A431WT cell line. Interestingly, the deletion of *PDIA3* prevented the increase in TRPV6 protein (Figure 2E).



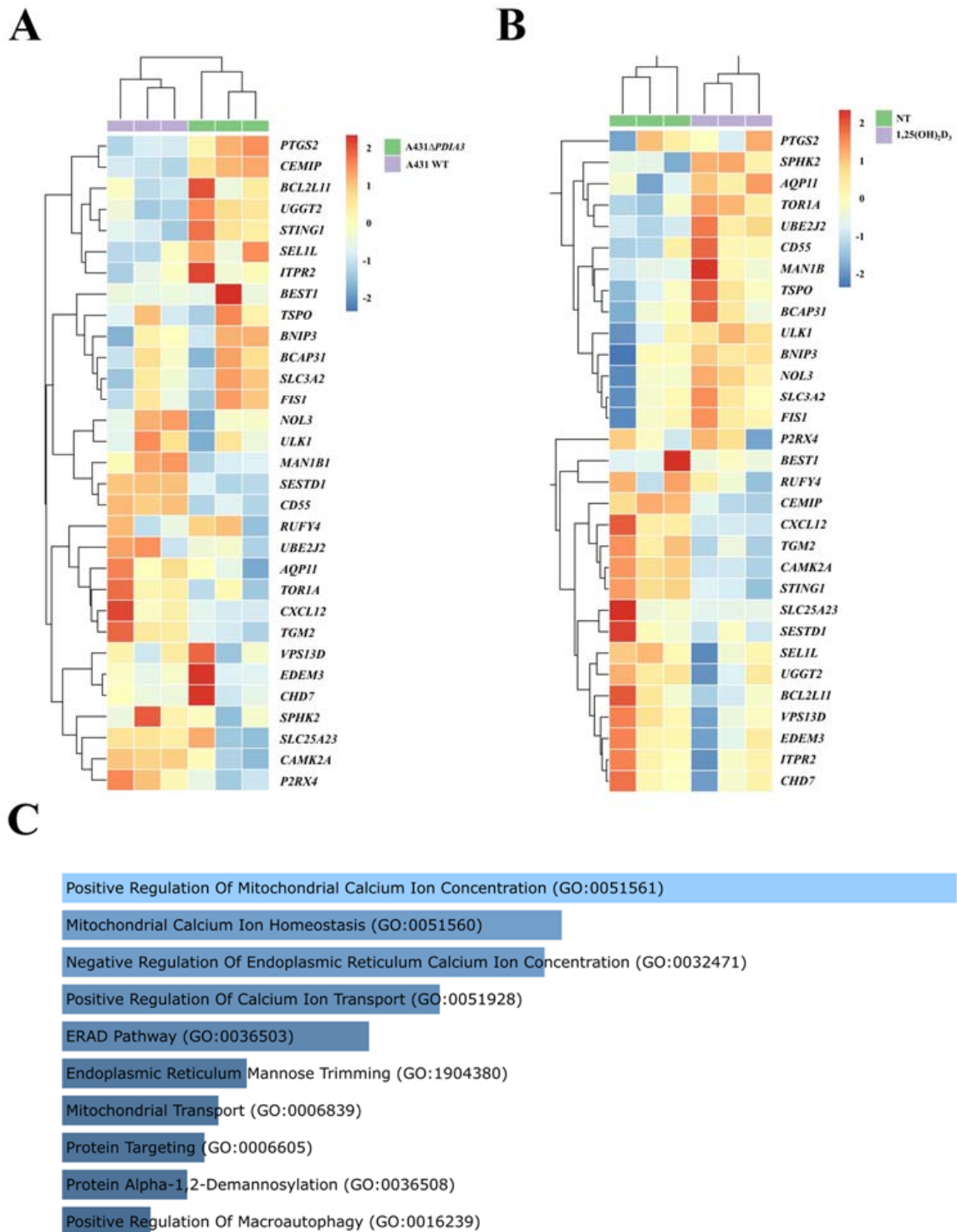


**Figure 1.** Changes in gene expression connected to calcium metabolism and endoplasmic reticulum homeostasis in human squamous carcinoma cell lines (A431). Heatmaps of selected genes with a statistically significant change in expression level after (A) PDIA3 knockout and (B) after 1,25(OH)<sub>2</sub>D<sub>3</sub> treatment solely in A431ΔPDIA3 cells. The color of cells represents the Z-score of normalized gene expression values. (C) Gene ontology biological process analysis of calcium-associated genes disrupted after PDIA3 deletion. Color intensity and length correspond to the *p*-value of the GO biological process.

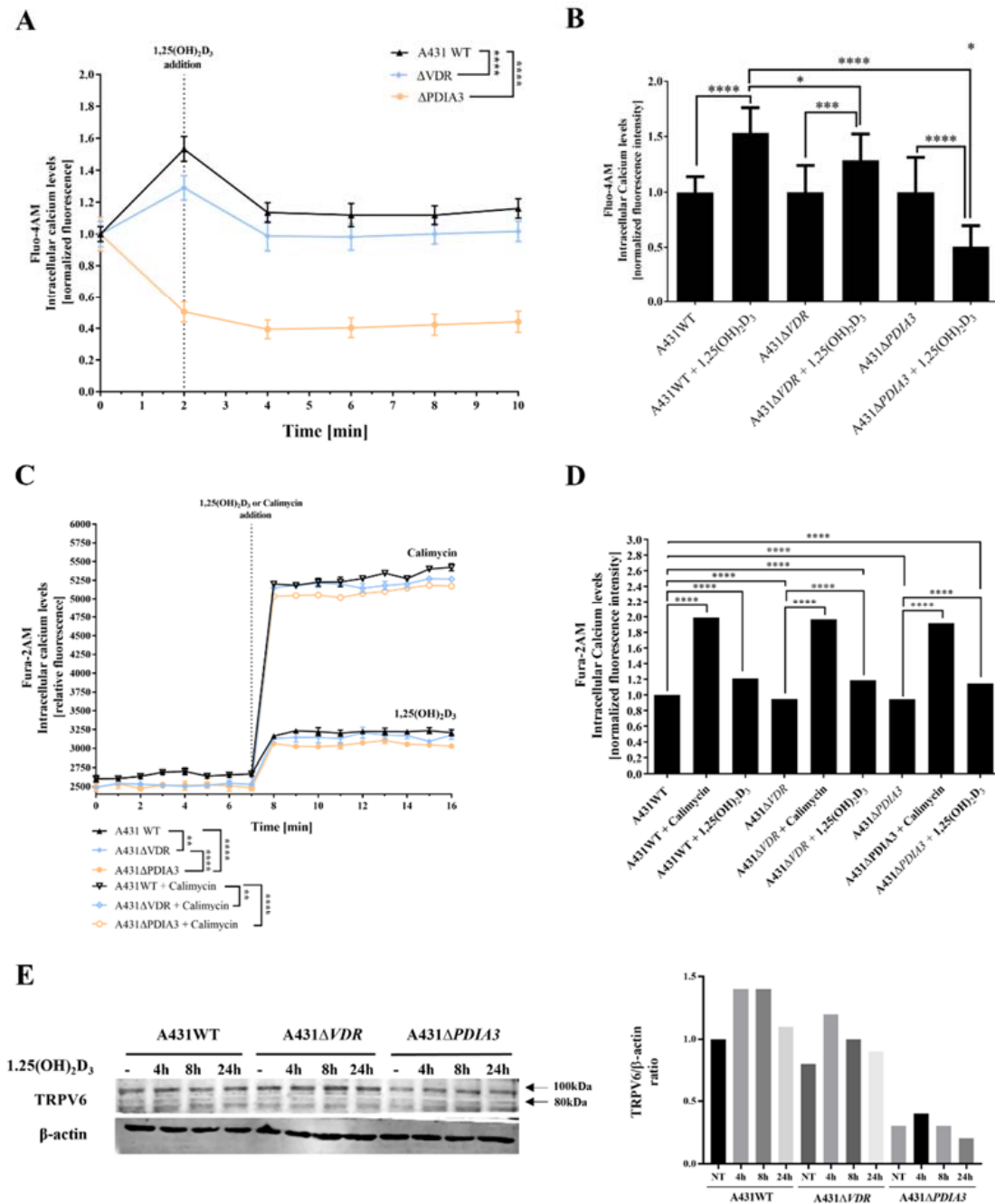


**Figure 2.** Deletion of *PDIA3* decreases calcium levels after  $1,25(\text{OH})_2\text{D}_3$  treatment in squamous cell carcinoma. **(A)** Intracellular calcium levels monitored with Fluo-4AM fluorescence probe in A431 cell lines with live cell time-lapse microscopy. **(B)** Normalized fluorescence intensity at 0 and 2 min time points. **(C)** Time-resolved analysis of intracellular calcium levels measured with Fura-2AM probe on microplate reader in A431. Results were calculated as a mean  $\pm$  SD of triplicates. Statistically significant differences are illustrated with asterisks: \*  $p < 0.05$ , \*\*  $p < 0.01$ , \*\*\*  $p < 0.001$ , or \*\*\*\*  $p < 0.0001$ . **(D)** Alterations of normalized fluorescence intensity at the 7th and 8th minute of the experiment. Representative results were presented in the graph. **(E)** Analysis of TRPV6 protein levels in A431 cell lines with *VDR* or *PDIA3* deletion. Two bands represent glycosylated (100 kDa) and non-glycosylated (80 kDa). The quantity of non-glycosylated TRPV6 (80 kDa) was calculated as a protein/ $\beta$ -actin ratio. Protein levels are calculated as means from three independent experiments. Representative pictures are shown.

Since the transcriptome analysis revealed numerous changes in gene expression after *PDIA3* deletion [13] and, most importantly, among calcium-associated genes, the effects of *VDR* and *PDIA3* deletion on the activity of the calcium-associated nuclear factor of activated T-cells (NFAT) and vitamin D response elements (VDRE) were investigated. VDRE served as additional control. Briefly, after the transfection of A431WT, A431 $\Delta$ *VDR*, and A431 $\Delta$ *PDIA3* with NFAT or VDRE luciferase reporter vectors, cells were treated with 100 nM 1,25(OH) $_2$ D $_3$  and luciferase activity was measured (Figure 3). The NFAT is a transcription factor activated by calcium signaling and was previously linked to the immunosuppressive activity of 1,25(OH) $_2$ D $_3$  [26,27]. The NFAT activity was increased almost threefold in A431WT cells after 8 h of 1,25(OH) $_2$ D $_3$  treatment (Figure 3A). The deletion of *VDR* did not affect NFAT activity (Figure 3B). Interestingly, in A431 $\Delta$ *PDIA3* cells, 1,25(OH) $_2$ D $_3$  treatment elicited a rapid increase in NFAT activity after 4 h with further decrease in activity after 8 and 24 h (Figure 3C). In wild-type A431 cell line, 1,25(OH) $_2$ D $_3$  treatment increased the activity of VDRE most efficiently after 24 h (Figure 3D). The deletion of *VDR* completely eliminated effect of 1,25(OH) $_2$ D $_3$  treatment on vitamin D response element (Figure 3E). In contrast, *PDIA3* deletion slightly enhanced VDRE activation by 1,25(OH) $_2$ D $_3$  in comparison to A431WT cells, and the effect was noticeable after 4 or 8 h of incubation (Figure 3F).

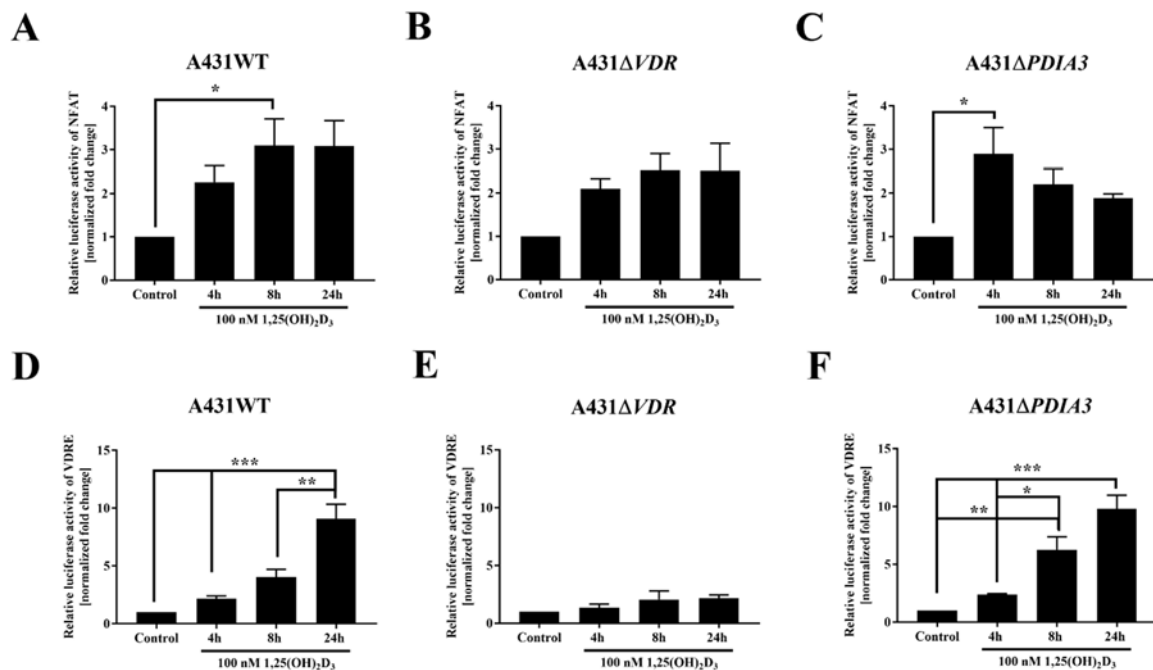


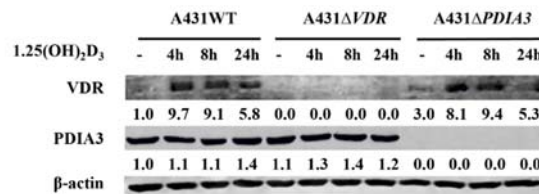
**Figure 3.** Changes in the activity of VDRE and NFAT response element to 1,25(OH) $_2$ D $_3$  in A431 cell lines. The bar graphs indicate the normalized fold change of the firefly/*Renilla* luciferase ratio of NFAT (A–C) and VDRE (D–F) in A431WT,  $\Delta$ *VDR*, and  $\Delta$ *PDIA3*. Dual luciferase reporter assay results are represented as means  $\pm$  SEM of triplicate samples. Statistically significant differences are illustrated with asterisks: \*  $p < 0.05$ , \*\*  $p < 0.01$ , or \*\*\*  $p < 0.001$ .

### 3.3. *VDR* and *PDIA3* Deletion Disrupts Membrane Response to 1,25(OH) $_2$ D $_3$ in Squamous Cell Carcinoma

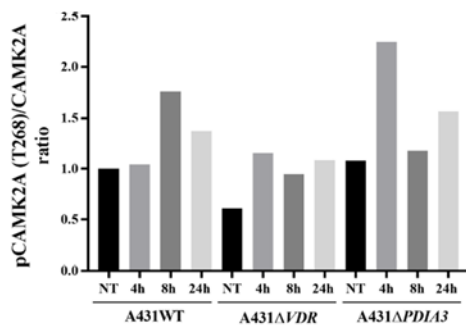
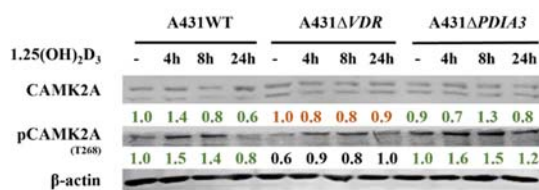
Calcium is a known secondary messenger, which activates several downstream targets such as PKC or CAMKII. Thus, we decided to investigate the downstream targets of calcium signaling as a part of membrane response to 1,25(OH) $_2$ D $_3$  and the role of *VDR* and *PDIA3* proteins in this process. Thus, time-resolved analysis of the levels of calcium-related protein in A431 cell with deletion of either *VDR* or *PDIA3* was performed (Figure 4A). It was observed that *VDR* deletion alone increased baseline levels of the phosphorylated form of extracellular signal-regulated kinase 1/2 (pERK1/2; Thr202/Tyr204) while de-

creasing the phosphorylated form of calcium/calmodulin-dependent protein kinase II alpha (pCAMKII $\alpha$ ; T268) (Figure 4B,C). Interestingly, the deletion of *PDIA3* increased baseline levels Erk1/2. The total amount of CAMKII $\alpha$  was not affected by either *VDR* or *PDIA3* deletion.

**A**



**B**



**C**

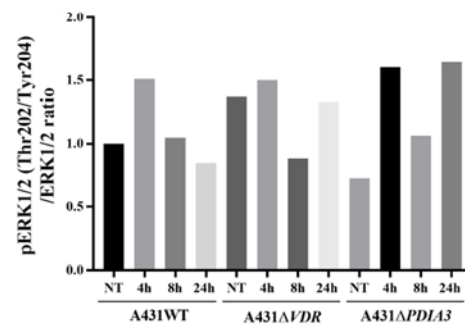
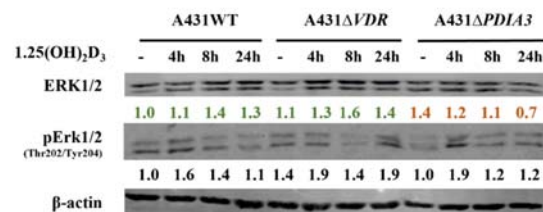


**Figure 4.** Effects of *PDIA3* and *VDR* deletion on 1,25(OH)<sub>2</sub>D<sub>3</sub> signaling pathways in human squamous carcinoma cells (A431). (A) Validation of *VDR* and *PDIA3* knockout in A431 cells. Ratio of phosphorylated forms of (B) CAMK2A (T268) and (C) Erk1/2 (Thr202/Tyr204) proteins. The red color illustrates a decrease in protein level, while green marks an increase. The quantity of each protein was calculated as a protein/β-actin ratio. Protein levels are calculated as means from three independent experiments. Representative pictures are shown for each protein. The red color illustrates a decrease in protein level, while green marks the increase.

*Doroudi M* and coworkers have shown that *PDIA3* is essential for the activation of PLAA, PLC $\gamma$ , and PKC $\alpha$  signaling cascade by 1,25(OH)<sub>2</sub>D<sub>3</sub> [18]. Although we observed that the baseline total levels of PLAA, PLC $\gamma$ , and PKC $\alpha$  were increased by *PDIA3* deletion (Supplementary Figure S2), the change in PLAA and PKC $\alpha$  activity measured by ELISA assays after 1,25(OH)<sub>2</sub>D<sub>3</sub> stimulation was not observed on our cellular model (not shown). Finally, the knockout of the *PDIA3* gene disrupted the response of Erk1/2 and its phosphorylation after 1,25(OH)<sub>2</sub>D<sub>3</sub> treatment (Figure 4C). *VDR* knockout also abolished the response of CAMKII $\alpha$  and its phosphorylation (Figure 4B). Interestingly, 1,25(OH)<sub>2</sub>D<sub>3</sub> treatment induced a slight increase in *PDIA3* level after 24 h incubation, and *VDR* deletion enhanced this effect.

#### 4. Discussion

Complementary to our previous research on the topic of non-genomic responses to  $1,25(\text{OH})_2\text{D}_3$  in squamous cell carcinoma [13,21], we further explored the role of PDIA3 in calcium homeostasis and membrane signaling after  $1,25(\text{OH})_2\text{D}_3$  treatment.

Recently, it has been shown that PDIA3 is strongly involved in the regulation of mitochondrial bioenergetics [20,21]. Here, we have shown that the deletion of the *PDIA3* gene affected the expression of calcium-associated genes and modulated their responses to  $1,25(\text{OH})_2\text{D}_3$ . Those genes were mainly involved in calcium-related processes within mitochondria and endoplasmic reticulum. Interestingly, the expression of some of those genes (*TGM2*, *BNIP3*, *FIS1*) has been linked as prognostic markers in squamous cell carcinomas [28,29]. The silencing of *PDIA3* and  $1,25(\text{OH})_2\text{D}_3$  treatment reversed the expression of those cancer-related genes in A431 cells. In accordance with our previous study, we observed that deletion of *VDR* completely eliminates  $1,25(\text{OH})_2\text{D}_3$ -dependent gene expression [22]. Furthermore, we observed that in cells lacking *VDR*, the activation of the vitamin D response element was completely eliminated, while the deletion of *PDIA3* modulated the activity of VDRE to some extent, especially after 8 h of  $1,25(\text{OH})_2\text{D}_3$  treatment.

Calcium acts as a second messenger molecule and is critical for proper cell physiology and signal transduction [30,31]. Here, we showed the deletion of either *VDR* or *PDIA3* decreased baseline calcium levels in squamous cell carcinoma A431 cells and further impaired calcium influx induced by  $1,25(\text{OH})_2\text{D}_3$ . Those findings were in accordance with our other study on PDIA3's role in calcium signaling. He and coworkers showed that the knockdown of *PDIA3* inhibited mitochondrial calcium uptake within HeLa cells, possibly through the regulation of mitochondrial calcium uniporter (MCU) expression [32]. Additionally, it was shown that the reduction in *VDR* levels in the intestine blunts the  $1,25(\text{OH})_2\text{D}_3$ -regulated absorption of calcium [33]. Furthermore, it was shown in mice models that the transient receptor potential vanilloid type 6 (TRPV6) is essential for vitamin D-induced active calcium transport in the intestine [34]. TRPV6 is a well-known classical target for  $1,25(\text{OH})_2\text{D}_3$  action and plays a vital role in the transcellular transport of calcium ions and uptake [35]. TRPV6 occurs in two forms, glycosylated (gTRPV6, 100 kDa) and non-glycosylated (TRPV6, 80 kDa). It was suggested that glycosylation determines the stability and assembly of TRPV6 [36]. In our previous research, it was shown that *PDIA3* deletion significantly impaired the expression of the *TRPV6* gene and its responsiveness to  $1,25(\text{OH})_2\text{D}_3$  in A431 $\Delta$ *PDIA3* cells [13]. Bianco et al. have shown that the deletion of the TRPV6 calcium channel resulted in no response to PTH or  $1,25(\text{OH})_2\text{D}_3$  treatment on mice models [37]. Here, we have shown that the expression of both forms of *TRPV6* was also impaired by *PDIA3* deletion in A431 cells. Decreased levels of TRPV6 in A431 $\Delta$ *PDIA3* may explain the partial impairment of calcium influx observed with a Fura-2AM probe. Thus, our results indicate that PDIA3 plays a major role in the regulation of calcium homeostasis, including the vitamin D-induced uptake of  $\text{Ca}^{2+}$  or intracellular storage and trafficking with the possible involvement of epithelial channel TRPV6 and the regulation of its stability.

PDIA3 is a protein necessary to maintain normal cellular physiology, and its dysfunction may lead to numerous diseases, including cancers, neurodegenerative diseases, or respiratory pathologies [38–42]. Multiple studies linked PDIA3 to the rapid response of cells to  $1,25(\text{OH})_2\text{D}_3$  [17,18] but the exact mechanism of its action remains unclear. In our previous report, we showed that the deletion of the *PDIA3* gene strongly modulates the effect of  $1,25(\text{OH})_2\text{D}_3$  on the gene expression profile of A431 cells, suggesting that it can directly (as a transcription factor or modulator) or indirectly (through activation of other signaling pathways and/or transcription factors [20,43,44]) affect the genomic activity of vitamin D. Among those genes, PDIA3 deletion increased the expression of PKC $\alpha$  [45]. Here, the total amount of PKC $\alpha$  was also disrupted and the effect of  $1,25(\text{OH})_2\text{D}_3$  was reduced. This is in accordance with the study of Wang et al., where the deletion of PDIA3 impaired the  $1,25(\text{OH})_2\text{D}_3$ -induced activity of PKC [14]. Our results presented here demonstrate that both *VDR* and *PDIA3* proteins are indeed involved in the  $1,25(\text{OH})_2\text{D}_3$  membrane response of A431 cells [46]. Nevertheless, it seems that the cooperation of both is essential



for membrane response. PDIA3 was co-localized with VDR in caveolae, and it was proven that both proteins can interact with caveolin-1 [17]. Another study by Doroudi and coworkers showed that CAMKIIA is required for mediating the rapid actions of  $1,25(\text{OH})_2\text{D}_3$  [47]. However, in our study, only the deletion of VDR attenuated the impact of  $1,25(\text{OH})_2\text{D}_3$  on levels of CAMKIIA. It was shown recently that the activation of PLC $\gamma$ -mediated signaling results in the release of calcium from intracellular stores and induces an influx of ions across the plasma membrane [48]. Here, we observed that the deletion of PDIA3 had the most prominent effect on the expression of PLC $\gamma$ ; however, a change in its activity was not observed, and thus, the involvement of PLC $\gamma$  in  $1,25(\text{OH})_2\text{D}_3$  signaling in the A431 squamous cell carcinoma cell line requires further investigation. Decreased levels of PKC $\alpha$  to  $1,25(\text{OH})_2\text{D}_3$  in A431 $\Delta$ PDIA3 cells are in accordance with the observations of Boyan and colleagues, who showed that the partial deletion of PDIA3 impaired the activation of PKC through PLAA induction due to lack of interaction between PDIA3/Cav1/PLAA [49].

Here, we showed a major role of PDIA3 in membrane response to an active form of vitamin D. Our results indicate that PDIA3 is not solely responsible for the activation of the non-genomic pathway of  $1,25(\text{OH})_2\text{D}_3$ , but that VDR is also required for this action. However, it seems that VDR and PDIA3 affect different targets of the  $1,25(\text{OH})_2\text{D}_3$  membrane response. Our results are further supported by a previous study in which we stated that PDIA3 is a modulator of the genomic actions of vitamin D [13]. Moreover, it seems that VDR and PDIA3 are required for the regulation of calcium influx induced by  $1,25(\text{OH})_2\text{D}_3$  in squamous cell carcinoma. The proposed involvement of PDIA3 and VDR in  $1,25(\text{OH})_2\text{D}_3$  action is shown in Figure 5.

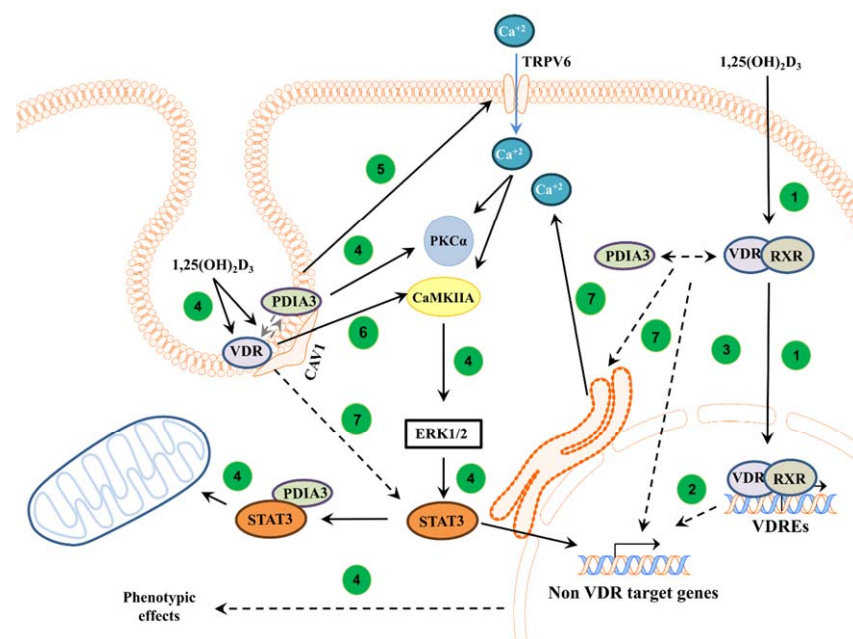


**Figure 5.** Proposed mechanism of action of VDR and PDIA3 to  $1,25(\text{OH})_2\text{D}_3$  membrane response in squamous cell carcinoma. In the classical pathway,  $1,25(\text{OH})_2\text{D}_3$  is bound by a heterodimer of VDR/RXR proteins and, subsequently, the complex is translocated into the nucleus where it regulates the transcription of vitamin D target genes [1] (1). Further, primary VDR target transcription factors can regulate secondary non-vitamin D target genes [50] (2). It was also postulated that PDIA3 can modulate genomic response to  $1,25(\text{OH})_2\text{D}_3$  [13] (3). In non-genomic pathways, VDR and PDIA3 were shown to interact with caveolin-1 [17]. PDIA3 was shown to be essential to activate PKC after  $1,25(\text{OH})_2\text{D}_3$  treatment [14] (4). Moreover, PDIA3 affects TRPV6 levels within SCC cells, possibly disrupting calcium response (5). Either PDIA3 or VDR are needed to activate STAT3, possibly regulating mitochondrial bioenergetics and non-VDR target genes [13,21] (4). Interestingly, it seems that VDR is required to activate CAMK2IIA kinase (6), while either protein is essential for valid calcium signaling (7).

Taken together, our results presented here emphasize the importance of PDIA3 in 1,25(OH)<sub>2</sub>D<sub>3</sub> signaling in squamous cell carcinoma cell line A431. The deletion of *PDIA3* not only affected membrane signaling but also genomic responses to vitamin D. Moreover, it seems that both VDR and PDIA3 are required for the regulation of calcium signaling induced by 1,25(OH)<sub>2</sub>D<sub>3</sub> in A431 squamous cell carcinoma.

## 5. Conclusions

In conclusion, this study demonstrated that both VDR and PDIA3 are needed to regulate membrane response to active forms of vitamin D in A431 squamous cell carcinoma, possibly through CAMKII $\alpha$  and impaired calcium influx, respectively. The proposed roles of PDIA3 and VDR in the regulation of intracellular response to 1,25(OH)<sub>2</sub>D<sub>3</sub> are summarized in Figure 5.

**Supplementary Materials:** The following supporting information can be downloaded at: <https://www.mdpi.com/article/10.3390/cells13010011/s1>, Figure S1: Time-resolved analysis of intracellular calcium levels measured with Fura-2AM probe on a microplate reader. A431 sublines were stimulated with (A) 1  $\mu$ M, (B) 100 nM or (C) 10 nM 1,25(OH)<sub>2</sub>D<sub>3</sub>. Please, note that panel C was taken from Figure 2C for comparison. Results were calculated as a mean  $\pm$  SD of triplicates. Statistically significant differences are illustrated with asterisks: \*  $p < 0.05$ , \*\*  $p < 0.01$ , \*\*\*  $p < 0.001$ , or \*\*\*\*  $p < 0.0001$ . Figure S2: Analysis of PLAA, PLC $\gamma$ , PKC $\alpha$  protein levels in A431 sublines after 1,25(OH)<sub>2</sub>D<sub>3</sub> treatment. The red color illustrates a decrease in protein level, while green marks the increase. The quantity of each protein was calculated as a protein/ $\beta$ -actin ratio. Protein levels are calculated as a mean from three independent experiments. Representative pictures were shown for each protein.

**Author Contributions:** Conceptualization, M.A.Ž. and R.B.; methodology, J.I.N., M.G., J.M.W. and A.M.O.; software, J.I.N. and M.G.; validation, M.A.Ž., J.I.N. and R.B.; investigation, J.I.N., M.G. and A.M.O.; resources, M.A.Ž.; data curation, J.I.N. and M.A.Ž.; writing—original draft preparation, J.I.N.; writing—review and editing, M.A.Ž.; visualization, J.I.N., M.G.; supervision, M.A.Ž.; funding acquisition, M.A.Ž. All authors have read and agreed to the published version of the manuscript.

**Funding:** The study was supported by a National Science Center OPUS Program under contract 2017/25/B/NZ3/00431.

**Institutional Review Board Statement:** Not applicable.

**Informed Consent Statement:** Not applicable.

**Data Availability Statement:** Data are contained within the article and Supplementary Materials.

**Conflicts of Interest:** The authors declare that they have no competing interests.

## Abbreviations

1,25-MARRS	Membrane-Associated, Rapid Response Steroid-binding
BNIP3	BCL2 Interacting Protein 3
CAMK2A	Calcium/Calmodulin-Dependent Protein Kinase II Alpha
CAV-1	Caveolin 1
CAV-3	Caveolin 3
Erk1/2	Extracellular Signal-Regulated Kinase 1/2
ERp57	Endoplasmic Reticulum Resident Protein 57
FIS1	Fission, Mitochondrial 1
NFAT	Nuclear Factor of Activated T-cells
PDIA3	Protein Disulfide Isomerase Family A Member 3
PKC $\alpha$	Protein Kinase C-alpha
PLAA	Phospholipase A2-Activating Protein
PLC $\gamma$	Phospholipase C Gamma 1
RXR	Retinoid X Receptor
A431	Squamous Cell Carcinoma cell line

STAT3	Signal Transducer and Activator of Transcription 3
TGM2	Transglutaminase 2
TRPV6	Transient Receptor Potential Cation Channel Subfamily V Member 6
VDR	Vitamin D Receptor
VDRE	Vitamin D Response Elements

## References

- Haussler, M.R.; Jurutka, P.W.; Mizwicki, M.; Norman, A.W. Vitamin D receptor (VDR)-mediated actions of  $1\alpha,25(\text{OH})_2$  vitamin D<sub>3</sub>: Genomic and non-genomic mechanisms. *Best Pract. Res. Clin. Endocrinol. Metab.* **2011**, *25*, 543–559. [[CrossRef](#)] [[PubMed](#)]
- Whitfield, G.K.; Jurutka, P.W.; Haussler, C.A.; Hsieh, J.C.; Barthel, T.K.; Jacobs, E.T.; Dominguez, C.E.; Thatcher, M.L.; Haussler, M.R. CHAPTER 13—Nuclear Vitamin D Receptor: Structure-Function, Molecular Control of Gene Transcription, and Novel Bioactions. In *Vitamin D (Second Edition)*; David, F., Ed.; Academic Press: Burlington, NJ, USA, 2005; pp. 219–261. [[CrossRef](#)]
- Zmijewski, M.A. Vitamin D and Human Health. *Int. J. Mol. Sci.* **2019**, *20*, 145. [[CrossRef](#)] [[PubMed](#)]
- Christakos, S.; Dhawan, P.; Verstuyf, A.; Verlinden, L.; Carmeliet, G. Vitamin D: Metabolism, Molecular Mechanism of Action, and Pleiotropic Effects. *Physiol. Rev.* **2016**, *96*, 365–408. [[CrossRef](#)] [[PubMed](#)]
- Schwartz, N.; Verma, A.; Bivens, C.B.; Schwartz, Z.; Boyan, B.D. Rapid steroid hormone actions via membrane receptors. *Biochim. Biophys. Acta* **2016**, *1863*, 2289–2298. [[CrossRef](#)]
- Civitelli, R.; Kim, Y.S.; Gunsten, S.L.; Fujimori, A.; Huskey, M.; Avioli, L.V.; Hruska, K.A. Nongenomic activation of the calcium message system by vitamin D metabolites in osteoblast-like cells. *Endocrinology* **1990**, *127*, 2253–2262. [[CrossRef](#)]
- Sterling, T.M.; Nemere, I. 1,25-dihydroxyvitamin D<sub>3</sub> stimulates vesicular transport within 5 s in polarized intestinal epithelial cells. *J. Endocrinol.* **2005**, *185*, 81–91. [[CrossRef](#)]
- Nemere, I.; Schwartz, Z.; Pedrozo, H.; Sylvia, V.L.; Dean, D.D.; Boyan, B.D. Identification of a membrane receptor for 1,25-dihydroxyvitamin D<sub>3</sub> which mediates rapid activation of protein kinase C. *J. Bone Miner. Res.* **1998**, *13*, 1353–1359. [[CrossRef](#)]
- Nemere, I.; Safford, S.E.; Rohe, B.; DeSouza, M.M.; Farach-Carson, M.C. Identification and characterization of 1,25D<sub>3</sub>-membrane-associated rapid response, steroid (1,25D<sub>3</sub>-MARRS) binding protein. *J. Steroid Biochem. Mol. Biol.* **2004**, *89–90*, 281–285. [[CrossRef](#)]
- Hettinghouse, A.; Liu, R.; Liu, C.J. Multifunctional molecule ERp57: From cancer to neurodegenerative diseases. *Pharmacol. Ther.* **2018**, *181*, 34–48. [[CrossRef](#)]
- Nemere, I.; Garbi, N.; Hämmerling, G.J.; Khanal, R.C. Intestinal cell calcium uptake and the targeted knockout of the 1,25D<sub>3</sub>-MARRS (membrane-associated, rapid response steroid-binding) receptor/PDIA3/Erp57. *J. Biol. Chem.* **2010**, *285*, 31859–31866. [[CrossRef](#)]
- Nemere, I.; Farach-Carson, M.C.; Rohe, B.; Sterling, T.M.; Norman, A.W.; Boyan, B.D.; Safford, S.E. Ribozyme knockdown functionally links a 1,25(OH)<sub>2</sub>D<sub>3</sub> membrane binding protein (1,25D<sub>3</sub>-MARRS) and phosphate uptake in intestinal cells. *Proc. Natl. Acad. Sci. USA* **2004**, *101*, 7392–7397. [[CrossRef](#)] [[PubMed](#)]
- Nowak, J.I.; Olszewska, A.M.; Piotrowska, A.; Myszczynski, K.; Domzalski, P.; Zmijewski, M.A. PDIA3 modulates genomic response to 1,25-dihydroxyvitamin D(3) in squamous cell carcinoma of the skin. *Steroids* **2023**, *199*, 109288. [[CrossRef](#)] [[PubMed](#)]
- Wang, Y.; Chen, J.; Lee, C.S.; Nizkorodov, A.; Riemenschneider, K.; Martin, D.; Hyzy, S.; Schwartz, Z.; Boyan, B.D. Disruption of Pdia3 gene results in bone abnormality and affects 1 $\alpha$ ,25-dihydroxy-vitamin D<sub>3</sub>-induced rapid activation of PKC. *J. Steroid Biochem. Mol. Biol.* **2010**, *121*, 257–260. [[CrossRef](#)] [[PubMed](#)]
- Garbi, N.; Tanaka, S.; Momburg, F.; Hämmerling, G.J. Impaired assembly of the major histocompatibility complex class I peptide-loading complex in mice deficient in the oxidoreductase ERp57. *Nat. Immunol.* **2006**, *7*, 93–102. [[CrossRef](#)] [[PubMed](#)]
- Wang, Y.; Nizkorodov, A.; Riemenschneider, K.; Lee, C.S.; Olivares-Navarrete, R.; Schwartz, Z.; Boyan, B.D. Impaired bone formation in Pdia3 deficient mice. *PLoS ONE* **2014**, *9*, e112708. [[CrossRef](#)] [[PubMed](#)]
- Chen, J.; Doroudi, M.; Cheung, J.; Grozier, A.L.; Schwartz, Z.; Boyan, B.D. Plasma membrane Pdia3 and VDR interact to elicit rapid responses to  $1\alpha,25(\text{OH})_2$ D(3). *Cell. Signal.* **2013**, *25*, 2362–2373. [[CrossRef](#)] [[PubMed](#)]
- Doroudi, M.; Schwartz, Z.; Boyan, B.D. Membrane-mediated actions of 1,25-dihydroxy vitamin D<sub>3</sub>: A review of the roles of phospholipase A2 activating protein and Ca(2+)/calmodulin-dependent protein kinase II. *J. Steroid Biochem. Mol. Biol.* **2015**, *147*, 81–84. [[CrossRef](#)] [[PubMed](#)]
- Yang, W.S.; Yu, H.; Kim, J.J.; Lee, M.J.; Park, S.K. Vitamin D-induced ectodomain shedding of TNF receptor 1 as a nongenomic action: D<sub>3</sub> vs D<sub>2</sub> derivatives. *J. Steroid Biochem. Mol. Biol.* **2016**, *155*, 18–25. [[CrossRef](#)]
- Keasey, M.P.; Razskazovskiy, V.; Jia, C.; Peterknecht, E.D.; Bradshaw, P.C.; Hagg, T. PDIA3 inhibits mitochondrial respiratory function in brain endothelial cells and *C. elegans* through STAT3 signaling and decreases survival after OGD. *Cell Commun. Signal.* **2021**, *19*, 119. [[CrossRef](#)]
- Nowak, J.I.; Olszewska, A.M.; Król, O.; Zmijewski, M.A. Protein Disulfide Isomerase Family A Member 3 Knockout Abrogate Effects of Vitamin D on Cellular Respiration and Glycolysis in Squamous Cell Carcinoma. *Nutrients* **2023**, *15*, 4529. [[CrossRef](#)]
- Olszewska, A.M.; Nowak, J.I.; Myszczynski, K.; Slominski, A.; Zmijewski, M.A. Dissection of an Impact of Vdr and Rxra on Genomic Activity of 1,25(OH)<sub>2</sub>D<sub>3</sub> in A431 Squamous Cell Carcinoma. *Mol. Cell Endocrinol.* **2023**, *in press*. [[CrossRef](#)]
- Chaiprasongsuk, A.; Janjetovic, Z.; Kim, T.K.; Jarrett, S.G.; D’Orazio, J.A.; Holick, M.F.; Tang, E.K.Y.; Tuckey, R.C.; Panich, U.; Li, W.; et al. Protective effects of novel derivatives of vitamin D(3) and lumisterol against UVB-induced damage in human keratinocytes involve activation of Nrf2 and p53 defense mechanisms. *Redox Biol.* **2019**, *24*, 101206. [[CrossRef](#)] [[PubMed](#)]



24. Tuckey, R.C.; Li, W.; Shehabi, H.Z.; Janjetovic, Z.; Nguyen, M.N.; Kim, T.K.; Chen, J.; Howell, D.E.; Benson, H.A.; Sweatman, T.; et al. Production of 22-hydroxy metabolites of vitamin d3 by cytochrome p450scc (CYP11A1) and analysis of their biological activities on skin cells. *Drug Metab. Dispos.* **2011**, *39*, 1577–1588. [[CrossRef](#)] [[PubMed](#)]
25. Tunsophon, S.; Nemere, I. Protein kinase C isotypes in signal transduction for the 1,25D3-MARRS receptor (ERp57/PDIA3) in steroid hormone-stimulated phosphate uptake. *Steroids* **2010**, *75*, 307–313. [[CrossRef](#)]
26. Takeuchi, A.; Reddy, G.S.; Kobayashi, T.; Okano, T.; Park, J.; Sharma, S. Nuclear factor of activated T cells (NFAT) as a molecular target for 1 $\alpha$ ,25-dihydroxyvitamin D3-mediated effects. *J. Immunol.* **1998**, *160*, 209–218. [[CrossRef](#)] [[PubMed](#)]
27. Park, Y.J.; Yoo, S.A.; Kim, M.; Kim, W.U. The Role of Calcium–Calcineurin–NFAT Signaling Pathway in Health and Autoimmune Diseases. *Front. Immunol.* **2020**, *11*, 195. [[CrossRef](#)] [[PubMed](#)]
28. Jin, T.; Lin, H.X.; Lin, H.; Guo, L.B.; Ge, N.; Cai, X.Y.; Sun, R.; Chen, W.K.; Li, Q.L.; Hu, W.H. Expression TGM2 and BNIP3 have prognostic significance in laryngeal cancer patients receiving surgery and postoperative radiotherapy: A retrospective study. *J. Transl. Med.* **2012**, *10*, 64. [[CrossRef](#)] [[PubMed](#)]
29. Fan, S.; Chen, W.X.; Lv, X.B.; Tang, Q.L.; Sun, L.J.; Liu, B.D.; Zhong, J.L.; Lin, Z.Y.; Wang, Y.Y.; Li, Q.X.; et al. miR-483-5p determines mitochondrial fission and cisplatin sensitivity in tongue squamous cell carcinoma by targeting FIS1. *Cancer Lett.* **2015**, *362*, 183–191. [[CrossRef](#)]
30. Sukumaran, P.; Nascimento Da Conceicao, V.; Sun, Y.; Ahamad, N.; Saraiva, L.R.; Selvaraj, S.; Singh, B.B. Calcium Signaling Regulates Autophagy and Apoptosis. *Cells* **2021**, *10*, 2125. [[CrossRef](#)]
31. Patergnani, S.; Danese, A.; Bouhamida, E.; Aguiari, G.; Previati, M.; Pinton, P.; Giorgi, C. Various Aspects of Calcium Signaling in the Regulation of Apoptosis, Autophagy, Cell Proliferation, and Cancer. *Int. J. Mol. Sci.* **2020**, *21*, 8323. [[CrossRef](#)]
32. He, J.; Shi, W.; Guo, Y.; Chai, Z. ERp57 modulates mitochondrial calcium uptake through the MCU. *FEBS Lett.* **2014**, *588*, 2087–2094. [[CrossRef](#)] [[PubMed](#)]
33. Song, Y.; Fleet, J.C. Intestinal resistance to 1,25 dihydroxyvitamin D in mice heterozygous for the vitamin D receptor knockout allele. *Endocrinology* **2007**, *148*, 1396–1402. [[CrossRef](#)] [[PubMed](#)]
34. Benn, B.S.; Ajibade, D.; Porta, A.; Dhawan, P.; Hediger, M.; Peng, J.B.; Jiang, Y.; Oh, G.T.; Jeung, E.B.; Lieben, L.; et al. Active intestinal calcium transport in the absence of transient receptor potential vanilloid type 6 and calbindin-D9k. *Endocrinology* **2008**, *149*, 3196–3205. [[CrossRef](#)] [[PubMed](#)]
35. Khattar, V.; Wang, L.; Peng, J.B. Calcium selective channel TRPV6: Structure, function, and implications in health and disease. *Gene* **2022**, *817*, 146192. [[CrossRef](#)] [[PubMed](#)]
36. Hoenderop, J.G.; Voets, T.; Hoefs, S.; Weidema, F.; Prenen, J.; Nilius, B.; Bindels, R.J. Homo- and heterotetrameric architecture of the epithelial Ca<sup>2+</sup> channels TRPV5 and TRPV6. *Embo J.* **2003**, *22*, 776–785. [[CrossRef](#)] [[PubMed](#)]
37. Bianco, S.D.; Peng, J.B.; Takanao, H.; Suzuki, Y.; Crescenzi, A.; Kos, C.H.; Zhuang, L.; Freeman, M.R.; Gouveia, C.H.; Wu, J.; et al. Marked disturbance of calcium homeostasis in mice with targeted disruption of the Trpv6 calcium channel gene. *J. Bone Miner. Res.* **2007**, *22*, 274–285. [[CrossRef](#)] [[PubMed](#)]
38. Hoffman, S.M.; Chapman, D.G.; Lahue, K.G.; Cahoon, J.M.; Rattu, G.K.; Daphtary, N.; Aliyeva, M.; Fortner, K.A.; Erzurum, S.C.; Comhair, S.A.; et al. Protein disulfide isomerase-endoplasmic reticulum resident protein 57 regulates allergen-induced airways inflammation, fibrosis, and hyperresponsiveness. *J. Allergy Clin. Immunol.* **2016**, *137*, 822–832.e827. [[CrossRef](#)]
39. Hoffman, S.M.; Tully, J.E.; Nolin, J.D.; Lahue, K.G.; Goldman, D.H.; Daphtary, N.; Aliyeva, M.; Irvin, C.G.; Dixon, A.E.; Poynter, M.E.; et al. Endoplasmic reticulum stress mediates house dust mite-induced airway epithelial apoptosis and fibrosis. *Respir. Res.* **2013**, *14*, 141. [[CrossRef](#)]
40. Diaz Cruz, M.A.; Karlsson, S.; Szekeres, F.; Faresjö, M.; Lund, D.; Larsson, D. Differential expression of protein disulfide-isomerase A3 isoforms, PDIA3 and PDIA3N, in human prostate cancer cell lines representing different stages of prostate cancer. *Mol. Biol. Rep.* **2021**, *48*, 2429–2436. [[CrossRef](#)]
41. Ramos, F.S.; Serino, L.T.; Carvalho, C.M.; Lima, R.S.; Urban, C.A.; Cavalli, I.J.; Ribeiro, E.M. PDIA3 and PDIA6 gene expression as an aggressiveness marker in primary ductal breast cancer. *Genet. Mol. Res.* **2015**, *14*, 6960–6967. [[CrossRef](#)]
42. Gonzalez-Perez, P.; Woehlbier, U.; Chian, R.J.; Sapp, P.; Rouleau, G.A.; Leblond, C.S.; Daoud, H.; Dion, P.A.; Landers, J.E.; Hetz, C.; et al. Identification of rare protein disulfide isomerase gene variants in amyotrophic lateral sclerosis patients. *Gene* **2015**, *566*, 158–165. [[CrossRef](#)] [[PubMed](#)]
43. Hu, W.; Zhang, L.; Li, M.X.; Shen, J.; Liu, X.D.; Xiao, Z.G.; Wu, D.L.; Ho, I.H.T.; Wu, J.C.Y.; Cheung, C.K.Y.; et al. Vitamin D3 activates the autolysosomal degradation function against Helicobacter pylori through the PDIA3 receptor in gastric epithelial cells. *Autophagy* **2019**, *15*, 707–725. [[CrossRef](#)] [[PubMed](#)]
44. Wu, W.; Beilhardt, G.; Roy, Y.; Richard, C.L.; Curtin, M.; Brown, L.; Cadieux, D.; Coppolino, M.; Farach-Carson, M.C.; Nemere, I.; et al. Nuclear translocation of the 1,25D3-MARRS (membrane associated rapid response to steroids) receptor protein and NFkappaB in differentiating NB4 leukemia cells. *Exp. Cell Res.* **2010**, *316*, 1101–1108. [[CrossRef](#)] [[PubMed](#)]
45. Zmijewski, M.A.; Carlberg, C. Vitamin D receptor(s): In the nucleus but also at membranes? *Exp. Dermatol.* **2020**, *29*, 876–884. [[CrossRef](#)]
46. Zmijewski, M.A. Nongenomic Activities of Vitamin D. *Nutrients* **2022**, *14*, 5104. [[CrossRef](#)]
47. Doroudi, M.; Chen, J.; Boyan, B.D.; Schwartz, Z. New insights on membrane mediated effects of 1 $\alpha$ ,25-dihydroxy vitamin D3 signaling in the musculoskeletal system. *Steroids* **2014**, *81*, 81–87. [[CrossRef](#)]

48. Gusev, K.; Glouchankova, L.; Zubov, A.; Kaznacheyeva, E.; Wang, Z.; Bezprozvanny, I.; Mozhayeva, G.N. The store-operated calcium entry pathways in human carcinoma A431 cells: Functional properties and activation mechanisms. *J. Gen. Physiol.* **2003**, *122*, 81–94. [[CrossRef](#)]
49. Boyan, B.D.; Chen, J.; Schwartz, Z. Mechanism of Pdia3-dependent  $1\alpha,25$ -dihydroxy vitamin D3 signaling in musculoskeletal cells. *Steroids* **2012**, *77*, 892–896. [[CrossRef](#)]
50. Warwick, T.; Schulz, M.H.; Günther, S.; Gilsbach, R.; Neme, A.; Carlberg, C.; Brandes, R.P.; Seuter, S. A hierarchical regulatory network analysis of the vitamin D induced transcriptome reveals novel regulators and complete VDR dependency in monocytes. *Sci. Rep.* **2021**, *11*, 6518. [[CrossRef](#)]

**Disclaimer/Publisher’s Note:** The statements, opinions and data contained in all publications are solely those of the individual author(s) and contributor(s) and not of MDPI and/or the editor(s). MDPI and/or the editor(s) disclaim responsibility for any injury to people or property resulting from any ideas, methods, instructions or products referred to in the content.

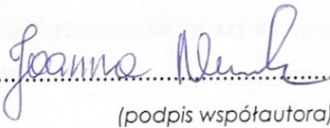
## **XI. STATEMENTS OF CO-AUTHORS**

Gdańsk, dnia 7 grudnia 2023r.

mgr Joanna Nowak  
(tytuł zawodowy, imię i nazwisko)

### OŚWIADCZENIE

Jako współautor pracy pt. „*PDIA3 modulates genomic response to 1,25-dihydroxyvitamin D3 in squamous cell carcinoma of the skin*” oświadczam, iż mój własny wkład merytoryczny w przygotowanie, przeprowadzenie i opracowanie badań oraz przedstawienie pracy w formie publikacji to konceptualizacja i przeprowadzenie badań, opracowanie metodologii, wizualizacja uzyskanych wyników, napisanie manuskryptu.

  
.....  
(podpis współautora)

Gdańsk, dnia 7 grudnia 2023r.

dr Anna Olszewska  
(tytuł zawodowy, imię i nazwisko)

### OŚWIADCZENIE

Jako współautor pracy pt. „*PDIA3 modulates genomic response to 1,25-dihydroxyvitamin D3 in squamous cell carcinoma of the skin*” oświadczam, iż mój własny wkład merytoryczny w przygotowanie, przeprowadzenie i opracowanie badań oraz przedstawienie pracy w formie publikacji to pomoc w przeprowadzeniu badań.

Jednocześnie wyrażam zgodę na przedłożenie w/w pracy przez mgr Joannę Nowak jako część rozprawy doktorskiej w formie spójnego tematycznie zbioru artykułów opublikowanych w czasopismach naukowych.

Oświadczam, iż samodzielna i możliwa do wyodrębnienia część ww. pracy wykazuje indywidualny wkład mgr Joanny Nowak przy opracowywaniu koncepcji, wykonywaniu części eksperymentalnej, opracowaniu i interpretacji wyników tej pracy.

*Anna Olszewska*

(podpis współautora)



Gdańsk, dnia 7 grudnia 2023r.

dr Kamil Myszczyński  
(tytuł zawodowy, imię i nazwisko)

### OŚWIADCZENIE

Jako współautor pracy pt. „*PDIA3 modulates genomic response to 1,25-dihydroxyvitamin D3 in squamous cell carcinoma of the skin*” oświadczam, iż mój własny wkład merytoryczny w przygotowanie, przeprowadzenie i opracowanie badań oraz przedstawienie pracy w formie publikacji to obróbka danych wraz z walidacją i wizualizacją wyników analizy transkryptomicznej.

Jednocześnie wyrażam zgodę na przedłożenie w/w pracy przez mgr Joannę Nowak jako część rozprawy doktorskiej w formie spójnego tematycznie zbioru artykułów opublikowanych w czasopismach naukowych.

Oświadczam, iż samodzielna i możliwa do wyodrębnienia część ww. pracy wykazuje indywidualny wkład mgr Joanny Nowak przy opracowywaniu koncepcji, wykonywaniu części eksperymentalnej, opracowaniu i interpretacji wyników tej pracy.

  
.....  
(podpis współautora)

Gdańsk, dnia 7 grudnia 2023r.

mgr Paweł Domżański  
(tytuł zawodowy, imię i nazwisko)

### OŚWIADCZENIE

Jako współautor pracy pt. „*PDIA3 modulates genomic response to 1,25-dihydroxyvitamin D3 in squamous cell carcinoma of the skin*” oświadczam, iż mój własny wkład merytoryczny w przygotowanie, przeprowadzenie i opracowanie badań oraz przedstawienie pracy w formie publikacji to przygotowanie metodologii związanej z analizą real-time PCR.

Jednocześnie wyrażam zgodę na przedłożenie w/w pracy przez mgr Joannę Nowak jako część rozprawy doktorskiej w formie spójnego tematycznie zbioru artykułów opublikowanych w czasopismach naukowych.

Oświadczam, iż samodzielna i możliwa do wyodrębnienia część ww. pracy wykazuje indywidualny wkład mgr Joanny Nowak przy opracowywaniu koncepcji, wykonywaniu części eksperymentalnej, opracowaniu i interpretacji wyników tej pracy.



(podpis współautora)



Gdańsk, dnia 7 grudnia 2023r.

prof. dr hab. Michał Żmijewski  
(tytuł zawodowy, imię i nazwisko)

### OŚWIADCZENIE

Jako współautor pracy pt. „PDIA3 modulates genomic response to 1,25-dihydroxyvitamin D3 in squamous cell carcinoma of the skin” oświadczam, iż mój własny wkład merytoryczny w przygotowanie, przeprowadzenie i opracowanie badań oraz przedstawienie pracy w formie publikacji to konceptualizacja badań, pozyskanie źródła finansowania badań, nadzór merytoryczny, walidacja pozyskanych danych, opracowanie metodologii, wizualizacja uzyskanych wyników oraz opracowanie manuskryptu publikacji.

Jednocześnie wyrażam zgodę na przedłożenie w/w pracy przez mgr Joannę Nowak jako część rozprawy doktorskiej w formie spójnego tematycznie zbioru artykułów opublikowanych w czasopismach naukowych.

Oświadczam, iż samodzielna i możliwa do wyodrębnienia część ww. pracy wykazuje indywidualny wkład mgr Joanny Nowak przy opracowywaniu koncepcji, wykonywaniu części eksperymentalnej, opracowaniu i interpretacji wyników tej pracy.

Katedra i Zakład Histologii  
Gdański Uniwersytet Medyczny

Prof. dr hab. Michał Żmijewski

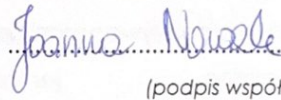
.....  
(podpis współautora)

Gdańsk, dnia 7 grudnia 2023r.

mgr Joanna Nowak  
(tytuł zawodowy, imię i nazwisko)

### OŚWIADCZENIE

Jako współautor pracy pt. „Protein Disulfide Isomerase Family A Member 3 Knockout Abrogate Effects of Vitamin D on Cellular Respiration and Glycolysis in Squamous Cell Carcinoma” oświadczam, iż mój własny wkład merytoryczny w przygotowanie, przeprowadzenie i opracowanie badań oraz przedstawienie pracy w formie publikacji to udział w projektowaniu, planowaniu i wykonywaniu doświadczeń, analiza uzyskanych wyników wraz z ich wizualizacją oraz opracowanie manuskryptu publikacji.

  
.....  
(podpis współautora)

Gdańsk, dnia 7 grudnia 2023r.

dr Anna Olszewska  
(tytuł zawodowy, imię i nazwisko)

### OŚWIADCZENIE

Jako współautor pracy pt. „*Protein Disulfide Isomerase Family A Member 3 Knockout Abrogate Effects of Vitamin D on Cellular Respiration and Glycolysis in Squamous Cell Carcinoma*” oświadczam, iż mój własny wkład merytoryczny w przygotowanie, przeprowadzenie i opracowanie badań oraz przedstawienie pracy w formie publikacji to udział w projektowaniu, planowaniu i wykonywaniu doświadczeń oraz udział w analizie pozyskanych danych.

Jednocześnie wyrażam zgodę na przedłożenie w/w pracy przez mgr Joannę Nowak jako część rozprawy doktorskiej w formie spójnego tematycznie zbioru artykułów opublikowanych w czasopismach naukowych.

Oświadczam, iż samodzielna i możliwa do wyodrębnienia część ww. pracy wykazuje indywidualny wkład mgr Joanny Nowak przy opracowywaniu koncepcji, wykonywaniu części eksperymentalnej, opracowaniu i interpretacji wyników tej pracy.

*Anna Olszewska*  
.....

(podpis współautora)



Gdańsk, dnia 7 grudnia 2023r.

mgr Oliwia Król  
(tytuł zawodowy, imię i nazwisko)

### OŚWIADCZENIE

Jako współautor pracy pt. „*Protein Disulfide Isomerase Family A Member 3 Knockout Abrogate Effects of Vitamin D on Cellular Respiration and Glycolysis in Squamous Cell Carcinoma*” oświadczam, iż mój własny wkład merytoryczny w przygotowanie, przeprowadzenie i opracowanie badań oraz przedstawienie pracy w formie publikacji to wykonanie testów metabolicznych z użyciem sprzętu Seahorse XF24 .

Jednocześnie wyrażam zgodę na przedłożenie w/w pracy przez mgr Joannę Nowak jako część rozprawy doktorskiej w formie spójnego tematycznie zbioru artykułów opublikowanych w czasopismach naukowych.

Oświadczam, iż samodzielna i możliwa do wyodrębnienia część ww. pracy wykazuje indywidualny wkład mgr Joanny Nowak przy opracowywaniu koncepcji, wykonywaniu części eksperymentalnej, opracowaniu i interpretacji wyników tej pracy.

.....  
Oliwia Król

(podpis współautora)

Gdańsk, dnia 7 grudnia 2023r.

prof. dr hab. Michał Żmijewski  
(tytuł zawodowy, imię i nazwisko)

### OŚWIADCZENIE

Jako współautor pracy pt. „*Protein Disulfide Isomerase Family A Member 3 Knockout Abrogate Effects of Vitamin D on Cellular Respiration and Glycolysis in Squamous Cell Carcinoma*” oświadczam, iż mój własny wkład merytoryczny w przygotowanie, przeprowadzenie i opracowanie badań oraz przedstawienie pracy w formie publikacji to stworzenie i zaplanowanie projektu, nadzór merytoryczny prowadzonych badań, analiza uzyskanych wyników wraz z opracowaniem manuskryptu publikacji.

Jednocześnie wyrażam zgodę na przedłożenie w/w pracy przez mgr Joannę Nowak jako część rozprawy doktorskiej w formie spójnego tematycznie zbioru artykułów opublikowanych w czasopismach naukowych.

Oświadczam, iż samodzielna i możliwa do wyodrębnienia część ww. pracy wykazuje indywidualny wkład mgr Joanny Nowak przy opracowywaniu koncepcji, wykonywaniu części eksperymentalnej, opracowaniu i interpretacji wyników tej pracy.

Katedra i Zakład Histologii  
Gdański Uniwersytet Medyczny

Prof. dr hab. Michał Żmijewski

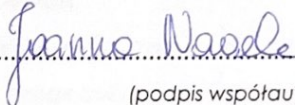
.....  
(podpis współautora)

Gdańsk, dnia 7 grudnia 2023r.

mgr Joanna Nowak  
(tytuł zawodowy, imię i nazwisko)

### OŚWIADCZENIE

Jako współautor pracy pt. „VDR and PDIA3 are essential for activation of calcium signaling and membrane response to 1,25(OH)<sub>2</sub>D<sub>3</sub> in squamous cell carcinoma cells” oświadczam, iż mój własny wkład merytoryczny w przygotowanie, przeprowadzenie i opracowanie badań oraz przedstawienie pracy w formie publikacji to zaplanowanie i wykonywanie części eksperymentalnej, analiza i wizualizacja uzyskanych wyników oraz napisanie manuskryptu publikacji.

  
.....  
(podpis współautora)



Gdańsk, dnia 7 grudnia 2023r.

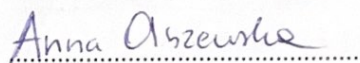
dr Anna Olszewska  
(tytuł zawodowy, imię i nazwisko)

### OŚWIADCZENIE

Jako współautor pracy pt. „VDR and PDIA3 are essential for activation of calcium signaling and membrane response to 1,25(OH)2D3 in squamous cell carcinoma cells” oświadczam, iż mój własny wkład merytoryczny w przygotowanie, przeprowadzenie i opracowanie badań oraz przedstawienie pracy w formie publikacji to udział w wykonywaniu doświadczeń oraz udział w analizie pozyskanych danych.

Jednocześnie wyrażam zgodę na przedłożenie w/w pracy przez mgr Joannę Nowak jako część rozprawy doktorskiej w formie spójnego tematycznie zbioru artykułów opublikowanych w czasopismach naukowych.

Oświadczam, iż samodzielna i możliwa do wyodrębnienia część ww. pracy wykazuje indywidualny wkład mgr Joanny Nowak przy opracowywaniu koncepcji, wykonywaniu części eksperymentalnej, opracowaniu i interpretacji wyników tej pracy.



(podpis współautora)



Gdańsk, dnia 7 grudnia 2023r.

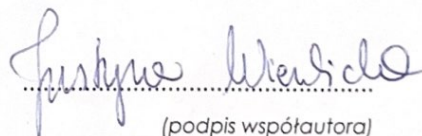
dr Justyna Wierzbicka  
(tytuł zawodowy, imię i nazwisko)

### OŚWIADCZENIE

Jako współautor pracy pt. „VDR and PDIA3 are essential for activation of calcium signaling and membrane response to 1,25(OH)2D3 in squamous cell carcinoma cells” oświadczam, iż mój własny wkład merytoryczny w przygotowanie, przeprowadzenie i opracowanie badań oraz przedstawienie pracy w formie publikacji to udział w interpretacji pozyskanych wyników.

Jednocześnie wyrażam zgodę na przedłożenie w/w pracy przez mgr Joannę Nowak jako część rozprawy doktorskiej w formie spójnego tematycznie zbioru artykułów opublikowanych w czasopismach naukowych.

Oświadczam, iż samodzielna i możliwa do wyodrębnienia część ww. pracy wykazuje indywidualny wkład mgr Joanny Nowak przy opracowywaniu koncepcji, wykonywaniu części eksperymentalnej, opracowaniu i interpretacji wyników tej pracy.



(podpis współautora)

Gdańsk, dnia 7 grudnia 2023r.

dr Magdalena Gebert  
(tytuł zawodowy, imię i nazwisko)

### OŚWIADCZENIE

Jako współautor pracy pt. „VDR and PDIA3 are essential for activation of calcium signaling and membrane response to 1,25(OH)2D3 in squamous cell carcinoma cells” oświadczam, iż mój własny wkład merytoryczny w przygotowanie, przeprowadzenie i opracowanie badań oraz przedstawienie pracy w formie publikacji to wykonanie testów aktywności czynników transkrypcyjnych (Dual luciferase reporter assay).

Jednocześnie wyrażam zgodę na przedłożenie w/w pracy przez mgr Joannę Nowak jako część rozprawy doktorskiej w formie spójnego tematycznie zbioru artykułów opublikowanych w czasopismach naukowych.

Oświadczam, iż samodzielna i możliwa do wyodrębnienia część ww. pracy wykazuje indywidualny wkład mgr Joanny Nowak przy opracowywaniu koncepcji, wykonywaniu części eksperymentalnej, opracowaniu i interpretacji wyników tej pracy.

*Magdalena Gebert*

(podpis współautora)

Gdańsk, dnia 7 grudnia 2023r.

prof. dr hab. Rafał Bartoszewski  
(tytuł zawodowy, imię i nazwisko)

## OŚWIADCZENIE

Jako współautor pracy pt. „*VDR and PDIA3 are essential for activation of calcium signaling and membrane response to 1,25(OH)2D3 in squamous cell carcinoma cells*” oświadczam, iż mój własny wkład merytoryczny w przygotowanie, przeprowadzenie i opracowanie badań oraz przedstawienie pracy w formie publikacji to konceptualizacja badań oraz opracowanie finalnej wersji manuskryptu.

Jednocześnie wyrażam zgodę na przedłożenie w/w pracy przez mgr Joannę Nowak jako część rozprawy doktorskiej w formie spójnego tematycznie zbioru artykułów opublikowanych w czasopiśmie naukowym.

Oświadczam, iż samodzielna i możliwa do wyodrębnienia część ww. pracy wykazuje indywidualny wkład mgr Joanny Nowak przy opracowywaniu koncepcji, wykonywaniu części eksperymentalnej, opracowaniu i interpretacji wyników tej pracy.

Zakład Biofizyki  
KIEROWNIK

  
prof. dr hab. Rafał Bartoszewski

(podpis współautora)



Gdańsk, dnia 7 grudnia 2023r.

prof. dr hab. Michał Żmijewski  
(tytuł zawodowy, imię i nazwisko)

## OŚWIADCZENIE

Jako współautor pracy pt. „VDR and PDIA3 are essential for activation of calcium signaling and membrane response to 1,25(OH)2D3 in squamous cell carcinoma cells” oświadczam, iż mój własny wkład merytoryczny w przygotowanie, przeprowadzenie i opracowanie badań oraz przedstawienie pracy w formie publikacji to konceptualizacja oraz pozyskanie źródła finansowania badań, nadzór merytoryczny, walidacja pozyskanych danych, opracowanie, opracowanie manuskryptu publikacji.

Jednocześnie wyrażam zgodę na przedłożenie w/w pracy przez mgr Joannę Nowak jako część rozprawy doktorskiej w formie spójnego tematycznie zbioru artykułów opublikowanych w czasopiśmie naukowych.

Oświadczam, iż samodzielna i możliwa do wyodrębnienia część ww. pracy wykazuje indywidualny wkład mgr Joanny Nowak przy opracowywaniu koncepcji, wykonywaniu części eksperymentalnej, opracowaniu i interpretacji wyników tej pracy.

Katedra i Zakład Histologii  
Gdański Uniwersytet Medyczny  
Prof. dr hab. Michał Żmijewski

.....  
(podpis współautora)